EXCITATION ENERGY TRANSFER AND CHARGE SEPARATION DYNAMICS IN PHOTOSYSTEM II: HOLE-BURNING STUDY

by

KHEM ACHARYA

M.S., TRIBHUVAN UNIVERSITY, 1997

AN ABSTRACT OF A DISSERTATION

submitted in partial fulfillment of the requirements for the degree

DOCTOR OF PHILOSOPHY

Department of Chemistry
College of Arts and Sciences

KANSAS STATE UNIVERSITY
Manhattan, Kansas

2012

Abstract

The constituents of oxygen-evolving photosystem II core complexes—antenna proteins (CP43 and CP47) and reaction center (RC)—have been the subject of many studies over the years. However, the various issues related to electronic structure, including the origin/composition of the lowest-energy traps, origin of various emission bands, excitation energy transfer (EET), primary charge separation (CS) processes and pigment site energies remain yet to be fully resolved. Exploiting our state-of-the-art techniques such as low-T absorption, fluorescence, and hole burning (HB) spectroscopies, we resolved some of the issues particularly related to CP47 and isolated RC protein complexes. For example, we demonstrated that the fluorescence origin band maximum (~695 nm) originates from the lowest-energy state ~693 nm of intact CP47. In intact CP47 in contrast to destablished protein complexes, the band (~695 nm) does not shift in the temperature range of 5–77 K unless hole-burning takes place. We also studied a large number of isolated RC preparations from spinach, and wild-type *Chlamydomonas reinhardtii* (at different levels of intactness), as well as its mutant (D2-L209H), in which the active branch pheophytin ($Pheo_{D1}$) has been genetically replaced with chlorophyll *a* (Chl *a*). We showed that the Q_x-/Q_y-region site-energies of $Pheo_{D1}$ and $Pheo_{D2}$ are ~545/680 nm and ~541.5/670 nm, respectively, in good agreement with our previous assignment [Jankowiak et al. *J. Phys. Chem. B* **2002**, *106*, 8803]. Finally, we demonstrated that the primary electron donor in isolated algal RCs from *C. reinhardtii* (referred to as RC684) is P_{D1} and/or P_{D2} of the special Chl pair (analogous to P_L and P_M, the special BChl pair of the bacterial RC) and not Chl_{D1}. However, the latter can also be the primary electron donor (minor pathway) in RC684 depending on the realization of the energetic disorder. We further demonstrate that transient HB spectra in RC684 are very similar to $P^+Q_A^-$ - PQ_A spectra measured in PSII core, providing the first evidence that RC684 represent *intact* isolated RC that also possesses the secondary electron acceptor, Q_A. In summary, a new insight into possible charge separation pathways in isolated PSII RCs has been provided.

EXCITATION ENERGY TRANSFER AND CHARGE SEPARATION DYNAMICS IN PHOTOSYSTEM II: HOLE-BURNING STUDY

by

KHEM ACHARYA

M.S., TRIBHUVAN UNIVERSITY, 1997

A DISSERTATION

submitted in partial fulfillment of the requirements for the degree

DOCTOR OF PHILOSOPHY

Department of Chemistry
College of Arts and Sciences

KANSAS STATE UNIVERSITY
Manhattan, Kansas

2012

Approved by:

Major Professor
Ryszard Jankowiak

Copyright

Abstract

The constituents of oxygen-evolving photosystem II core complexes—antenna proteins (CP43 and CP47) and reaction center (RC)—have been the subject of many studies over the years. However, the various issues related to electronic structure, including the origin/composition of the lowest-energy traps, origin of various emission bands, excitation energy transfer (EET), primary charge separation (CS) processes and pigment site energies remain yet to be fully resolved. Exploiting our state-of-the-art techniques such as low-T absorption, fluorescence, and hole burning (HB) spectroscopies, we resolved some of the issues particularly related to CP47 and isolated RC protein complexes. For example, we demonstrated that the fluorescence origin band maximum (~695 nm) originates from the lowest-energy state ~693 nm of intact CP47. In intact CP47 in contrast to destablished protein complexes, the band (~695 nm) does not shift in the temperature range of 5–77 K unless hole-burning takes place. We also studied a large number of isolated RC preparations from spinach, and wild-type *Chlamydomonas reinhardtii* (at different levels of intactness), as well as its mutant (D2-L209H), in which the active branch pheophytin ($Pheo_{D1}$) has been genetically replaced with chlorophyll *a* (Chl *a*). We showed that the Q_x-/Q_y-region site-energies of $Pheo_{D1}$ and $Pheo_{D2}$ are ~545/680 nm and ~541.5/670 nm, respectively, in good agreement with our previous assignment [Jankowiak et al. *J. Phys. Chem. B* **2002**, *106*, 8803]. Finally, we demonstrated that the primary electron donor in isolated algal RCs from *C. reinhardtii* (referred to as RC684) is P_{D1} and/or P_{D2} of the special Chl pair (analogous to P_L and P_M, the special BChl pair of the bacterial RC) and not Chl_{D1}. However, the latter can also be the primary electron donor (minor pathway) in RC684 depending on the realization of the energetic disorder. We further demonstrate that transient HB spectra in RC684 are very similar to $P^+Q_A^-$ - PQ_A spectra measured in PSII core, providing the first evidence that RC684 represent *intact* isolated RC that also possesses the secondary electron acceptor, Q_A. In summary, a new insight into possible charge separation pathways in isolated PSII RCs has been provided.

Table of Contents

List of Figures ix
Acknowledgements xiv
Dedication xvi
Chapter 1 - Introduction 1
1.1. Photosynthesis overview 1
1.1.1 A glimpse of photosynthesis 1
1.1.2 Anoxygenic photosynthesis 2
1.1.3 Oxygenic photosynthesis 2
1.1.3.1 Photosystem II and I 5
1.1.3.2 PSII core 6
1.2. An overview of key principles of HB theory 8
1.2.1 Zero-phonon lines and electron phonon coupling 8
1.2.2 Inhomogeneous broadening 13
1.2.3 Spectral hole burning 15
1.2.3.1 Mechanism of HB 16
1.3. Excitation energy transfer and charge separation mechanism 20
References 27
Chapter 2 - On the Unusual Temperature Dependent Emission of the CP47 Antenna Protein Complex of Photosystem II 33
2.1 Introduction 34
2.2 Result and discussion 36
2.3 Conclusion 46
References 48
Chapter 3 - Site-Energies of Active and Inactive Pheophytins in the Reaction Center of Photosystem II from *Chlamydomonas reinhardtii* 51
3.1. Introduction 53
3.2. Materials and methods 57
3.2.1. Preparation of PSII RC from WT *C. reinhardtii* and its D2-L209H mutant. 57

3.2.2. Spectroscopic measurements. 59
3.2.3. Monte Carlo simulations of the WT minus the mutant RC absorption difference spectrum. 60
3. 3. Results 61
3.3.1. Low temperature absorption spectra of the RC from WT *C. reinhardtii* and its D2-L209H mutant—site energies of PheoD1 and PheoD2. 61
3.3.2. Comparison of absorption, persistent, and transient hole spectra obtained for the RCs from *C. reinhardtii* and spinach. 64
3.3.3. Absorption and nonresonant HB spectra obtained for damaged *C. reinhardtii* RCs.. 67
3.3.4. Optical spectra obtained for the C. reinhardtii D2-L209H mutant. 69
3.3.5. Monte Carlo simulations of the absorption difference spectra of *C. reinhardtii* and its D2-L209H mutant. 72
3.4. Discussion 73
3.4.1. Nonresonant persistent holes. 73
3.4.2. Destabilized (damaged) RC samples. 75
3.4.3. More on site energies of $Pheo_{D1}$ and $Pheo_{D2}$. 78
3.4.4. Excitonic calculations. 79
4. Conclusions. 81
References 84
Chapter 4 - Primary Electron Donor(s) in Isolated Reaction Center of Photosystem II from *Chlamydomonas reinhardtii* 90
4.1. Introduction 92
4.2. Experimental section 96
4.3. Results 97
4.3.1 Low temperature absorption spectra for isolated RC of *C. reinhardtii*. 97
4.3.2. Nonresonant transient HB spectra. 99
4.3.3. Resonant hole-burned (HB) spectra. 105
4.4. Discussion 107
4.4.1. Absorption spectra of RC684 and RC680 RCs isolated from *C. reinhardtii*. 108
4.4.2. On triplet formation and the nature of the electrochromic shift in RC684. 111
4.4.3. Charge separation pathway(s) in RC680 and RC684. 115

4.5. Concluding Remarks..... 121
References..... 123
Chapter 5 - Conclusion and Future Direction..... 126
References..... 130
Appendix A - New Insight into the Electronic Structure of the CP47 Antenna Protein Complex of Photosystem II: Hole Burning and Fluorescence Study..... 132
Appendix B - Supporting Information for the Chapter number two: Experimental Strategy and Fitting Algorithm for Temperature Dependent Fluorescence Spectra. 136

List of Figures

Figure 1-1 Organization of photosynthetic units and the light-driven reactions taking place in thylakoid membrane of plants. 3

Figure 1-2 Arrangement of various antennas (CP29, CP26 and LHCII) around the core protein complexes (CP43, CP47 and RC) in PSII. 5

Figure 1-3 Arrangement of pigments in PSII core monomer. Chlorophylls in CP43 and CP47 are in gray, except: Chla 526 (blue), 523 (red), 481 (purple), and 477 (cyan) ultimately involving in energy transfer to RC. RC cofactors are in green. All β-carotene are shown in pink. 8

Figure 1-4 Schematic of potential energy curves for weak and strong linear (i.e. $\omega_g = \omega_e$) el-ph couplings. Electronic transitions between ground (E_0) and excited (E_1) states are indicated by vertical arrows in accordance with Franck Condon approximation. 12

Figure 1-5 Schematic of homogeneous versus inhomogeneous broadening. In the upper frame, absorbers are in perfect host matrix (left one), experiencing perfect periodic potential (middle one), and resulting in homogeneous lineshape (right one). In the lower frame, absorbers are in amorphous matrix (left), experience rugged potential (middle) and resulting in inhomogeneously broadened band (right most). 13

Figure 1-6 Schematic of the NPHB mechanism. Extrinsic TLS with ground (g) and excited electronic states, labeling as g and e, respectively, of a pigment. Δ_α and Δ_β are the double well asymmetry parameters in the ground and excited state, respectively. q is the intermolecular coordinate, and ω_B is the burn frequency. 17

Figure 1-7 Nonphotochemical spectral hole-burning. In the top panel, the dashed (red) and the solid (blue) lines represent the pre-burn and the post-burn absorption spectra, respectively. In the bottom panel is shown the difference spectrum (post-burn minus pre-burn absorption spectra). See text for details. 19

Figure 1-8 Schematic of the electronic coupling between the two pigments P_1 and P_2, giving rise to either EET or electron transfer from P^*_1 to P_2. 20

Figure 1-9 Schematic showing the mechanism of EET: a) Columbic mechanism, as suggested by Förster, and b) electron exchange mechanism, as suggested by Dexter. 25

Figure 2-1 Arrangement of CP47 Chls and carotenes (in brown) on the stromal and lumenal side of the membrane. Chls 521, 523, 524 and 526 are shown in red. Chls 511, 514, and 517 are in blue. Remaining Chls are in green; the pigments are numbered as in.[22] 35
Figure 2-2 Temperature dependent emission spectra of various CP47 complexes. Frame A: digitized spectra as presented in.[3] Spectra shown in frames B and C represent spectra of destabilized and intact CP47 complexes (this work), respectively. 37
Figure 2-3 Normalized (integrated) fluorescence intensity of CP47 complexes shown in Figure 2-2 plotted as a function of temperature; black squares, red circles, and blue triangles represent data shown in Figure 2-2, frames A, B, and C, respectively. The inset shows fluorescence of intact CP47 at excitation wavelengths of 496.5 nm (top), 630.0 nm, and 660.0 nm (bottom curve). The green stars and open circles, shown for comparison, correspond to the normalized relative quantum yields of PS II core reported in[18] and[11], respectively. 38
Figure 2-4 Temperature dependence of the fluorescence spectrum (top curve) obtained for sample with saturated non-resonant hole at 5 K; its maximum is near 692 nm. The remaining spectra were obtained at higher temperatures. The dotted curve is the pre-burn 50 K spectrum from Figure 2-2C scaled for comparison with the post-burn curve. The inset show the shifts of the broad non-resonant holes (blue squares) and positions of the corresponding maxima of the origin bands (red circles), obtained at different burn fluences. 41
Figure 2-5 Comparison of experimental CP47 fluorescence spectra (black curves) with calculated emission spectra (blue dashed curves) at 5, 50, 100, and 150 K. The red and green curves correspond to the calculated lowest-state emission and higher-states emission, respectively. 43
Figure 3-1 Cofactor arrangement in the active (D1) and inactive (D2) branches of the PSII RC based on the crystal structure of *T. vulcanus* at 1.9 Å resolution, PDB ID 3ARC. The left frame shows the arrangement in WT RCs (chls, green; carotenes, yellow; pheophytins, purple; plastoquinones, gray; non-heme iron, red; and nitrogen, blue). The right frame shows the arrangement of selected pigments and their ligands (water, orange; histidine, red; leucine, cyan) in the D2-L209H RC mutant. The substituents of the cofactors are truncated for clarity. 54

Figure 3-2 Spectra a and b correspond to the absorption spectra of intact WT and D2-L209H mutant RCs, respectively, measured at T = 5K. The areas of curve a and b are scaled to 7.0 and 7.5, respectively, based on the normalized oscillator strength of the cofactors. Curve c is the difference between spectra b and a. The inset shows the corresponding Q_x-region (see text for detail). 61

Figure 3-3 Absorption, nonresonant persistent hole, and transient HB spectra obtained for RCs from *C. reinhardtii* and spinach RC are shown in frames A/C/E and B/D/F, respectively. The insets in frames A and B show the Q_x absorption band of both pheophytins near 544 and 543 nm, while those in frames E and F illustrate the Q_x response (in the pheophytin region) in the transient spectra. All HB spectra were obtained with a λ_B of 665 nm and were measured at 5K. 64

Figure 3-4 *Frame A*: Absorption spectrum (curve a) of partly damaged PSII RC from *C. reinhardtii* (see text). Curve b is the absorption spectrum obtained for intact WT RCs. Absorption spectra in the corresponding Q_x-region of pheophytins are shown in the inset, as curves a′ and b′, respectively. Curves c and c′ are the difference spectra (i.e., c = a – b and c′ = a′ – b′). The green curve d is the persistent (nonresonant) HB spectrum obtained with λ_B = 664.9 nm; the arrow points to the ZPH. Curve d′ shows the response in persistent HB spectrum in the Q_x-region of pheophytins. The sharp spikes observed in the 675–687 nm spectral range in curves d (re-plotted on a cm^{-1} scale in the upper left insets of frames A and B) are Chl *a* vibronic satellite holes. *Frame B* shows the same spectra, as in frame A, but obtained for WT RCs of *C. reinhardtii* exposed to the excess of TX-100 detergent (see text for details). All spectra were obtained at T = 5 K. 68

Figure 3-5 Figure 3-5. Curves a, a', b, and c correspond to the absorption, fluorescence, persistent, and transient HB spectra obtained for the D2-L209H mutant of *C. reinhardtii*. Both HB spectra were obtained with a λ_B of 665.0 nm, and recorded at 5 K. 69

Figure 3-6 The red curve a (curve c from Figure 3-2) corresponds to absorbance difference spectrum obtained for WT RC and its D2-L209H mutant, assuming a dipole strength ratio of Pheo a/Chl a of 0.5. The blue curve (spectrum b) was obtained using excitonic calculations (see text). 80

Figure 4-1 Cofactor arrangement in the active (D1) and inactive (D2) branches of photosystem II reaction center from crystal structure of *T. vulcanus* at 1.9 Å resolution, PDB ID 3ARC.[2]

The cofactors are color coded as, chls: green, carotenes: yellow, pheophytins: purple, plastoquinones: gray, non-heme iron: red, and Nitrogen: blue. The substituents of the cofactors are truncated for clarity..... 92

Figure 4-2 Normalized absorption spectra (at Q_x transition of Pheos) of three representative RC samples RC_{S1}, RC_{S2}, and RC_{S3} (obtained from *C. reinhardtii*) are shown in the frames A, B, and C, respectively. Corresponding transient HB spectra are shown in frames D, E, and F. The insets in frames A, B and C show the Q_x absorption band of pheophytins. All HB spectra were obtained with λ_B = 665.0 nm and laser intensity of ~100 mW/cm^2. The dotted gray curve in frames A and B is the absorption spectrum from frame C and is shown for easy comparison. All spectra were measured at T = 5 K. 98

Figure 4-3. Transient HB spectra. Curves a and b represent the transient HB spectra of intact and partly damaged RC_{S3d} obtained with λ_B = 665.0 nm and laser intensities I = 100 mW/cm^2, respectively. The difference between curves b and a is shown as curve c. 101

Figure 4-4 Transient HB spectra. Frames A and B represent the transient HB spectra of RC_{S2} and RC_{S3}, respectively, obtained with λ_B of 665.0 nm (curves, a/a') and 496.5 nm (curves, b/b'). The red curves c/c' are obtained as the difference of a/b and a'/b', which correspond to triplet bleach in RC680 and RC684, respectively..... 102

Figure 4-5 Transient hole-burned spectra of various RC samples. In the main frame, black curve represents the absorbance due to the oxidation of P_{D1} of RC_{S3}, obtained with λ_B of 665 nm and intensity of 100 mW/cm^2. Left inset corresponds to the absorption of P_{D1}^+ in RC_{S2} obtained with λ_B of 682 nm and laser burn intensities (I) of 1, 5, 50, and 150 mW/cm^2. Right inset represents the electrochromic shift in Pheo Q_x-band of spinach RC sample (black), RC_{S2} (blue), and RC_{S3} (red) obtained with λ_B of 665.0 nm. 104

Figure 4-6 Resonant transient HB spectra obtained for RC_{S3} sample. Spectra a, b, c, and d (resolution 1 cm^{-1}) were obtained with λ_B of 682.0, 684.0, 686.0, and 688.0 nm, respectively. Black dashed curve was obtained at λ_B = 496.5 nm. The inset corresponds to the Lorentzian fit (black curve) of ZPH of curve b..... 106

Figure 4-7 Extracted absorption spectra for RC684 (frame A) and RC680 (frame B) complexes. The curves a/b and a′/b′ correspond to the extracted absorption spectra of two subsets of RCs, RC684 (intact) and RC680 (destablished) complexes, respectively (see text for details). Transient spectrum c (inverted curve d from Figure 7) shows a good agreement

with the low-energy absorption tail of extracted absorption spectrum of RC684. Curve d (in frame B) was obtained as the difference of absorption spectra of intact and partly damaged RC_{S3} preparation, which corresponds to the destabilized RC680..... 109

Figure 4-8 Comparison of various ($P^+Q_A^-$– PQ_A) spectra: curve a (black) represents the ($P^+Q_A^-$– PQ_A) obtained for the isolated RC_{S3} from *C. reinhardtii,* adopted from curve b' of Figure 4B. Curve (a') is resonant transient HB spectrum of RC_{S3} sample obtained at the 688.0 nm. Spectra b and c are the flash induced absorption difference ($P^+Q_A^-$– PQ_A) spectra of PSII core complexes from *Synechocystis* sp. PCC 6803 at 80 K[23] and *T. elongatus* at 5 K[30], respectively. 112

Figure B-1 Emission spectra of CP47 complex at T = 5 K with two different concentrations of β-DM; solid black line (0.03%) and dotted blue line (0.015%). 139

Acknowledgements

Jesus Christ, how time is flying! It is hard to believe that my life as a graduate student has come to an end. First and foremost, I would like to express my deepest appreciation and thanks to my research advisor and committee chair, Professor Ryszard Jankowiak. Your wisdom, generosity and knowledge have stimulated and guided me thoroughly during my graduate studies. Thank you for your continuous support and encouragement, and for the things, especially modus operandi in the scientific arena, that I have learned from you. Serdecznie dziękuję!!!

It is my pleasure and honor to thank my Graduate Committee Members: Professor Paul Smith, Professor Viktor Chikan, and Professor Robert Szoszkiewicz for the invaluable time and suggestions. I would also like to sincerely thank Professor Douglas McGregor for being an outside chairperson of my graduate committee. Special thanks to our collaborators and sample providers, Prof. Michael Seibert and Prof. Rafael Picorel for kindly providing samples for my research. Thank you all K-State faculty members and staff for your direct or indirect support during my graduate study. Thanks to Earline Dikeman for your help in teaching courses. Thank you so much Ron Jackson, Tobe Eggers, and Jim Hodgson for your helping-hands with fixing the lab equipment.

I would like to thank all the lab members in the Jankowiak group. Special thanks to past members: Dr. Raja Chinnappan, Dr. Nhan C. Dang and Mike Reppert for sharing their lab experiences. Wow! I almost forgot to thank my nearest and dearest current lab mates: Dr. Ximao Feng, Bhanu Neupane, Mukund Koirala, Lin Chen, and Adam Kell for your helpfulness and ever-smiling faces! Thank you so much Majka Jankowiak for your maternal-like care in

preparing birthday cakes and other delicious foods, and organizing parties in your house, providing a homely environment for us in the foreign soil. The group as a whole has been a second family to me.

My very special thanks go to my family and relatives. Thanks to my parents, especially my mother who solely took care of me after my father passed away; I am really indebted to you, mom! Thanks to my family members: sister Khima Dahal-Acharya, brother-in-law Ganga Dhar Dahal, and brother Krishna Hari Acharya for your love and affection. I always enshrine my maternal uncle (Mama) Bhanu Bhakta Sharma in my bosom for fulfilling paternal-like responsibilities regarding my education; I've been philosophically inspired by your examples of being honest, hardworking, social and patriotic. My lovely wife, Sattya, thank you! Thanks for your everlasting love and support. Thanks to my daughter, Aadima Acharya (Apu), and son, Aadim Acharya, for making me a cheerful dad! Finally, thanks to myself for honestly and successfully driving the life….

Dedication

My parents

(Mother Manrupa Acharya and Father Ganga Dhar Acharya)

Chapter 1 - Introduction

1.1. Photosynthesis overview

1.1.1 A glimpse of photosynthesis

Photosynthesis is the most important biological process on earth that harvests light energy to produce the various biological components required to support nearly all life on earth.[1] The process is of great importance for our planet as it provides food and oxygen for our survival. All fossil fuels, an oxygenic atmosphere, and formation of the ozone layer are all direct or indirect consequences of photosynthesis. An understanding of the structures and molecular details of photosynthesis, which nature has developed and optimized over 2.5 billion years, has huge implications for the future of mankind, especially for solving the energy crisis.[2] Discovery of molecular mechanisms will form the basis for the development of new routes towards a sustainable bioenergy source. In all photosynthesis, light is captured by huge antenna systems and funneled to nanoscale biosolar energy converters, called photosynthetic reaction centers (RC). The captured sun light then drives a transmembrane charge separation which builds up a membrane potential, thereby driving the synthesis of high energy products such as ATP and NADPH[3,4], which are later used in "dark" reactions to build up carbohydrates and all other biomolecules needed for survivals. Only after understanding these remarkable tasks in photosynthesis, we will be better-equipped to secure the energy needs of humans by the conversion and utilization of solar energy.[2]

1.1.2 Anoxygenic photosynthesis

There are two types of photosynthesis: anoxygenic and oxygenic. Purple bacteria, green sulfur bacteria, green filamentous bacteria and heliobacteria are all the classes of non-oxygenic photosynthetic bacteria.[5,6] Anoxygenic photosynthesis is out of the main focus of this dissertation, so only a brief description will be discussed. Purple bacteria are the most diverse, simple and highly studied among the non-oxygenic bacteria; which, like the oxygenic photosystem, comprise of antenna and reaction systems. The antenna system is very complicated and, in general, consists of LHI and LHII. LHI (also called B875) directly surrounds the RC, which in turn is surrounded by LHII (also called B800-850).[5,6] Anoxygenic bacteria, the oldest photosynthetic organisms on earth, contain a single RC and are not able to use water as an electron source for photosynthesis. Based on the photoreaction center, these bacteria can be divided into two classes: type-I and type-II reaction centers, containing either FeS or quinones as the terminal electron acceptors, respectively.[2] The RC of purple bacteria represents a type-II reaction center, whereas green-sulfur bacteria and heliobacteria represent type-I reaction centers. While detailed crystal structure[7-10] information on type-II reaction centers is available from purple bacteria, only biochemical, biophysical, and molecular biological studies have been performed on the structural composition and organization of type-I reaction centers, not yet crystallized. The purple bacterial RC was the first membrane protein to have been crystallized, and led to the Nobel Prize in 1988 for the work.

1.1.3 Oxygenic photosynthesis

It is the oxygenic photosynthesis that changed the atmosphere from anoxic to oxygen-rich, by using water as the electron donor and producing oxygen, which is required to sustain life on Earth. Higher plants, algae, and cyanobacteria (ancestors of oxygenic photosynthesis) are the

organisms that carry out oxygenic photosynthesis.[11-13] The overall process of oxygenic photosynthesis involves four concurrently working multi-subunit protein complexes: PSII, PSI, cytochrome b_6f, and F-ATPase, embedded in thylakoid membranes inside the chloroplast.[14] The basic arrangement of these four proteins is schematically shown in Figure 1-1.

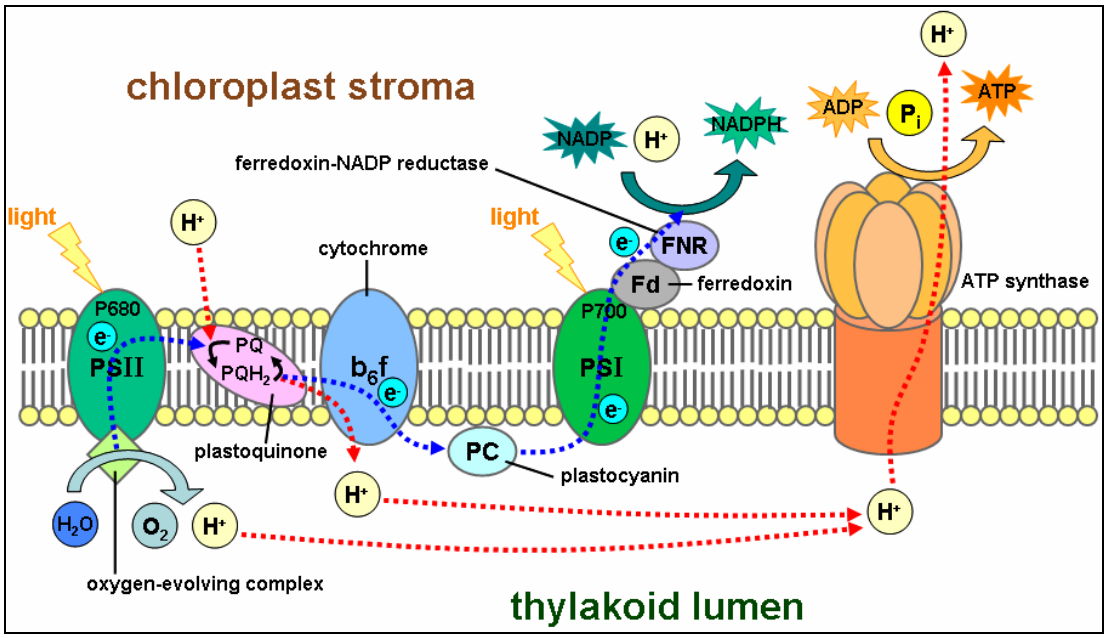

Figure 1-1 Organization of photosynthetic units and the light-driven reactions taking place in thylakoid membrane of plants.[15]

While all photosynthetic RCs are derived from a common ancestor, the peripheral antenna systems have developed differently in different organisms to increase cross section for light absorption.[16] For examples, purple bacterial have developed LHI and LHII; green non-sulfur bacteria (which contain a type-II RC) and green sulfur bacteria (which contain a type-I RC) – chlorosomes; and cyanobacteria and red algae – phycobilisomes, unique and highly developed antenna systems, which are able to absorb green light, and thus the full spectrum of visible light.[2] Although phycobilisomes mainly serve as peripheral antenna for PSII, they can also move to PSI in the process of state transition to balance light capturing capacity between the

two photosystems. Green algae and higher plants on the other hand contain membrane integral antenna complexes, light harvesting complexes I and II (LHCI and LHCII), as peripheral antenna for PSI and PSII, respectively. Integral membrane antennas are complexes in which the pigment-protein crosses the lipid bilayer. While LHCI is exclusively associated to PSI, LHCII can move, like phycobilisome, from PSII to PSI to adjust the distribution of excitation energy between the two photosystems in the process of state transitions. It can also play an important role in photoprotection by dissipating excess energy under high light intensities. Note that LHCII is the second most abundant protein on earth. Unlike core antenna systems of PSI and PSII that contain only Chla, LHCI and LHCII contain both Chla and Chlb, allowing more light to be absorbed from the visible spectrum. The recent crystal structure[17] of LHCII has revealed that each monomer of LHCII contains 8 Chla and 5 Chlb. For more information about the structure and function of LHCII, the following references[18-20] are suggested. Besides LHCII, other peripheral antennas associated with PSII are CP24 and CP29 transferring energy to CP47, and CP26 transferring energy to CP43. The recent crystal structure[21] of CP29 has confirmed 13 chlorophyll-binding sites – eight Chl *a* sites, four Chl *b* and one putative mixed site occupied by both Chl *a* and *b*. A simple figure that shows the basic arrangement of proteins in the PSII supercomplex is shown in Figure 1-2.

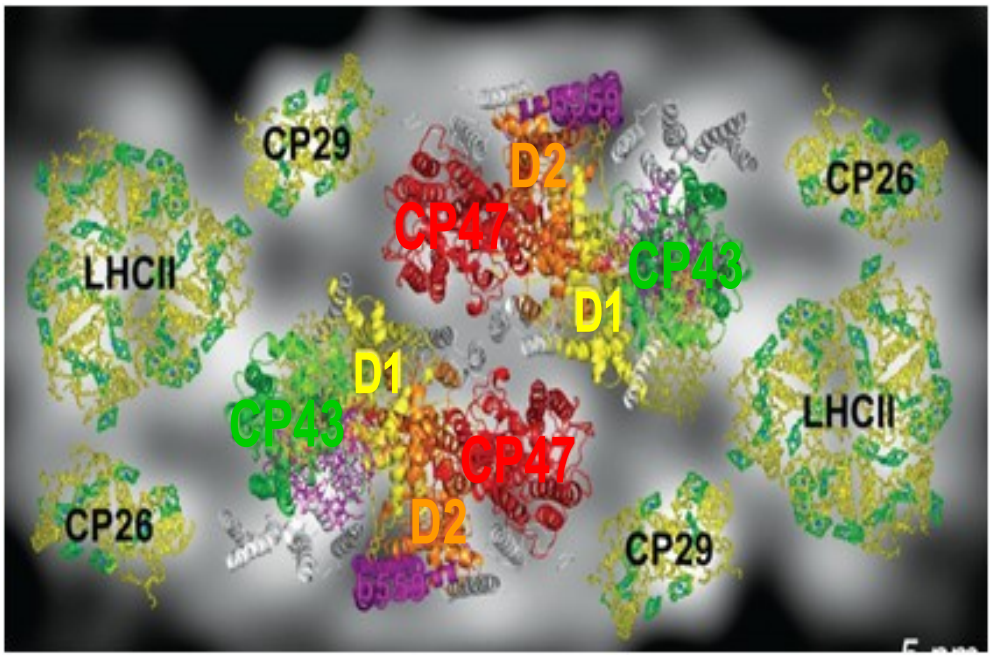

Figure 1-2 Arrangement of various antennas (CP29, CP26 and LHCII) around the core protein complexes (CP43, CP47 and RC) in PSII.[19]

1.1.3.1 Photosystem II and I

Unlike anoxygenic photosynthesis, all oxygenic photosynthetic organisms contain two photosystems. Photosystem I contains a type-I RC with three 4Fe4S clusters as final electron acceptors. It catalyzes the light-driven electron transfer from the luminal electron carriers plastocyanine or cytochrome c_6 to ferredoxin/flavodoxin at the stromal side of the membrane. Photosystem II contains a type-II RC which catalyzes the light-driven electron transport from water to a plastoquinone.[2] Photosystem II is unique and important as it is the only enzyme on earth which is able to split water into protons and oxygen by the use of visible light.[14] PSI and PSII work in series and are functionally coupled by the cytochrome b6f complex. In cyanobacteria, PSI is a trimer with a molecular mass of 1MDa, which is the largest membrane protein for which a structure has been determined. The high resolution crystal structure of PSI[22]

reveals that each monomer contains 96 Chlorophylls, 22 carotenoids, 4 lipids, 3 4Fe4S clusters, 2 phylloquiones, and 1 Ca^{2+} ion.

1.1.3.2 PSII core

The minimal PSII assembly capable of catalyzing light driven water oxidation is the PSII core (considered as a solar battery), consisting of the central D1/D2/cytb559 RC pigment-protein complex surrounded by inner antenna complexes CP43 and CP47[23], and other low molecular mass proteins. Photosystems II in cyanobacteria, green algae and plants are structurally similar dimers[24]; however, one monomer represents one functional unit. The crystal structure of the PSII[25-27] core has confirmed that the central part of the PSII core consists of the D1/D2 heterodimeric RC protein and two core antenna proteins, CP43 and CP47, flank D1 and D2 proteins on each side. The CP43 and CP47 proteins contain 13 and 16 Chl *a* molecules, respectively, making a total of 35 Chls *a* in each PSII core monomer. These Chls provide a light harvesting system for the reaction centers. On the other hand, PSII RC complex is confirmed, by high-resolution crystal structure, to contain six Chl and two Pheo molecules, two plastoquinones, one or two cytochromes b-559 (Cyt b-559), two β-carotene molecules, and a non-heme iron. [25-27] The arrangement of Chls is depicted in the figure 1-3. More details about CP47 and PSII RC – the protein complexes which are mainly studied in this dissertation – are discussed in chapter 1, and 3 and 4, respectively.

PSI and PSII perform the first step in photosynthesis: the light-induced charge separation across the photosynthetic membrane.[28] Upon photoexcitation of P680 in the PSII RC, charge separation takes place, resulting in the transfer of an electron to the neighboring $Pheo_{D1}$ and subsequently to a plastoquinone cofactor (Q_A and Q_B).[29] The special feature of this chlorophyll ($P680^+$) is due to its very high positive redox potential of ~ 1.26 V, one of the most oxidizing

redox potential found in nature and sufficient in extracting electrons from water.[28] The hole moves from P_{680}^{+} to the redox active tyrosine, $Tyr_{Z,}$ and then to a tetra-nuclear manganese cluster associated with an oxygen evolving complex (OEC), where it extracts four electrons from the OEC in four subsequent electron transfer events.[28] The extraction of an electron by $P680^{+}$ from $(Mn)_4$ cluster via tyrosine is absolutely unique to PSII and has no counterpart in any other protein in nature. The reduced OEC is now able to oxidize water, producing molecular oxygen and four protons after four subsequent oxidation steps (*viz* S0 to S4). At the acceptor side of PSII, two electrons are transferred to the mobile phylloquinone electron acceptor Q_B, enabling it to take two protons to produce plastohydroquinone (PQH_2).[28] While the proton forms the transmembrane pH gradient, driving force for ATP synthesis, the electron finally moves via cytochrome b_6f and plastocyanin to the ferredoxin of PSI. The reduced ferredoxin first reduces FNR (Ferredoxin: NADP+: oxidoreductase), and finally reduces NADP+ to NADPH, thereby providing reduced hydrogen for the synthesis of sugar from CO_2. The special feature of the primary donor in PSI (P700*) is due to its very high negative redox potential of -1.1 V, enabling it to reduce ferredoxin.[28] Both photosystems are functionally coupled by a pool of plastoquinones and another large membrane protein complex, cytochrome b6f, mediating the electron transfer between two photosystems, which in turn reduces the oxidized primary donor of PSI , P700.

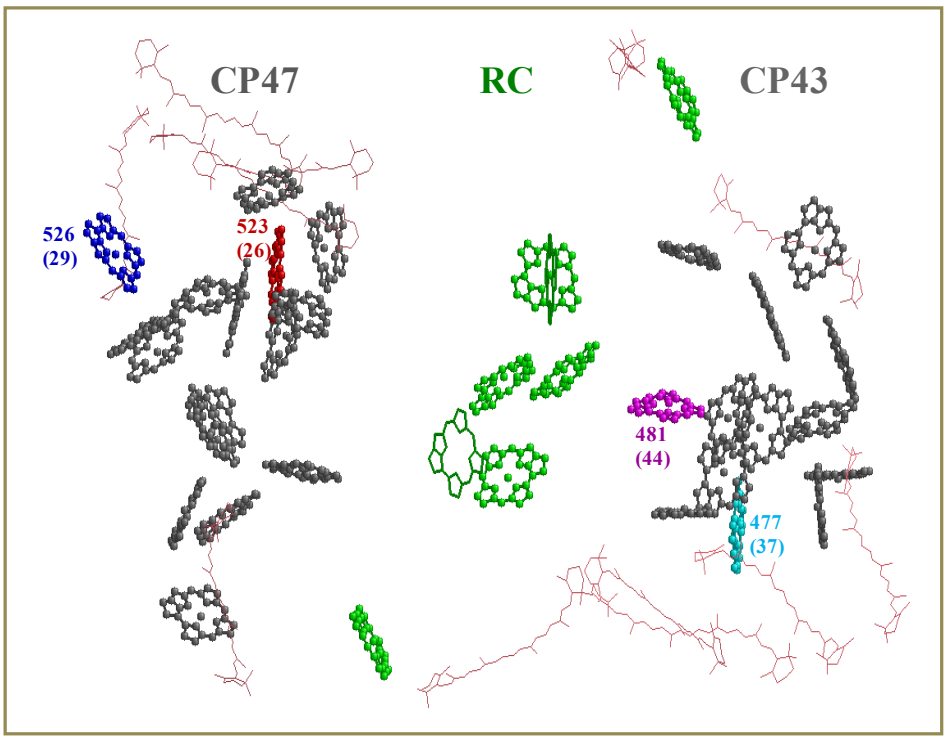

Figure 1-3 Arrangement of pigments in PSII core monomer.[27] Chlorophylls in CP43 and CP47 are in gray, except: Chla 526 (blue), 523 (red), 481 (purple), and 477 (cyan) ultimately involving in energy transfer to RC. RC cofactors are in green. All β-carotene are shown in pink.

1.2. An overview of key principles of HB theory

1.2.1 Zero-phonon lines and electron phonon coupling

An optical transition of a chromophore is quantum mechanical in nature and follows the Heisenberg uncertainty principle,

$$\Delta E \Delta t = \frac{h}{2\pi}, \tag{1-1}$$

where t is the time the electron spends in a particular energy state of energy E.[30] Because of the time uncertainty of an electron residing in a particular energy state, the spectral lineshape of an

optical transition gets broadened, called *uncertainty* or *homogeneous broadening*[31], and the lineshape is called *natural* or *homogeneous lineshape*.

At absolute zero (0 K), the homogeneous linewidth of an optical transition of a chromophore (impurity) in a solid matrix is related to a characteristic time T_1 according to the equation,[32]

$$\Gamma_{hom} = \frac{1}{2\pi c T_1}, \tag{1-2}$$

where Γ_{hom} is the homogeneous linewidth in cm^{-1}, c is the speed of light in cm/s, and T_1 is the relaxation time or the decay time of the excited state in s. At T = 0 K, the typical width of Γ_{hom} lies in the range of $10^{-4} - 10^{-3}$ cm^{-1}, which corresponds to a T_1 of $10^{-7} - 10^{-8}$ cm^{-1},[32] which purely corresponds to the excited state lifetime. As temperature increases, the lineshape starts to broaden due to dephasing processes induced by thermally activated phonon modes of the host matrix. These phonon modes result in a change in the phase of the excited electronic state wavefunction of the chromophore, so that the time dependent part, $\exp(iE_{ex}t/\hbar)]$, acquires an additional random phase factor shorting the excited state lifetime. Introducing this time (time required to change this phase) as another uncertainty factor of broadening, the Γ_{hom} can be rewritten as[32],

$$\Gamma_{hom} = \frac{1}{2\pi c T_2} = \frac{1}{2\pi c T_1} + \frac{1}{\pi c T_2^*}, \tag{1-3}$$

where T_2 is the total dephasing time and T_2^* is the phase relaxation or transverse relaxation or pure dephasing time, which is determined by the thermally induced fluctuation of the optical transition frequency. In other words, T_2^* is the time of the time-dependent part of the excited state wavefunction required to change from $\exp(iE_{ex}t/\hbar)$ to $\exp[i(E_{ex}t/\hbar + \delta)]$. At higher

temperatures (above 3 – 4 K), the increased number of thermally activated phonons lead to faster phase relaxation (T_2^* decreases) of the excited electronic wave function of the guest molecules. As T_2^* decreases, the second term starts to dominate the linewidth.[33]

For pure electronic and vibronic transitions, where no matrix phonons are created or destroyed, the homogeneous lineshape is called the zero-phonon line (ZPL), which is Lorentzian in shape. However, electronic transitions of guest molecules also couple to matrix phonons, called electron-phonon coupling. The transition accompanying net creation or destruction of phonons results in a broad continuous band, called the phonon side band (PSB), on the higher or lower energy side of the ZPL of absorption or emission spectrum, respectively. The shapes of the PSB, in a single site absorption spectrum, at lower and higher energy are Gaussian and Lorentzian, respectively. The structure and width of the PSB depends on local lattice dynamics at the impurity center, electron-phonon coupling and temperature.[33] The band shape of the single site absorption or fluorescence profile, as shown in Figure 1-4, consists of two parts: ZPL and PSB, which can be written as

$$L(\omega,T) = \phi_{ZPL}(\omega,T) + \phi_{PSB}(\omega,T), \qquad (1\text{-}4)$$

where the first and second parts respectively describe the ZPL and PSB. At T = 0, the width of ZPL is defined by lifetime broadening only. However, due to the presence of electron-phonon coupling and interactions with the low-energy excitations (i.e. TLS) the width of ZPL increases and becomes temperature dependent.[34-38] In this case, quadratic electron-phonon is to be considered in lieu of linear one, which leads to PSB with no effect on ZPL width.[1] The temperature dependence of homogeneous linewidth is given by $\sim T^{1+\mu}$ with $\mu \sim 0.3$ below 5 K .[1, 32,39,40]

The strength of the PSB is determined by the change in geometry of an impurity molecule in an excited state relative to the ground state, and can be explained by the Franck-Condon principle.[32] Figure 1-4 illustrates the potential energy curves for the strong and weak cases of electron-phonon coupling. For the weak coupling, the change in equilibrium geometry (Δq_i) in the excited state relative to the ground state is small and the main feature is the ZPL along with a small PSB. For the strong electron-phonon coupling, the large change in Δq_i during the electronic excitation leads to a significant PSB compared to the ZPL. The relative intensity of the ZPL and PSB can be characterized by the Debye-Waller factor, α (also called Franck-Condon factor), given by[41],

$$\alpha = \frac{I_{ZPL}}{I_{ZPL} + I_{PSB}}, \tag{1-5}$$

where I_{ZPL} and I_{PSB} are the integrated intensities of the ZPL and PSB, respectively. In the harmonic oscillator model at T ~ 0 K for N phonon modes, the DWF factor is given by[35,41-43]

$$\alpha = \exp(-S), \tag{1-6}$$

where S is the dimensionless Stokes shift, also known as the Huang-Rays factor and is defined as:

$$S(T=0) = \frac{M_i \omega_i}{2\hbar} \sum_i (\Delta q_i)^2, \tag{1-7}$$

where M_i and ω_i are the reduced mass and frequency of the phonon mode i, respectively, and Δq_i is the change of the equilibrium position corresponding to the lattice normal coordinate q_i. As equation 1.7 shows, $S \propto (\Delta q_i)^2$, and can be used to characterize the strength of the electron-phonon coupling; for strong coupling S > 1and for weak coupling S < 1.[33] For very strong coupling (S ≥ 10), no ZPL is observed, and the transition is said to be F-C forbidden.[1]

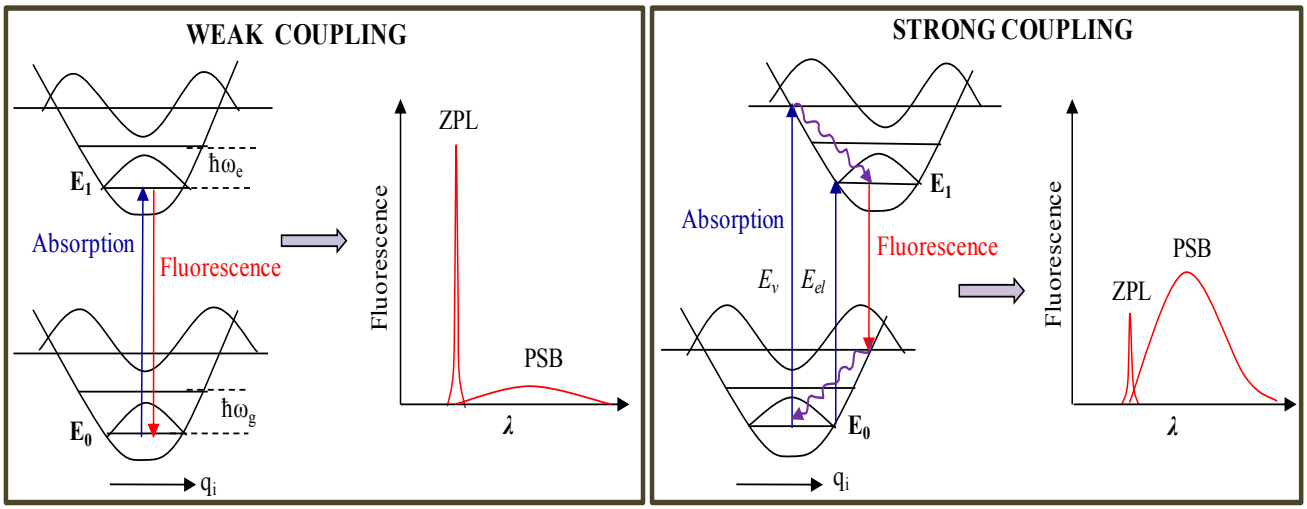

Figure 1-4 Schematic of potential energy curves for weak and strong linear (i.e. $\omega_g = \omega_e$) el-ph couplings. Electronic transitions between ground (E_0) and excited (E_1) states are indicated by vertical arrows in accordance with Franck Condon approximation.

Both local lattice dynamics, the strength of the PSB and the DWF are temperature dependent. The DWF decreases rapidly and, usually, monotonically as temperature increases, i.e., increasing temperature results in a rapidly deceasing ZPL intensity. The temperature dependent DWT is given by[33],

$$\alpha(T) = \exp\left[-\sum_{i}^{N} S(2\bar{n}_i + 1)\right], \qquad (1\text{-}8)$$

where $\bar{n}_i = \left[\exp(\hbar\omega_i / kT) - 1\right]^{-1}$ is the thermal occupation number, which is defined as the average number of phonons of mode *i* at temperature *T*. $\alpha(T)$ reaches its maximum value at very low temperatures (T $\leq$ 10 K for most organic glasses).

1.2.2 Inhomogeneous broadening

In the preceding section, an ideal broadening mechanism of a single chromophore embedded in a host matrix — where the chromophore experiences a perfect periodic potential and the same immediate local environment — has been discussed. This type of broadening is referred to as Γ_{hom} and is characterized by the ZPL. However, for an amorphous bulk sample,

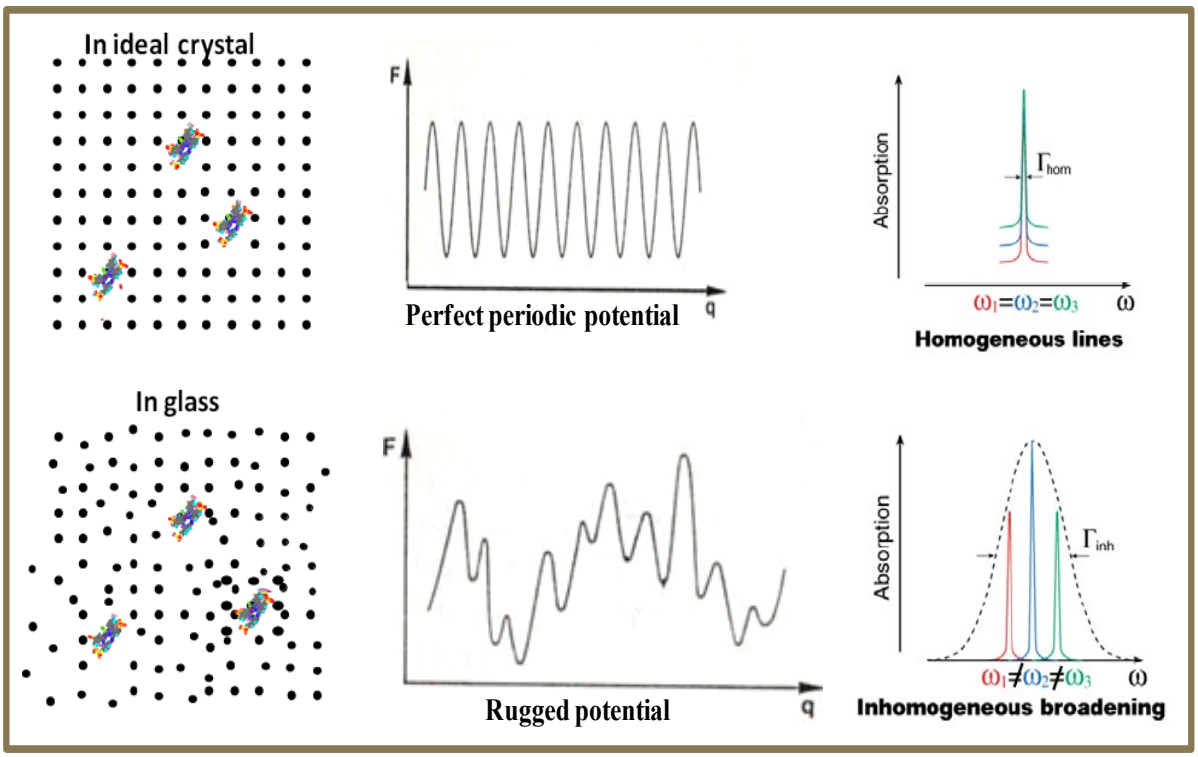

Figure 1-5 Schematic of homogeneous versus inhomogeneous broadening. In the upper frame, absorbers are in perfect host matrix (left one), experiencing perfect periodic potential (middle one), and resulting in homogeneous lineshape (right one). In the lower frame, absorbers are in amorphous matrix (left), experience rugged potential (middle) and resulting in inhomogeneously broadened band (right most).

because of the rugged potential energy surface, each molecule experiences slightly different local environments, arising from the particular inhomogeneities in the host matrix. Mechanisms leading to Γ_{inh} are defects, strains, stress filed variation, random electric fields, irregular molecular ordering, and interaction between centers/chromophores.[41,44,45] As a result, the ground and excited states of even identical chromophores are different and absorb at different frequencies, giving rise to a distribution of homogeneous lineshape frequencies, *inhomogeneous broadening*.[32,46]

In general, inhomogeneous broadening is the statistical distribution of the single site absorption spectrum and can be characterized by an inhomogeneous or site distribution function (IDF or SDF), $G(\omega)$, which has a Gaussian profile with a full width at half maximum of Γ_{inh}.[32,46,47] However, the experimental absorption spectrum of a bulk sample is the convolution of a single site absorption spectrum (including the ZPL and PSB) with the SDF of these sites, $G(\omega)$. Hence the width of the absorption spectrum (at half-maximum) is $\sim \Gamma_{inh} + S\omega_m$, where S is the Huang-Rhys factor and ω_m is the mean phonon frequency. [1,32, 42] Similarly, the width of fluorescence spectrum is $\sim \Gamma_{inh} + S\omega_m$, so the resulting Stokes shift is about $2\ S\omega_m$. There is deviation from this formula for large values of S. Γ_{inh} is always greater than Γ_{hom}. For example, for proteins and glasses Γ_{inh} is about 100 – 400 cm^{-1}, which is about a factor of 10^5 broader than Γ_{hom} (~ 0.0001 cm^{-1}). Even for molecules in a Shpol'skii matrix (organic molecules embedded in microcrystalline alkane hosts),[48] Γ_{inh} is around 1 – 5 cm^{-1}, which is still 3 – 4 orders of magnitude greater than Γ_{hom}. To obtain the dynamic information of a molecule, the primary task is to extract the Γ_{hom} from the obscurity of inhomogeneous broadening by applying site-selective spectroscopic techniques such as spectral hole burning, [32,44,49-51] fluorescence line narrowing (FLN)[52], single molecule spectroscopy (SMS)[53,54], all in frequency-domain, and photon echoes

(PE)[55-58] in the time-domain. The site-selective techniques have great utility and importance because of their ability to unravel hidden spectral information by improving spectral resolution by a factor of 10^3 to 10^5 as compared to conventional spectroscopy at room temperature.

1.2.3 Spectral hole burning

In the preceding section, the origins of homogeneous and inhomogeneous broadening have been discussed. This section discusses how the ZPL — which carries tremendous information regarding the dynamics of molecules — can be extracted from the intricacy of inhomogeneous broadening by using hole-burning techniques. Spectral hole burning, like fluorescence line narrowing, single molecule, and photon echo spectroscopies, is a powerful technique to investigate the excitonic structure, electron/energy transfer dynamics, and pigment-protein interaction in photosynthetic complexes.[1,42,59] The information provided by SHB includes[1]: i) excitation energy or electron transfer time by measuring Γ_{hom}, ii) Γ_{inh}, derived by measuring zero-phonon action (ZPA) spectra, iii) extent of correlation and excitonic interaction between the different bands within S_1 (Q_y)-states, iv) Huang-Rhys factors by measuring shallow hole at lowest state, and v) frequencies of Chl modes by vibronic satellite holes.

Upon optical excitation, if a molecule relaxes to the original ground state, there is no change in transition frequency of this molecule, and hence the absorption remains the same. However, if the molecule relaxes to a different ground state because of a photochemical or nonphotochemical transformation, a spectral hole appears in the absorption spectrum and this process is called spectral hole burning (SHB). If the hole fills up as soon as the laser is turned off, the hole is called a transient hole, and if it persistently remains as long as low temperature is maintained, the hole is called a persistent hole. While photochemical hole burning (PHB) is due to light-induced chemical reactions such as tautomerization, isomerization, or bond breaking,

non-photochemical hole burning is due to the rearrangement of the local environment around the excited molecule, resulting in a change in transition frequencies. As the HB is the central tool employed for the research studies in this dissertation, its types and mechanism are separately discussed below.

Four conditions are generally required to observe the spectral hole. First, the absorption spectrum must be inhomogeneously broadened. Second, a transition-frequency change mechanism must exist upon photo excitation. Third, the pump source must have a narrower bandwidth than the homogeneous linewidth. Fourth, the hole refilling process must be slower than the burning process, so HB experiments are performed at low temperature below 130 K.[33,52]

1.2.3.1 Mechanism of HB

Hayes and Small, for the first time in 1978, proposed a mechanism based on a static distribution of extrinsic two level systems (TLS_{ext}), coupled to an impurity, to explain the transition frequency change in persistent nonphotochemical hole burning.[60] A schematic of TLS_{ext} is depicted in Figure 1-7, where the superscripts g and e represent the ground and excited states of the chromophore (impurity). Initially, the molecule is trapped in the left well (g) of the bistable configuration (TLS_{ext}). Upon electronic excitation of the molecule by the laser frequency (ω_b) in the left well, tunneling takes place in the excited state (e), and finally it relaxes back to the ground state in the right well and emits a photon of frequency ω_f, different than ω_B. At low temperature, the barrier in the ground states is higher than the thermal energy, so the chromophore will be trapped in this new configuration, resulting in a hole formation in the post-burn absorption spectrum along with a blue-shifted anti-hole. Note that the blue-shifted anti-hole is not always the general case (*vide infra*).

Later, optical dephasing studies[61] showed that a static distribution model alone (TLS_{ext}) is not enough to explain NPHB, so two types of TLS *viz* intrinsic (TLS_{int}) and extrinsic (TLS_{ext}) were proposed. TLS_{int} of the host are intimately associated with the excess free volume of the glasses[62] and were purposed to be responsible for the dynamic features of the ZPH, such as its width and optical dephasing properties. On the other hand, TLS_{ext} are closely associated with the impurity molecules and their inner shell of solvent molecules, which are responsible for the frequency change in hole burning. Thus, the optical excitation of the chromophores triggers the

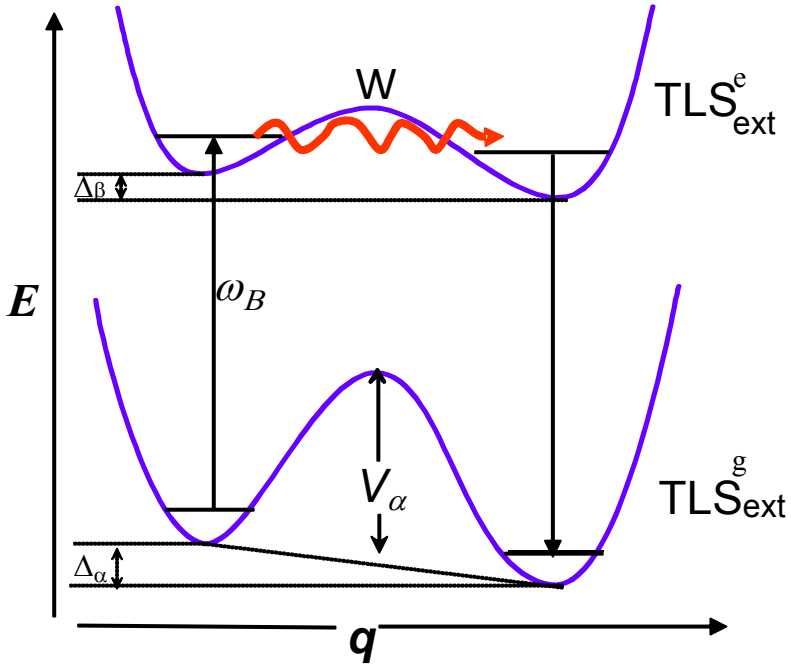

Figure 1-6 Schematic of the NPHB mechanism.[63,64] Extrinsic TLS with ground (g) and excited electronic states, labeling as g and e, respectively, of a pigment. Δ_α and Δ_β are the double well asymmetry parameters in the ground and excited state, respectively. *q* is the intermolecular coordinate, and ω_B is the burn frequency.

rearrangement of the host environment in the outer shell. This process initiates the phonon-assisted tunneling, leading to the hole formation. Therefore, phonon-assisted tunneling in the excited state of TLS_{ext} is the rate-determining step for hole formation. In Shu-small mechanism[62] for NPHB, a sequence of tunneling events begins in TLS_{int} of the outer shell, and terminates in TLS_{ext} of the inner shell. This final step is depicted in the Figure 1-6. The appearance of red-shifted anti-holes can be explained with the help of extrinsic multiple level system (MLS_{ext}) (Figure not shown for brevity).

Figure 1-7 depicts the hole formation in a typical guest-host system. If a narrow line width laser of frequency ω_B is used to selectively excite a subset of chromophores of the inhomogeneously broadened absorption spectrum, the molecules are excited resonantly via their ZPL. Once the molecule relaxes to a different ground state, a sharp ZPL appears in the post-burn absorption spectrum. Also, as the ZPL is accompanied by a PSB, the ZPH is accompanied by a phonon sideband hole (PSBH) on the higher energy side of the ZPH. At the same time, the laser frequency burns non-resonantly PSBs of other molecules lying at lower frequencies than ω_B. These phononic excitations, after relaxation, result in the formation of a pseudo-PSBH in the spectrum at a lower frequency than ω_B. In addition to phononic excitations, vibronic excitations are possible. These vibronic excitations rapidly relax to the zero vibrational level in their excitonically excited states, resulting in the formation of vibronic satellite holes at a frequencies of $\omega_A = \omega_B - \omega_v$, and/or at $\omega_C = \omega_B + \omega_v$ where ω_v is the vibrational frequency. The depth of vibronic satellite hole at ω_C is related to the depth at ω_B via respective Frank-Condon factor.[65] Note that the vibrational frequencies (ω_v) at lower and higher energy sides in general do not have to be identical. Note that, like in ZPHs, satellite holes are also accompanied by a PSBH and

pseudo-PSBH at higher and lower energy sites of the satellite holes, respectively. The real PSBH is hardly visible due to the interference by anti-holes.

The holes can be easily revealed by taking the difference of absorption spectra with (post-burn) and without (preburn) the laser-on, the difference spectrum is shown in the lower frame of Figure 1-7. ZPH width (Γ_{hole}), in the absence of all broadening mechanisms (fluence broadening, dephasing, and spectral diffusion), is the convolution of laser lineshape with the hole in both burning and detecting steps, i.e. $L_{hole} = L_{ZPL} \otimes L_B \otimes L_{ZPL} \otimes L_D$, where L_{ZPL}, L_B, and L_D are the lineshapes of the ZPL, burn laser, and detecting laser, respectively. If the hole is burned and detected with a narrow laser, $\Gamma_B = \Gamma_D << \Gamma_{hom}$, Γ_B and Γ_D become a delta function and $L_{hole} = 2\Gamma_{hom}$.

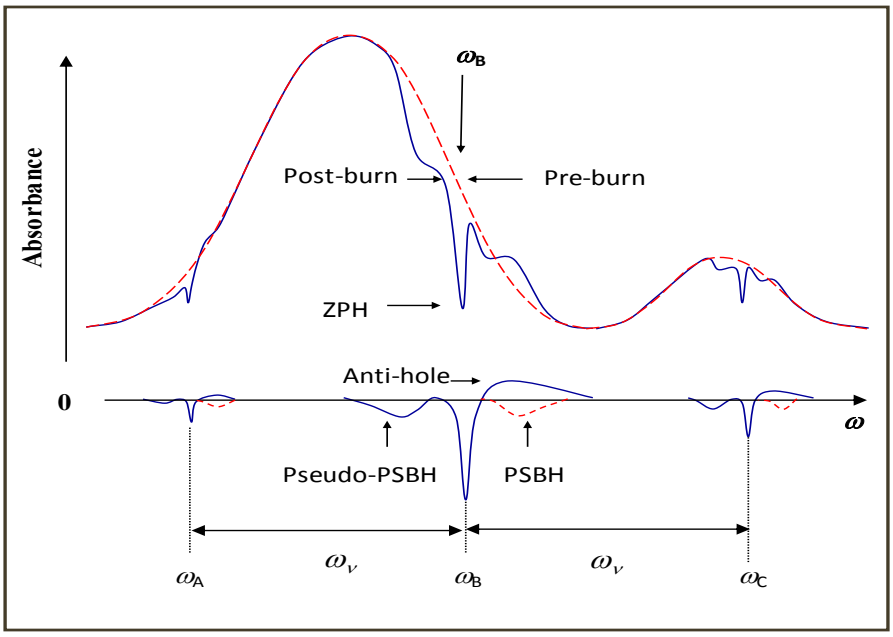

Figure 1-7 Nonphotochemical spectral hole-burning.[65] In the top panel, the dashed (red) and the solid (blue) lines represent the pre-burn and the post-burn absorption spectra, respectively. In the bottom panel is shown the difference spectrum (post-burn minus pre-burn absorption spectra). See text for details.

The second type of hole burning is the transient (triplet bottleneck) HB. The reason for the transient hole is the possibility of pumping some impurity molecules into long-lived metastable state via intersystem crossing from the singlet excited state. This leads to the depletion of ground state population, and hence the appearance of a hole in the absorption spectrum. The triplet state lifetime corresponds to the depletion time of ground state population.[66,67] As the transient hole is due to the short-lived state, the transient-absorption spectrum is measured while continuously exciting the sample.

1.3. Excitation energy transfer and charge separation mechanism

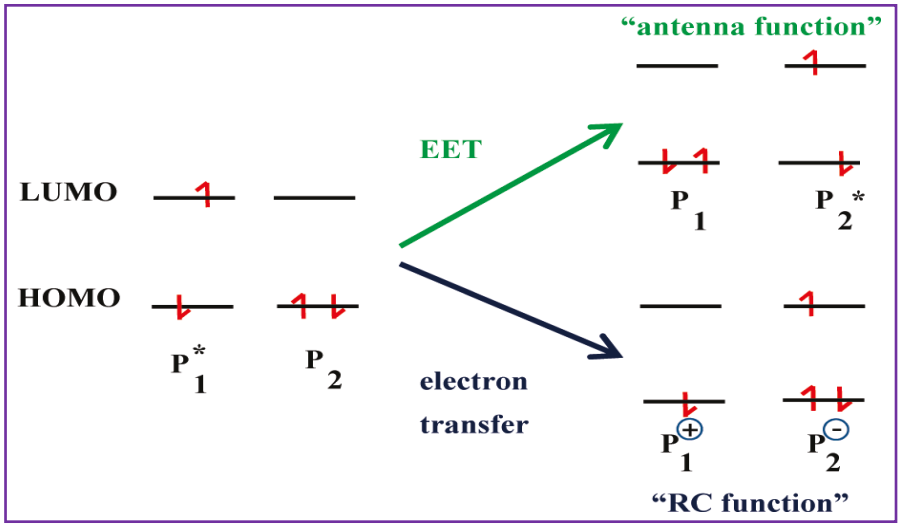

Figure 1-8 Schematic of the electronic coupling between the two pigments P_1 and P_2, giving rise to either EET or electron transfer from P^*_1 to P_2.[1]

As discussed in section 1.2, it is evident that the photosynthetic complexes perform, as shown in Figure 1-8, EET ("antenna function") and electron transport ("RC function") events within the networks of interacting pigments.[1] These pigment-protein interactions include: electrostatic interaction with nearby charged amino acids[68,69] and backbones, H-bonding,[70,71],

axial ligation of the central Mg[72] and distortion of the macrocycle[73]. According to the nature of these interactions (couplings), an appropriate theory needs to be chosen to properly describe the EET or electron transport events.[74,75] These interactions are responsible for the static shift of the site energies. Further, there is also dynamic regulation of the site energy because of the coupling of the electronic transition with the protein vibrations.[76,77] In order to study the energy transfer mechanism, an accurate estimate of the pigment site energy and strength of coupling must be made. In photosynthetic proteins, chromophores are so coupled that the electronic transition is delocalized over multiple chromophores leading to the formation of delocalized/mixed states called *excitonic states*. The excited state Hamiltonian for such systems is defined by[78]:

$$H = \sum_{n}(\varepsilon_n + d_n)|n\rangle\langle n| + \sum_{n,m} V_{nm}|n\rangle\langle m| \qquad (1\text{-}8)$$

where while $|n\rangle$ and $|m\rangle$ denote the localized monomer states, n and m refer to the number of pigments. ε_n is the average transition energy of monomer energy and d_n is the offset energy due to diagonal site excitation energy disorder. The symmetrical matrix H is of $n \times n$ dimension with the site energies in diagonal elements and the coupling $V_{n,m}$ in off diagonal elements. The excitonic energy (E_α) and wavefunction $|\alpha\rangle$ are then obtained after diagonalzing the matrix,

$$|\alpha\rangle = \sum_{n} c_n^{(\alpha)} \, |n\rangle \; . \qquad (1\text{-}9)$$

Since overlap is neglected, $\sum_n \left|c_n^{(\alpha)}\right|^2 = 1$. The excitonic transition dipoles can be calculated as:

$$\vec{\mu}_\alpha = \sum_{n} c_n^{(\alpha)} \; \vec{\mu}_n \qquad (1\text{-}10)$$

where $\vec{\mu}_n$ is the transition dipole of monomer pigment n. The absorption spectrum of the α^{th} exciton state, neglecting the phonons and intramolecular vibrations, is given by:

$$d_{\alpha}(\omega) = \left\langle |\vec{\mu}_{\alpha}|^2 \, \delta(\omega - \omega_{\alpha 0}) \right\rangle_{\text{dis}} \tag{1-11}$$

where $\omega_{\alpha 0}$ is the energy of the α^{th} exciton state and $\langle ... \rangle_{dis}$ denotes an average over disorder in site energies.[78] The net absorption spectrum is given as the sum over the absorption for all excitonic states after convolution with the appropriate single-site absorption spectra. The oscillator strength of each pigment for each excitonic band, also called as occupation number, is determined by $|c_{\alpha n}|^2$.[78]

Depending upon the extent of electronic coupling (V) between the donor and acceptor in photosynthetic complexes, the EET mechanism can be divided into two types – incoherent and coherent.[79,80] For weak coupling, $V/\Delta << 1$ (where Δ is the disorder or inhomogeneous broadening), and the EET is considered as an incoherent hopping process between the localized donor and acceptor. Such processes can be modeled with Förster[81] and Dexter[82] theories. For the strong coupling, $V/\Delta >> 1$, the initial excited state is delocalized and the process is viewed as a wave-like coherent process.[83]

Förster resonance energy transfer applies when the excitonic coupling *(V)* between two pigments is small compared to the difference of their site energies. This requires the large spatial separation of two pigments and localization of excitation energy on the individual pigments. Under this condition, V can be described using point-dipole approximation as:[84,85,86]

$$V_{12} = V_{21} = \frac{1}{4\pi\varepsilon_0\varepsilon_r}\left[\frac{\vec{\mu}_1 \cdot \vec{\mu}_2}{R^3_{12}} - \frac{3(\vec{\mu}_1 \cdot \vec{R}_{12})(\vec{\mu}_2 \cdot \vec{R}_{12})}{R^5_{12}}\right], \tag{1-12}$$

where μ_1 and μ_2 are the optical transition dipoles of pigments 1 and 2 and R is the distance between their centers. The dielectric constant ε_r accounts for the effects from the protein environment. The sign of V_{nm} (coupling matrix) depends on the relative orientation of the transition dipoles. Also, the transition energies for the upper (U) and lower (L) excitonic components in a dimer are given by:

$$\lambda_{L/U} = \frac{\varepsilon_1 + \varepsilon_2 \pm \sqrt{(\varepsilon_1 - \varepsilon_2)^2 + 4V_{12}{}^2}}{2} \tag{1-13}$$

where ε_1 and ε_2 are the site energies (transition frequencies) of the pigments in the absence of coupling. For the weak coupling case, the intra- and inter-molecular relaxation processes occur faster than EET, so the transfer rate constant ($k_{1\to2}$) is given by Fermi's Golden Rule as:

$$k_{1\to2} = \frac{4\pi^2}{h}\left|V_{1,2}\right|^2 \rho(E), \tag{1-14}$$

where $\rho(E)$ is called Franck-Condon (FC) weighted density of states, which is related to the energy matching of the energy levels of the donor and acceptor. The integral $\rho(E)$, encompassing all parameters related to vibrational states, is given by:

$$\rho(E) = \int_{E=0}^{\infty} dE G_D(E) G_A(E), \tag{1-15}$$

where $G_D(E)$ and $G_A(E)$ are normalized line shape functions for donor and acceptor molecules, respectively.

As $\rho(E)$ and $V_{1,2}$ are related to the absorption $\varepsilon_A(\omega)$ of the acceptor and fluorescence $f_D(\omega)$ of the donor, the Förster equation can be written as:[1]

$$k_{1\to2} = \frac{9\kappa^2 c^4 \phi_D}{8\pi n^4 \tau_D R^6} \int_{\omega} \varepsilon_A(\omega) f_D(\omega) \frac{d\omega}{\omega^4} \equiv \frac{3}{2}\frac{\kappa^2}{\tau_D}\left(\frac{R_0}{R}\right)^6, \tag{1-16}$$

where R_0 is the characteristic Förster radius (4 – 10 nm), which is the distance at which EET is 50% efficient, n is the refractive index, τ_D is the fluorescence lifetime, and ϕ_D is the quantum yield of the donor molecule. $\kappa^2 = (\cos\alpha - 3\cos\beta_1\cos\beta_2)^2$ is the orientation factor, where α is the angle between μ_1 and μ_2, and β_1 and β_2 are the angles between μ_1 and R_{12}, and μ_2 and R_{12}, respectively. Depending on the orientation, κ ranges from -2 to 2 and is 2/3 for randomly oriented chromophores.

In the case of strong coupling, for closely spaced chromophores (donor-acceptor distance < 1 nm), electronic wavefunction overlap strongly and EET takes place through an exchange mechanism, called Dexter theory. In the Förster model, EET is possible between pigments of the same spin, whereas Dexter does not have any spin restriction and permits EET from triplet state to a pigment in the ground singlet state. Therefore, quenching of Chl^T by carotenoids during photoprotection requires a Dexter (through bond) mechanism.[75,87,88]

In most of the light harvesting complexes, the pigments are densely packed and the excitonic coupling between them is very strong. The excitation is delocalized over multiple pigments simultaneously and the overall wavefunction can be viewed as the coherent superposition of locally excited states. Such coherent transfer exists when the energy transfer time is very fast compared to inter- and intra-molecular relaxation time, so that excited states do not have time to go out of phase so quickly.[1,89] In such a case, the relaxation of delocalized excitation states can be described by several theories – one widely used is Redfield relaxation theory.[77,90,91] In this theory, the nuclear relaxation is considered to be very fast compared to the energy transfer between different exciton states and a single phonon is considered in the exciton –nuclear interaction. However, this limitation breaks down in modified Redfield theories[92,93,94,95] where the nuclei relax into different equilibrium states n the strong exciton-vibrational coupling

conditions. Our group is in the progress of utilizing Redfield theory for the excitonic calculation of our low-*T* absorption and HB spectra.

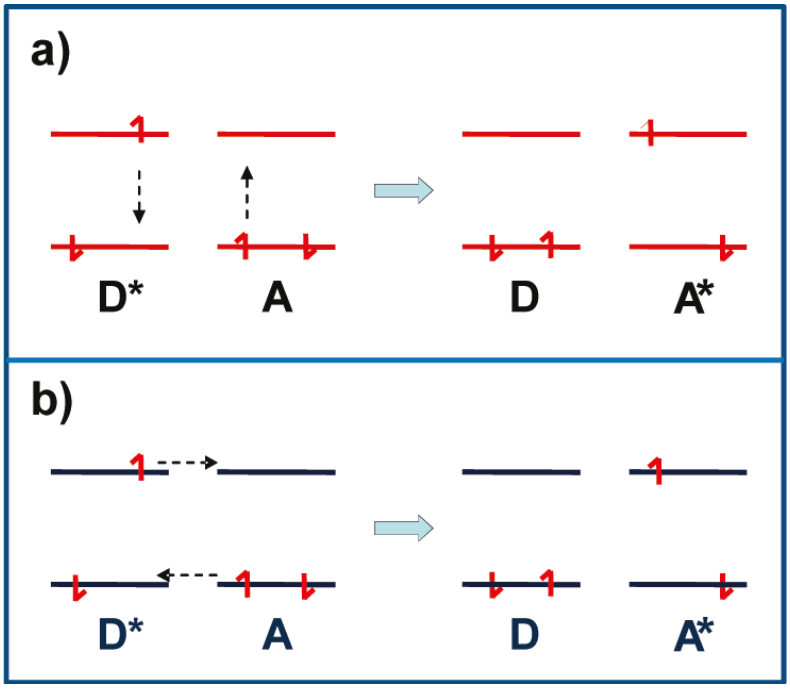

Figure 1-9 Schematic showing the mechanism of EET: a) Columbic mechanism, as suggested by Förster, and b) electron exchange mechanism, as suggested by Dexter.

The rate of electron transfer between donor and acceptor can be expressed as semi-classic expression as:[96,97]

$$k_{ET} = \frac{4\pi^2 H_{D-A}^2}{h\sqrt{4\pi\lambda k_B T}} \exp\left[-(\Delta G^0 + \lambda)^2 / 4\lambda k_B T\right], \qquad (1\text{-}17)$$

where k_B is the Boltzmann constant, h is Planck's constant and T is the temperature in Kelvin. λ is the reorganization energy which is defined as the energy required to distort the equilibrium geometry of donor state to acceptor state equilibrium geometry without electron transfer i.e. the energy required to reorient the nuclear components from the reactant to transition state. It has

been proposed that the protein matrix provides a rigid scaffold for the redox centers and thus reduces the reorganizational energy.[98] In general, λ increases with increase in polarity of the environment of D-A centers.

$H_{D\text{-}A}$ is the electronic coupling strength between D and A pairs and $H_{D\text{-}A}^2$ is the probability of electron tunneling. In the square potential barrier approximation, $H_{D\text{-}A}^2$ decreases exponentially with the distance ($r_{D\text{-}A}$) between donor and acceptor molecules as[99]

$$H_{D-A} = H^{\circ}_{D-A} \exp\left[-\beta(r_{D-A} - r_{\circ})\right] \qquad (1\text{-}18)$$

The β term is a coefficient tht describes the exponential decay of the electronic coupling with respect to distance (i.e. the barrier height).

ΔG° is the standard Gibbs free energy change, i.e. free energy difference between D-A states, and is related to the redox potential difference between donor and acceptor pairs as,

$$\Delta G^{o} = F(V^{ox} - V^{red}) + C, \qquad (1\text{-}19)$$

where F is the Faraday constant and C is the coulomb attractive energy.[100] The ET increases with $-\Delta G°$ and reaches maximum at $-\Delta G° = \lambda$ (called activation less transfer) and the rate decreases for $-\Delta G° > \lambda$ (called inverted regime). The classical Marcus theory is found to be very useful to explain the nature of biological electron transfer.

As my research work is primarily focused on experimental aspects, I hope the aforementioned theoretical discussions will be enough to understand the basic aspects of hole-burning spectroscopy and energy/electron transfer dynamics in photosynthetic complexes.

References

(1) Jankowiak, R.; Reppert, M.; Zazubovich, V.; Pieper, J.; Reinot, T. *Chem. Rev*. **2011,** *111,* 4546.

(2) Fromme, P. In *Photosynthetic Protein Complexes: A Structural Approach*, Wiley-VCH Verlag GmbH&Co. KGaA: Germany, 2008; p 1.

(3) Sauer, K. In *Bioenergetics of Photosynthesis* (ed. Govindjee), New York: Academic Press, 1975; p 115.

(4) Knox, R. S. In *Primary Process of Photosynthesis* (ed. J. Barber), Amsterdam: Elsevier, 1977; p 55.

(5) Hu, X.; Ritz, T.; Damjanovic, A.; Autenrieth, F.; Schulten, K. *Q. Rev. Biophys.* **2002**, *35*, 1.

(6) Hu, X.; Schulten, K. *Phys. Today* **1997**, *50*, 28.

(7) Deisenhofer, J.; Epp, O.; Sinning, I.; Michel, H. *J. Mol. Biol.* **1995**, *246*, 429.

(8) Deisenhofer, J.; Epp, O.; Miki, K.; Huber, R.; Michel, H. *Nature (London)* **1986**, *318*, 618.

(9) Deisenhofer, J.; Michel, H. *New Compr. Biochem.* **1992**, *23*, 103.

(10) Ermler, U.; Fritzsch, G.; Buchanan, S. K.; Michel, H. *Structure (London)* **1994**, *2*, 925.

(11) Barnes, C. R. *Bot. Gaz*. **1893**, *18*, 403.

(12) van Niel, C. B. *Arch. Mikrobiol* **1931**, *3*, 1.

(13) Clayton, R.; Sistrom, W. (eds.) In *The Photosynthetic Bacteria*, New York: Planum Press, 1978; p 1.

(14) Nelson, N.; Yocum, C. F. *Annu. Rev. Plant Biol*. **2006**, *57*, 521.

(15) Taiz, L.; Zeiger, E. *Plant Physiology*, 5th ed.; Sinauer Associates, Inc.,Sunderland, Massachusetts, 2010.

(16) Barber, J. *Quart. Rev. Biophys*. **2003**, *36*, 71.

(17) Liu, Z.; Yan, H.; Wang, K.; Kuang, T.; Zhang, J.; Gui, L.; An, X.; Chang, W. *Nature* **2004**, *428*, 287.

(18) van Amerongen, H.; van Grondelle, R. *J. Phys. Chem. B* **2001,** *105,* 604.

(19) Nield, J.; Barber, J. In *Photosynthesis. Energy from the Sun: 14th International Congress on Photosynthesis*(ed .J.F. Allen, E. Gantt, J.H. Golbeck, and B. Osmond), Springer, , 2008; p 357.

(20) Müller, M. G.; Lambrev, P.; Reus, M.; Wientijes, E; Croce, R.; Holzwarth, A. R. *ChemPhysChem*, **2010**, *11*, 1289.

(21) Pan, X.; Li, M; Wan, T.; Wang, L.; Jia, C.; Hou, Z.; Zhao, X.; Zhang, J.; Chang, W. *Nature* **2011**, *18*, 309.

(22) Jordan, P.; Fromme,P.; Witt, H. T.; Klukas, O.; Saenger, W.; Krauβ, N. *Nature* **2001**, *411*, 909.

(23) Krausz, E.; Hughes. J. L.; Smith, P.; Pace, R.; Årsköld, S. P. *Photochem. Photobiol. Sci.* **2005**, *4*, 744.

(24) Hankamer,B.; Morris, E. P.; Nield, J.; Gerle, C.; Barber, J. *J. Struct. Biol*. **2001**, *135*, 262.

(25) Guskov, A.; Kern, J.; Gabdulkhakov, A.; Broser, M.; Zouni, A.; Saenger,W. *Nat. Struct. Mol.Biol.* **2009**, *16*, 334.

(26) Loll, B.; Kern, J.; Saenger, W.; Zouni, A.; Biesiadka, J. *Nature* (London, U. K.) **2005**, *438*, 1040.

(27) Umena, Y.; Kawakami, K.; Shen, J.-R.; Kamiya, N. *Nature* **2011**, *473*, 55.

(28) Grotjohann, I.; Jolley, C.; Fromme, P. *Phys. Chem. Chem. Phys* **2004** , *6,*4743.

(29) Cox, N.; Hughes, J. L.; Steffen, R.; Smith, P. J.; Rutherford, A.W.; Pace, R. J.; Krausz, E. *J. Phys. Chem. B* **2009,** *113,* 12364.

(30) Levine, Ira N. *Quantum Chemistry*, 5th ed; Prentice Hall: new Jersely, **2000**; p 96.

(31) Ingle, J. D.; Crouch, S.R. In *Spectrochemical Analysis;* Prentice-Hall: New Jersey, 1988; p 209.

(32) Moerner, W. E. *Topics in current physics, Persistent spectral hole burning: Science and applications*; Springer-Verlag: New York, 1987; p 1.

(33) Rebane, K. K.; Rebane, L. A. In *Persistent Spectral Hole Burning: Science and Applications*; Moerner, W. E. Ed.; Springer-Verlag: New York, 1998; Chapter 2.

(34) Personov, R. I. In *Spectroscopy and Excitation Dynamics of Condensed Molecular Systems*; Agranovich, V. M., Hochstrasser, R. M., Eds.; Elsevier Science Ltd: Amsterdam, 1983; p 1.
(35) Osadko, I. S. In *Advances in Polymer Science*; Dusek, K., Ed.; Springer-Verlag: Berlin 1994; p 123.
(36) Hayes, J. M.; Lyle, P. A.; Small, G. J. *J. Phys. Chem.* **1994**, *98,* 7337.
(37) Flecher, G.; Friedrich, J.; *Chem. Phys. Lett.* **1977**, *50,* 32.
(38) Kikas, J. *Chem. Phys. Lett*. **1978**, *57*, 511.
(39) Koedijk, J. M. A.; Wannemacher, R.; Silbey, R. J.; Völker, S. *J. Phys. Chem.* **1996**, *100*, 19945.
(40) Jankowiak, R.; Small, G. J. In *Disorder Effects on Relaxation Processes*; Blumen, A., Richard, R., Eds.; Springer-Verlag: Berlin, 1994; p 425.
(41) Rebane, K. K. *Impurity Spectra of Solids*; Plenum: New York, 1970; p 1.
(42) Jankowiak, R.; Hayes, J. M.; Small, G. J. *Chem. Rev* **1993**, *93*, 1471.
(43) Personov, R. I. In *Spectroscopy and Excitation Dynamics of Condensed Molecular Systems*; Agranovich, V. M., Hochstrasser, R. M., Eds.; Elsevier Science Ltd: Amsterdam, 1983; p 1.
(44) Völker, S. In *Relaxation Processes in Molecular Excited States*; Fünfschilling, J., Ed.; Kluwer Academic Publishers: Dordrecht, 1989; p 113.
(45) Stoneham, A. M. *Rev. Mod. Phys.* **1969,** *41*, 82.
(46) Reddy, N. R. S.; Lyle, P. A.; Small, G. J. *Photosynth. Res*. **1992**, *31*, 169.
(47) Jankowiak, R.; Richert, R.; Bässler, H. *J. Phys. Chem*. **1985**, *89*, 4569.
(48) Gooijer, C., Ariese, F. and Hofstraat, J. W. (Eds): *Shpol'skii Spectroscopy and Other Site Selection Methods: Applications in Environmental Analysis, Bioanalytical Chemistry, and Chemical Physics*, A John Wiley & Son, Inc., New York, Chichester, Weinheim, Brisbane, Singapore, Toronto, 2000; p 1.
(49) Sild, O., Haller, K., (eds): *Zero-Phonon Lines and Spectral Hole Burning in Spectroscopy and Photochemistry*, Springer-Verlag, Berlin, Heidelberg, New York, London, Paris, Tokyo, 1988; p 1.

(50) Maier, H.; Kharlamov, B.; Haarer, D. In *Tunneling Systems in Amorphous and Crystalline Solids*, Esquinazi (Ed.), Springer, Berlin, Heidelberg, New York Barcelona, Budapest, Hong Kong, London, Milan, Paris, Singapore, Tokyo, 1998; p 317.

(51) Creemers, T. M. H.; Völker, S.; In *Shpol'skii Spectroscopy and Other Site Selection Methods: Applications in Environmental Analysis, Bioanalytical Chemistry, and Chemical Physics*, Gooijer, C., Ariese, F. and Hofstraat, J. W. (Eds)A John Wiley & Son, Inc., New York, Chichester, Weinheim, Brisbane, Singapore, Toronto, 2000, Chapter 9; p 273.

(52) Jankowiak, R. In *Shpol'skii Spectroscopy and Other Site Selection Methods: Applications in Environmental Analysis, Bioanalytical Chemistry, and Chemical Physics*, Gooijer, C., Ariese, F. and Hofstraat, J. W. (Eds)A John Wiley & Son, Inc., New York, Chichester, Weinheim, Brisbane, Singapore, Toronto, 2000, Chapter 8; p 235.

(53) Basche, Th.; Moerner, W. E.; Orrit, M.; Wild, U. (Eds): *Single Molecule Optical Detection, Imaging and Spectroscopy*, VCH, Weinheim, New York, Basel, Cambrigde, Tokyo, 1996; p 1.

(54) Basche, Th.; Orrit, M.; Rigler, R. (Eds): *Single Molecule Spectroscopy - Nobel Conference Lectures*, VCH, Weinheim, New York, Basel, Cambrigde, Tokyo, 1996.

(55) Mukamel, S., Principles of Nonlinear Optical Spectroscopy, New York: Oxford University Press, 1995, Chapter 9 – 11; p 261.

(56) Hesselink, W. H.; Wiersma, D. A. In *Spectroscopy and Excitation dynamics of Condensed Molecular Systems*, Agranivich, V. M. and Hochstrasser, R. M. (Eds), North-Holland, Amsterdam, 1983; p 249.

(57) Narasimhan, L. R.; Littau, K. A.; Pack, D. W.; Bai, Y. S.; Elschner, A.; Fayer, M. D. *Chem. Rev.*, **1990**, *90*, 439.

(58) Koedijk, J. M. A., Wannemacher, R., Silbey, R. J. and Völker, S., *J. Phys. Chem.* **1996**, *100*, 19945.

(59) Purchase, R.; Völker, S. *Photosynth. Res.* **2009**, *101*, 245.

(60) Hayes, J. M.; Small, G. J. *Chem. Phys.* **1978**, *27*, 151.

(61) Hayes, J. M., Stout, R. P., Small, G. J. *J. Phys. Chem.*, **1981**, *74*, 4266.

(62) Shu, L.; Small, G. J. *Chem. Phys* **1990**, *141*, 447.

(63) Reinot, T.; Zazubovich, W.; Hayes, J. M.; Small, G. J. *J. Phys. Chem. B.*, **2001**, *105*, 5083.

(64) Shu, L.; Small, G.J. *J. Opt. Soc. Am. B* **1992**, *9*, 724.

(65) Dang, N.C.; Ph. D. Thesis, Iowa state University, 2005.

(66) Szabo, A.; *Phys. Rev. Lett.* **1970**, *25*, 924.

(67) Erickson, L. E. *Phys. Rev. B.* **1975**, *11*, 4512.

(68) Eccles, J.; Honig, B. *Proc. Natl. Acad. Sci. USA* **1983,** *80*, 4959.

(69) Diner, B. A.; Schlodder, E.; Nixon P. J.; Coleman W. J.; Rappaport, F.; Lavergne, J.; Vermaas, W.F. J.; Chisholm, D. A. *Biochemistry* **2001,** *40,* 9265.

(70) Fowler, G. J.; Visschers, R. W.; Grief, G. G.; van Grondelle R.; Hunter, C. N. *Nature* **199**2, *355,* 848.

(71) Witt, H.; Schlodder, E.; Teutloff , C.; Niklas, J.; Bordignon, E.; Carbonera, D.; Kohler, S.; Labahn, A.; Lubitz, W. *Biochemistry* **2002,** *41*, 8557.

(72) Lin, S.; Jaschke, P. R.; Wang, H.; Paddock, M.; Tufts, A.; Allen, J. P.; Rosell, F. I.; Mauk, A. G.; Woodbury, N. W.; Beatty, J. T. *Proc. Natl. Acad. Sci. U. S. A.* **2009**, *106*, 8537.

(73) Lapouge, K.; Naveke, A.; Gall, A.; Ivancich, A.; Seguin, J; Scheer, H.; Sturgis, J. N.; Mattioli, T. A.; Robert, B. *Biochemistry* **1999,** *38,* 11115.

(74) van Amerongen, H.; Valkunas, L.; van Grondelle, R. *Photosynthetic Excitons*; World Scientific: Singapore, 2000; p 168.

(75) Shreve, A. P.; Trautman, J. K.; Frank, H. A.; Owens, T. G.; Albrecht, A. C. *Biochim. Biophys. Acta.* **1991**, *1058*, 280.

(76) Novoderezhkin, V.,I.; van Grondelle, R. *J Phys Chem B* **2002,** *106,* 6025.

(77) Yang, M.; Fleming, G. R. *Chem Phys* **2002**, *275,* 355.

(78) Reppert, M.; Acharya, K.; Neupane, B.; Jankowiak, R. *J. Phys. Chem. B* **2010**, *114*,11884.

(79) Rahman, T. S.; Knox, R. S.; Kenkre, V. M. *Chem. Phys*. **1979**, *44*, 197.

(80) Kühn, O.; Renger, T.; Voigt, J.; Pullerits, t.; Sundström, V. *Trends in Photochem. Photobiol*. **1997**, *4*, 213.

(81) Förster, T. *Ann. Phys. (Leipzig)* **1984**, *2*, 55

(82) Dexter, D. *J. Chem. Phys.* **1953**, *21*, 836

(83) Sunstrom, V.; Pullertis, T.; van Grondelle, R. *J. Phys. Chem. B* **1999**, *103*, 232.

(84) Renger, T. *Photosyn. Res.* **2009,** *102,* 471.

(85) Krueger, B. P.; Scholes, G. D.; Fleming, G. R. *J Phys Chem B* **1998,** *102*, 5378.

(86) Madjet, M. E.; Abdurahman, A.; Renger, T. *J Phys Chem B* **2006,** *110,*17268.

(87) Hu, X.; Ritz, T.; Damjanović, A.; Autenrieth, F.; Schulten, K. *Q. Rev. Biophys.* **2002**, *35*, 1.

(88) Blankenship, R. E. *Molecular Mechanisms of Photosynthesis*; Blackwell Science Ltd.: London, 2008; p 42.

(89) Renger, G. In *Bioenergetics*; Gräbner, P. Malazzio, G., Eds.; Birkhäuser Verlag: Basel, 1997; p 311.

(90) Redfield, A.G. *IBM J. Res. Dev.* **1957,** *1*, 19.

(91) Renger, T.; May, V.; Kühn, O. *Phys Rep* **2001** *343*, 138.

(92) Zhang, W.; Meier, T.; Chernyak, V.; Mukamel, S. *J.Chem. Phys.* **1998,***108*, 7763.

(93) Novoderezhkin, V.I.; Palacios, M.A.; van Amerongen, H.; van Grondelle R. *J. Phys. Chem. B* **2004,** *108*, 10363.

(94) Novoderezhkin, V.I.; Rutkauskas, D.; van Grondelle, R. *Biophys. J.* **2006,** *90*, 2890.

(95) Schröder, M.; Kleinekathöfer, U.; Schreiber, M. *J. Chem. Phys.* **2006,** *124*, 084903.

(96) Marcus, R. A.; Sutin, N. *Biochim. Biophys. Acta* **1985**, *811*, 265.

(97) Marcus, R. A. *Rev.Mod. Phys.* **1993**, *65*, 599.

(98) Stubbe, J.; Nocera, D. G.; Yee, C. S.; Chang, M. C. Y. *Chem. Rev.* **2003**, *103*, 2167.

(99) Hopfiled, J. J. *Proc. Natl. Acad. Sci. U.S.A.* **1974**, *71*, 3640.

(100) Fleming, G. R.; Martin, J. L.; Breton, J. *Nature* **1988**, *333*, 190.

Chapter 2 - On the Unusual Temperature Dependent Emission of the CP47 Antenna Protein Complex of Photosystem II

K. Acharya, B. Neupane, M. Reppert, X. Feng, and R. Jankowiak

Abstract

It is shown that the fluorescence origin band maximum (~695 nm) of the intact CP47 antenna protein complex of PSII from spinach does not shift in the temperature range of 5-77 K. However, emission shifts continuously to shorter wavelengths (~692 nm) if high fluence is used. and holeburning takes place. If permanent damage does not occur, this process is reversible by cycling the temperature. In contrast, the emission peaks previously observed near 685 nm and 691 nm are characteristic of destabilized complexes and cannot be eliminated by temperature cycling. We argue that the CP47 complex is extremely light sensitive at low temperatures and that its 695 nm emission band in the PSII core, in contrast to several literature reports, does not arise from excitations that are trapped on red-absorbing chlorophyll of the ~690 nm band, as 5 K emission of intact (non-aggregated) CP47 also peaks near 695 nm.

2.1 Introduction

Although Photosystem II (PSII) has been studied for decades, some aspects of the electronic structure and excitation energy transfer (EET) of PSII remain controversial. For example, even though many emission spectra at different temperatures from both the intact (oxygen evolving) and isolated reaction center (RC) and CP43 and CP47 inner antenna protein complexes of PSII from plants[1-15] and cyanobacteria[16-18] have been published, no coherent picture emerges when the published emission spectra of the above complexes are compared. This is in part due to the fact that complex biological systems are prone to photodamage and/or destabilization even at extremely low doses of photon density during the isolation and/or interrogation procedures. In this regard we showed recently[19] that the isolated (intact) CP47 antenna complex from PSII has a 5 K fluorescence emission maximum near 695 nm[19] and not, as previously reported, near 690-692 nm.[3,6,16] We have suggested that the previously measured 690-691 nm CP47 emission peak is a combination of emissions from the 695 nm emission of intact CP47 complexes with the lowest-energy state possessing very weak oscillator strength[19,20] and from the two trap emissions near 685 and 690 nm originating from photodamaged/destabilized complexes.[19,20] This interpretation is consistent with reports by Huyer et al.[8] (isolated CP47) and Komura et al.[12] (PSII core complexes) of multiple CP47 low-T emission bands in the 685 – 695 nm range resolved by time-domain spectroscopy. Note that only the 695 nm emission of CP47 is consistent with data obtained for more native (i.e. PSII core) complexes at 77 K.[9,11,13,18]

To shed more light into the emission of isolated CP47 complexes (the possibility of aggregation has been excluded) we measured fluorescence spectra at different temperatures and excitation wavelengths, as well as different levels of photobleaching of the lowest-energy state. We demonstrate that intact CP47 complexes have very different temperature dependent emission

in comparison with the previously published fluorescence spectra.[3] In particular, we show that the 695 nm emission peak of intact isolated CP47 does not shift significantly in the 5 – 77 K temperature range. This finding calls into question the previous interpretation[9,18] (used to explain spectroscopic data of CP47[21] and the PSII core.[9,11,13,18]) that the 77 K emission peak near 695 nm in the CP47-RC complex originates from a subset of CP47 pigment(s) (assigned to the 690 nm band) which are unable to transfer energy uphill to the RC, whereas the low temperature (5 K) CP47 emission peak near 690-691 nm originates from the entire distribution of lowest-energy

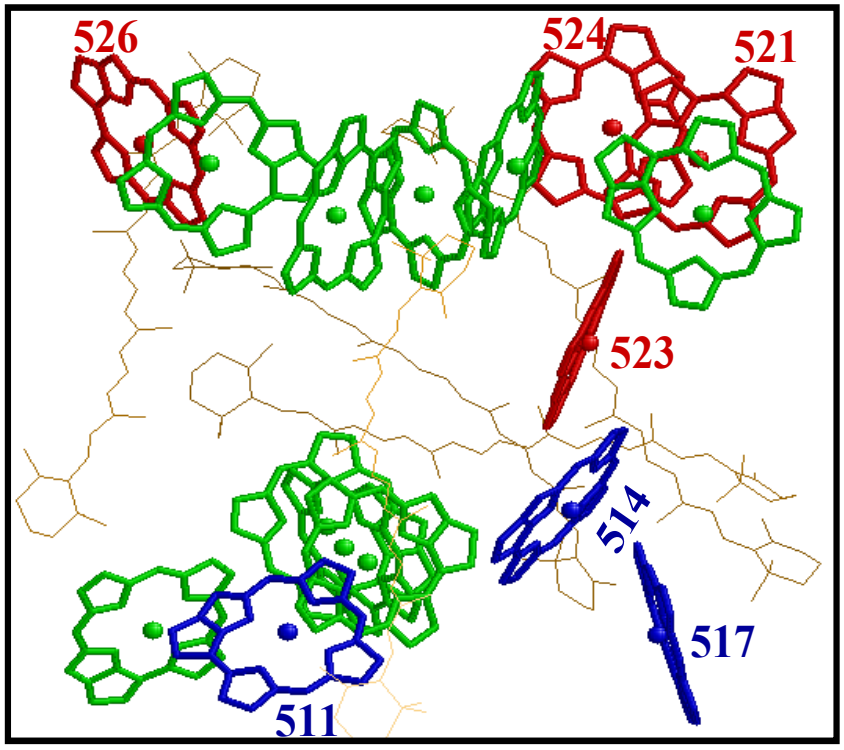

Figure 2-1 Arrangement of CP47 Chls and carotenes (in brown) on the stromal and lumenal side of the membrane. Chls 521, 523, 524 and 526 are shown in red. Chls 511, 514, and 517 are in blue. Remaining Chls are in green; the pigments are numbered as in.[22]

pigment states. In addition, we demonstrate that non-photochemical HB can produce a blue-shifted (reversible upon temperature annealing) contribution to the low temperature emission spectrum, which may help to explain some literature data. We argue that considerable reinterpretation of the low energy states and their emissive properties in this important antenna complex is warranted as only a proper understanding of CP47 emission will explain the long standing puzzle of PSII core emission and its temperature dependent profile,[9,11,13,18] where an unusual "red" shift of the PSII core fluorescence origin band with increasing temperature was observed. Figure 2-1 shows the arrangement of CP47 Chls and carotenes (in brown) on the stromal and lumenal side of the membrane.[22] Very recently, we have suggested that most likely Chl 523 (not Chl 526)[4] contributes strongly to the lowest-energy state, providing the low oscillator strength and specific excitonic interactions needed to fit the absorption and red-shifted (695 nm) emission spectra as well as the persistent hole-burning (HB) spectrum.[20]

2.2 Result and discussion

Figure 2-2 (frame A) shows typical temperature dependent emission spectra of the CP47 complex obtained from[3]. For comparison, Frames B and C show temperature dependent emission spectra for the destabilized and intact CP47 complexes, respectively, obtained recently in our laboratory. Note the 680.3 nm emission band (see frame B) was observed only in some preparations containing a small fraction of destabilized CP47 complexes in which energy transfer to the lowest- energy traps is disrupted. In all frames, at higher temperatures (i.e. above 100 K) the increase in temperature results not only in temperature broadening but also in a blue shift of the spectra due to the equilibrium of the excitation over the antenna pigments.

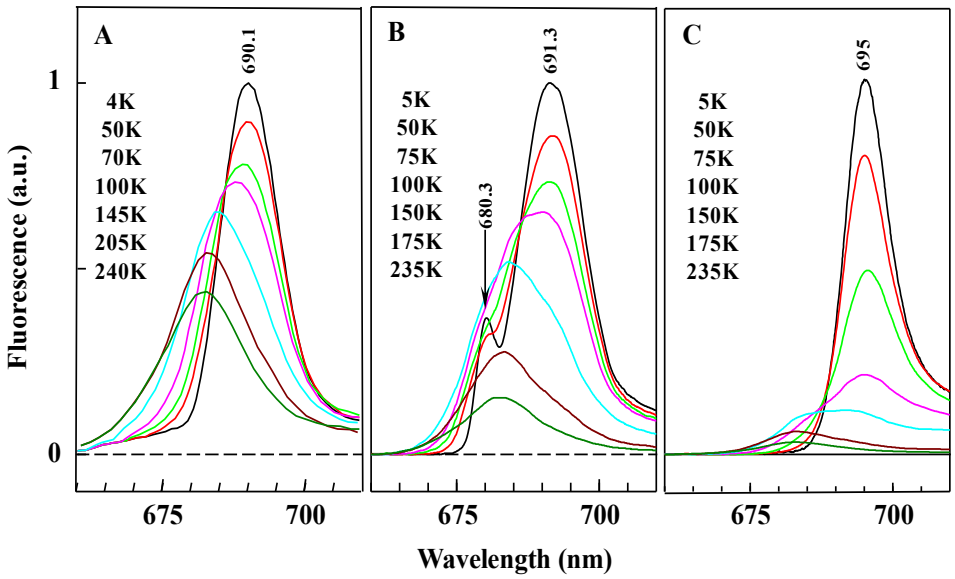

Figure 2-2 Temperature dependent emission spectra of various CP47 complexes. Frame A: digitized spectra as presented in.[3] Spectra shown in frames B and C represent spectra of destabilized and intact CP47 complexes (this work), respectively.

Interestingly, both the fluorescence maxima and bandwidths of the spectra shown in frame C (intact sample) are drastically different from those shown in frames A and B. The fluorescence maximum at 4 K obtained from[3] (Figure 2-2A; top spectrum) lies near 690 ± 1 nm with a full-width at half-maximum (*fwhm*) of ~12.5 nm. Similar spectra were reported in[6], while an even larger *fwhm* (~16.5 nm) was observed in[7]. Likewise, our 5 K emission spectrum for destabilized CP47 (frame B) peaks at 691.3 nm and has a *fwhm* of 13.3 nm. The above mentioned *fwhm* are by a factor of ~1.3-1.7 larger than that shown in frame C for intact CP47 which peaks at 694.8 nm and has a width of ~9.5 nm. In addition, as illustrated in Figure 2-3, the integrated (normalized) intensity of the fluorescence spectra from frames A, B, and C of Figure 2-2, plotted as black squares, red dots, and blue triangles, respectively, show very different behavior when plotted as a function of temperature.

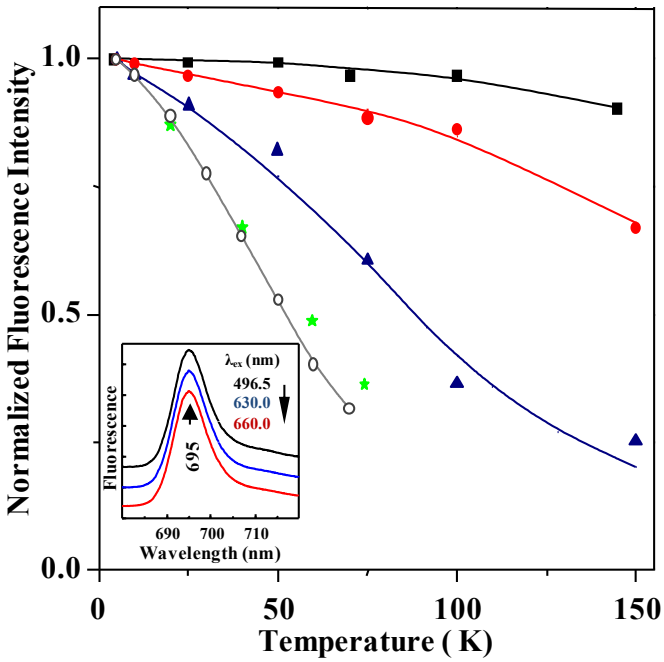

Figure 2-3 Normalized (integrated) fluorescence intensity of CP47 complexes shown in Figure 2-2 plotted as a function of temperature; black squares, red circles, and blue triangles represent data shown in Figure 2-2, frames A, B, and C, respectively. The inset shows fluorescence of intact CP47 at excitation wavelengths of 496.5 nm (top), 630.0 nm, and 660.0 nm (bottom curve). The green stars and open circles, shown for comparison, correspond to the normalized relative quantum yields of PS II core reported in[18] and[11], respectively.

The strong decrease of CP47 fluorescence as a function of temperature (particularly for the intact sample of Figure 2-2C and PSII core that must contain intact CP47) is most likely due to strong temperature dependent internal conversion. For comparison, the data points labeled by open circles show the integrated (normalized) fluorescence intensity for PSII core in the temperature range of 5 - 70 K taken from[11], while the green stars correspond to the normalized relative fluorescence quantum yields of the PS II core as reported in[18]. One must take some care in comparing the PSII and CP47 data: since all data sets are normalized to a value of unity close to 0 K, the values reported represent relative, not absolute, fluorescence yields; thus these data do not, for example, allow the determination of the absolute EET efficiency to the RC. Nonetheless, it is interesting to note that the relative yields of PSII core emission from[11,18] decrease even faster

than that of CP47. Although the presence of additional quenching processes in the PSII core cannot be excluded, this behavior suggests that in the intact PSII core complex, the fluorescence efficiency is determined by the rate of EET to the RC, rather than by competition with non-radiative processes. This in turn implies that the non-radiative decay processes which quench fluorescence in the isolated CP47 protein are not so fast as to quench EET to the RC in the intact PSII core complex (which would impair CP47 function as a light-harvester).

As seen in Figure 2-2C, the fluorescence origin band of the intact CP47 lies at ~695 nm, and its maximum does not shift significantly in the temperature range of 4-77 K. (A small shift in some samples from ~694.8 nm at 5 K to ~695.6 nm at 50 K is due to reversible HB as discussed below). The observation of the 695 nm emission band at 5 K in isolated CP47 complex is in contrast to 5 K spectra previously reported in the literature[3,6,7] (similar to those of frames A and B of Figure 2-2) and calls into question several previous interpretations of such experimental data.[9,11,13,18] For example, the puzzling observation in[18] of an unusual red-shift of CP47-RC fluorescence between 4 and 77 K (from 691 nm to 694 nm) led to the interpretation that, while emission at 5 K (691 nm) originated from all lowest-energy pigments in the CP47 subunit, the 694 nm 77 K emission peak was due only to pigments which are unable to transfer energy to the RC (leading to selective emission from red-absorbing Chls). The presence of 695 nm emission at 5 K from *isolated* CP47 complexes (for which EET to the RC is obviously impossible) indicates that this explanation (while feasible for the previously obtained data) is most likely incorrect since one should otherwise expect 691 nm emission at 5 K from the isolated complex as well. Similarly, since 685 nm emission at 77 K observed in previously studied samples, as shown in,[19] originates from destabilized CP47 complexes, we also reject the suggestion put forward in[11,18] that intact CP47 complex possesses a state (i.e. the 683/684 nm state) that slowly transfers

energy to the RC. This is consistent with our previous findings that intact CP47 complexes do not show a transient hole near 684 nm[19] which is, however, clearly observed in destabilized complexes.[21,23] Note that the emission maximum is independent of the excitation wavelength as shown in the inset of Figure 2-3. Thus we conclude that in the intact CP47 antenna, excitation energy is very efficiently transferred to the lowest-energy state at ~693 nm resulting in a narrow (*fwhm* ~9.5 nm) 695 nm emission band, and we see no reason to assume that in intact CP47 (residing in the intact PSII core complex) at ~5 K a considerable part of the absorbed energy cannot be used for charge separation as suggested in.[11,13,18] These findings emphasize that in order to elucidate the true EET dynamics in CP47 (and other photosynthetic complexes) the samples studied have to be free from contributions of partly destabilized/photodamaged complexes, especially when data are obtained in fluorescence and/or fluorescence excitation mode. This is because small subpopulations of disordered/photodamaged complexes with relatively large fluorescence quantum yield may strongly affect the composite emission signal.

Some of these effects become clearer when one considers emission originating from complexes with a modified (by HB) low-energy state, referred to in[19] as $A1_{mod}$. In[19] we showed that in the first approximation one can say that this is the lowest-energy state in CP47 in which the A1 state at 693 nm has been saturated, i.e., A1 ceases to be the lowest-energy state. In reality, of course, due to the continuous HB process (CP47 is quite sensitive to light and heat)[24] the lowest-energy state at 693 nm and the resulting fluorescence continually shift "blue" as a function of fluence (f). This is one reason why in some samples the emission origin band was slightly blue shifted. We hasten to add that the $A1_{mod}$ band can be eliminated by temperature cycling (re-creating the original A1 state) proving that no irreversible changes are introduced ($f < 4$ kJ/cm^2). It should be emphasized that these HB-induced shifts are distinct from the emission

peaks near 685 and 691 nm observed, for example in Figure 2-2A and 2-2B, due to destabilized complexes; these contributions (referred to as FT2 and FT1 in[19]) cannot be annealed by raising the temperature. The latter is consistent with[25] where the heterogeneity of CP47 was also revealed via observation of different fluorescence decay components. These authors suggested, in agreement with our recent HB and fluorescence studies,[19,20] that in destabilized CP47 samples the inter-chromophoric interactions must be disrupted and/or perturbed in different way(s) depending on the subpopulation of the CP47 complexes.

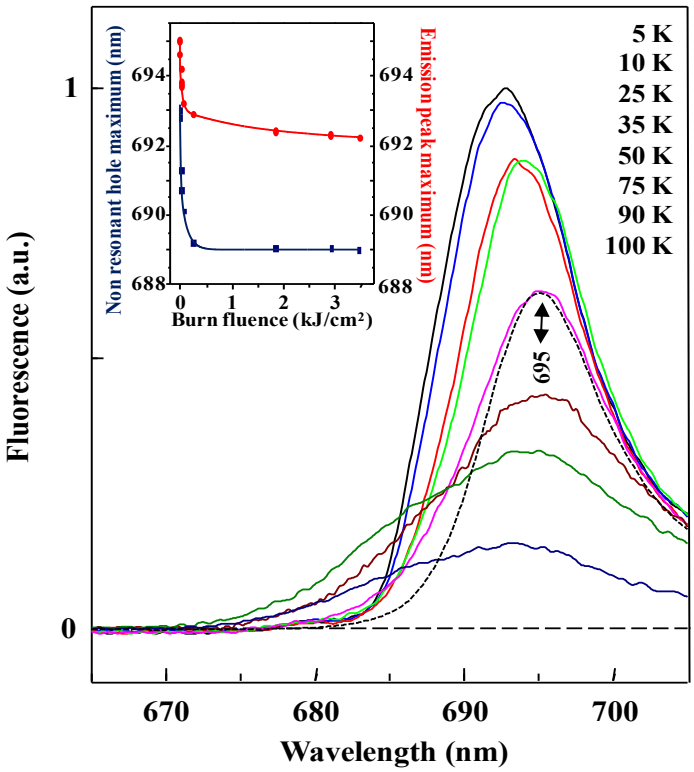

Figure 2-4 Temperature dependence of the fluorescence spectrum (top curve) obtained for sample with saturated non-resonant hole at 5 K; its maximum is near 692 nm. The remaining spectra were obtained at higher temperatures. The dotted curve is the pre-burn 50 K spectrum from Figure 2-2C scaled for comparison with the post-burn curve. The inset show the shifts of the broad non-resonant holes (blue squares) and positions of the corresponding maxima of the origin bands (red circles), obtained at different burn fluences.

The temperature dependence of CP47 emission from samples with saturated lowest-energy state ($A1_{mod}$) is shown in the main frame of Figure 2-4; the 5 K emission peaks near 692 nm, having been shifted from ~695 nm by HB. The inset in Figure 2-4 shows that the modified lowest-energy $A1_{mod}$ state shifts blue as revealed by the HB spectra; although the HB spectra are not shown here, the blue squares in the inset (that correspond to the spectral position of the hole maximum burned under non-resonant conditions using λ_{ex} of 496.5 nm) shift to shorter wavelengths as a function of fluence. A similar "blue" shift is observed in emission maxima (see the red circles in the same inset). The emission spectra shown in the main frame of Figure 2-4 clearly indicate that upon temperature annealing, the emission band shifts back to 695 nm as observed in intact (unburned) samples (see the double sided arrow) as the hole is thermally refilled. For comparison with the 50 K post-HB spectrum, the dotted curve in Figure 2-4 shows the 50 K emission spectrum from a fresh (unburned) sample. The two spectra peak at 695 nm, indicating that thermal processes have already mostly re-filled the burned hole. The slight broadening of the post-HB spectrum can be attributed to incomplete refilling due to complexes in which 50 K is not a high enough temperature to completely refill the spectral hole on the experimental timescale.

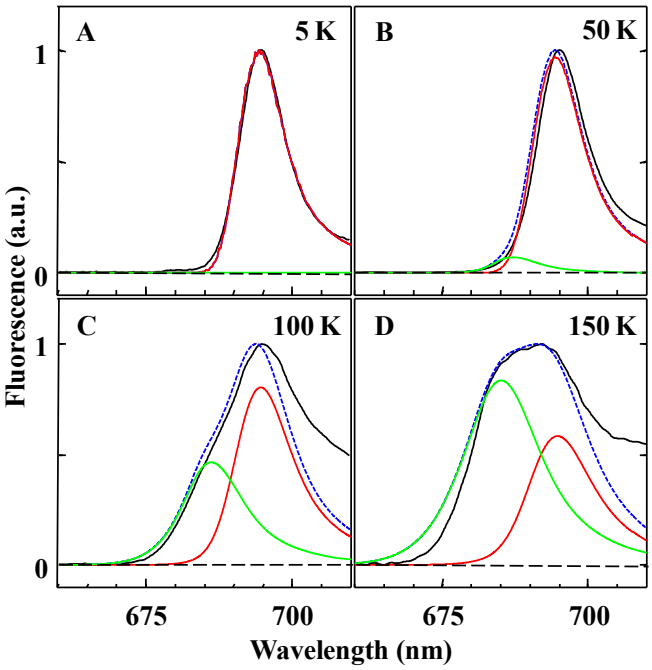

Figure 2-5 Comparison of experimental CP47 fluorescence spectra (black curves) with calculated emission spectra (blue dashed curves) at 5, 50, 100, and 150 K. The red and green curves correspond to the calculated lowest-state emission and higher-states emission, respectively.

The observed shift of these HB spectra from ~692 nm at 5 K to ~695 nm at 50 K may help to explain the unusual temperature dependence observed in[11,13,18]. In fact the behavior reported in[18], where the emission peak of the CP47-RC complex was observed to shift from ~691 nm at 4 K to 694 nm at 77 K, is almost identical to the behavior seen in Figure 2-4. The similarity of these data sets suggests that the CP47-RC data in[18] may be affected by HB contributions in the 4 K spectrum (which are erased as the temperature is raised), although new experiments with fresh CP47-RC preparations are necessary to confirm this suggestion. In general, depending on sample exposure to light and experimental conditions during emission measurements, the blue shifted emission observed in various CP47 samples reported over the

years,[3,6,7] is most likely caused by two effects: 1) a contribution from reversible photobleaching due to high photon densities used for excitation, and/or 2) a contribution from the differently destabilized (or photodamaged) complexes (irreversible damage) characterized by the FT1 and FT2 trap emissions.[19]

Finally, we note that the T-dependence of our intact (and unburned) CP47 sample is in excellent agreement with the theoretically predicted behavior for temperatures up to ~150 K. Figure 2-5 shows calculated (blue curves) and experimental (black) fluorescence spectra obtained at four temperatures: 5, 50, 100, and 150 K (see figure caption for details). Note that especially at low temperatures (5 and 50 K) the calculated spectra agree very well with the experimental curves (the discrepancy on the long-wavelength side at T = 100 and T = 150 K can be attributed to vibrational modes, which are not included in the calculations). The red curve in each frame shows emission from the lowest excitonic state, while the green curve shows the Boltzmann population-weighted emission from higher excitonic states, which is negligibly small even up to 50 K. As a result, up to about 80 K the maximum remains near 695 nm in agreement with our experimental data. All spectra were calculated using the excitonic states composition from[20] and the standard expression for the emission lineshape function, which (after applying a series expansion to the exponent in the expression shown in[26]) reads

$$D(\omega;T) \propto e^{-S(T)} \sum_{R=0}^{\infty} \frac{S(T)^R}{R!} l_R(-\omega;T),$$

where $S(T) = \int_{-\infty}^{\infty} p(\omega;T)d\omega$, $p(\omega;T) = (1+n(\omega;T))J(\omega) + n(-\omega;T)J(-\omega)$, $J(\omega)$ is the spectral density function, $l_0(\omega;T)$ is a delta function representing the zero-phonon line (ZPL),

$l_1(\omega;T) = S(T)^{-1} \cdot p(\omega;T)$, and for $R > 1$, $l_R(\omega;T)$ is the convolution $l_1(\omega;T)$ with itself R-1 times. For numerical calculations, the sum was truncated after a number of terms sufficient to account for 99.99% of the total intensity of the phonon-sideband. The best results were obtained with the Huang-Rhys factor S = 1 for all states (as obtained for the lowest state in[20]); for details see the Supporting Information in Appendix B. Note that at higher temperatures (70-150 K) as expected the emission band shifts to higher energies (blue shift) due to emission from higher states caused by the equilibrium of the excitation energy over the antenna Chls; this behavior is in contrast to the unusual red-shift observed in Figure 2-4 due to HB. Above 100 - 150 K the deviation of the simulated spectra from the experimental ones increases significantly, most likely due to thermal activation of vibrational modes, T-induced changes in pigment/protein/solvent interactions and/or quadratic/anharmonic electron-phonon coupling effects not accounted for in our simulations. These effects are beyond the scope of this communication and will be addressed elsewhere.

We anticipate that these data will provide more insight into the unusual temperature dependence of PSII core emission[11,13,18] and ultimately shed more light into the nature of EET from CP47 (and/or CP43) to the RC in PSII core complexes. Here, in light of the data discussed above, we only suggest that one of the conclusions in[11,13,18] that low-temperature PSII emission originates from CP43 and CP47 "slow-transfer" states may have to be revisited. That is, given the observed emission near 695 nm from *isolated* CP47 at all temperatures between 5 and 77 K, we do not think that the strong temperature dependence seen in PSII core, including the red shift of the emission observed between 4 and 77 K, can be attributed solely to the lowest-energy CP47 pigments maintaining some "slow transfer" character or being thermally excited in a PSII assembly that becomes increasingly equilibrated.[13] Instead, we suggest that the multiple emission

bands observed from the isolated PSII core complex[12] may originate from destabilized or photo-damaged subunits, leading to the unusual T-dependent profile.

2.3 Conclusion

In summary, we have shown that the fluorescence origin band of the intact CP47 antenna protein complex of PSII from spinach does not shift in the temperature range of 4-77 K, and has very different temperature dependence than previously reported in[3]. Temperature dependent emission spectra of CP47 obtained at different saturation levels of the lowest-energy state(s) near 693 nm offer more insight into the origin of the previously published CP47 fluorescence spectra. It has conclusively been shown that the emission maximum of CP47 and its bandwidth strongly depend on the degree of bleaching of the low-energy state(s) and/or destabilization of the protein complex. That is, the 695 nm emission shifts continuously to shorter wavelengths reaching, due to photobleaching, a position of ~692 nm at saturated HB conditions. This process is reversible by cycling the temperature. In contrast, the emission peaks previously observed near 685 nm and ~691 nm characteristic of destabilized complexes[19] cannot be eliminated by temperature cycling. Thus we conclude that the well-known 695 nm emission of CP47 previously observed only at 77 K[11,13] does not arise from excitations that are trapped on red-absorbing CP47 Chls of the 690 nm band, as 5 K emission of intact CP47 also peaks near 695 nm.[19,20] Likewise, we argue that the 685 nm emission in PSII cores does not arise from excitations that are transferred slowly from 683 nm states in CP47 to the RC, as suggested in[11,18], since the 683/684 nm state and its emission near 685 nm are absent in intact CP47. Instead we suggest that both the ~685 nm and ~690 emissions in the PSII core could originate from destabilized or photo-damaged complexes. Thus the slow EET dynamics observed in[13] may not be characteristic of the intact CP47 antenna, showing again that the EET dynamics in PSII deserves further study. These results highlight that

it is essential that general criteria of intactness are established; otherwise it will be difficult to compare data generated in different laboratories.

Acknowledgment. This work was supported by a U.S. Department of Energy EPSCoR grant (DE-FG02-08ER46504). Partial support for K. Acharya was provided by the K-State Center for Sustainable Energy. B. Neupane was supported by the NSF grant (EPS-0903806) and matching grants from the State of Kansas through Kansas Technology Enterprise Corporation. CP47 complexes were kindly provided by Drs. M. Seibert and R. Picorel from NREL (Golden, CO). MR acknowledges support from a Fulbright US Student Fellowship (2009-2010) for research in Warsaw, Poland.

References

(1) Groot, M.; Frese, R. N.; de Weerd, F. L.; Bromek, K.; Pettersson, Å.; Peterman, E. J. G.; van Stokkum, I. H. M.; van Grondelle, R.; Dekker, J. P. *Biophys. J.* **1999**, *77*, 3328.

(2) Dang, N. C.; Zazubovich, V.; Reppert, M.; Neupane, B.; Picorel, R.; Seibert, M.; Jankowiak, R. *J. Phys. Chem. B* **2008**, *112*, 9921.

(3) Groot, M.; Peterman, E. J. G.; van Stokkum, I. H. M.; Dekker, J. P.; van Grondelle, R. *Biophys. J.* **1995**, *68*, 281.

(4) Raszewski, G.; Renger, T. *J. Am. Chem. Soc.* **2008**, *130*, 4431.

(5) Alfonso, M.; Montoya, G.; Cases, R.; Rodriguez, R.; Picorel, R. *Biochemistry* **1994**, *33*, 10494.

(6) den Hartog, F. T. H.; Dekker, J. P.; van Grondelle, R.; Völker, S. *J. Phys. Chem. B* **1998**, *102*, 11007.

(7) van Dorssen, R. J.; Breton, J.; Plijter, J. J.; Satoh, K.; van Gorkom, H. J.; Amesz, J. *Biochim. Biophys. Acta, Bioenerg.* **1987**, *893*, 267.

(8) Huyer, J.; Eckert, H. J.; Irrgang, K. D.; Miao, J.; Eichler, H. J.; Renger, G. *J. Phys. Chem. B* **2004**, *108*, 3326.

(9) Dekker, J. P.; Hassoldt, A.; Pettersson, A.; van Roon, H.; Groot, M.; van Grondelle, R. In *In On the nature of the F695 and F685 emission of photosystem II.* Section Title: Plant Biochemistry; **1995**; Vol. 1, pp 53-56.

(10) van Dorssen, R. J.; Plijter, J. J.; Dekker, J. P.; Den Ouden, A.; Amesz, J.; van Gorkom, H. J. *Biochim. Biophys. Acta, Bioenerg.* **1987**, *890*, 134.

(11) Krausz, E.; Hughes, J. L.; Smith, P. J.; Pace, R. J.; Årsköld, S. P. *Photosynth. Res.* **2005**, *84*, 193.

(12) Komura, M.; Shibata, Y.; Itoh, S. *Biochim. Biophys. Acta, Bioenerg.* **2006**, *1757*, 1657.

(13) Krausz, E.; Hughes, J. L.; Smith, P.; Pace, R.; Peterson Årsköld, S. *Photochem. Photobiol. Sci.* **2005**, *4*, 744.

(14) Jankowiak, R.; Raetsep, M.; Picorel, R.; Seibert, M.; Small, G. J. *J. Phys. Chem. B* **1999**, *103*, 9759.

(15) Peterman, E. J. G.; van Amerongen, H.; van Grondelle, R.; Dekker, J. P. *Proc. Natl. Acad. Sci. U. S. A.* **1998**, *95*, 6128.

(16) Polivka, T.; Kroh, P.; Pšenčik, J.; Engst, D.; Komenda, J.; Hála, J. *J. Lumin.* **1997**, *72-74*, 600.

(17) Shen, G.; Vermaas, W. F. J. *Biochemistry* **1994**, *33*, 7379.

(18) Andrizhiyevskaya, E. G.; Chojnicka, A.; Bautista, J. A.; Diner, B. A.; van Grondelle, R.; Dekker, J. P. *Photosynth. Res.* **2005**, *84*, 173.

(19) Neupane, B.; Dang, N. C.; Acharya, K.; Reppert, M.; Zazubovich, V.; Picorel, R.; Seibert, M.; Jankowiak, R. *J. Am. Chem. Soc.* **2010**, *132*, 4214.

(20) Reppert, M.; Acharya, K.; Neupane, B.; Jankowiak, R. *J. Phys. Chem. B* **2010**, *114*,11884.

(21) de Weerd, F. L.; Palacios, M. A.; Andrizhiyevskaya, E. G.; Dekker, J. P.; van Grondelle, R. *Biochemistry* **2002**, *41*, 15224.

(22) Guskov, A.; Kern, J.; Gabdulkhakov, A.; Broser, M.; Zouni, A.; Saenger, W. *Nat. Struct. Mol. Biol.* **2009**, *16*, 334.

(23) Chang, H.-C.; Jankowiak, R.; Yocum, C. F.; Picorel, R.; Alfonso, M.; Seibert, M.; Small, G. J. *J. Phys. Chem.* **1994**, *98*, 7717.

(24) Wang, J.; Shan, J.; Xu, Q.; Ruan, X.; Gong, Y.; Kuang, T.; Zhao, N. *J. Photochem. Photobiol. , B* **1999**, *50*, 189.

(25) de Paula, J. C.; Liefshitz, A.; Hinsley, S.; Lin, W.; Chopra, V.; Long, K.; Williams, S. A.; Betts, S.; Yocum, C. F. *Biochemistry* **1994**, *33*, 1455.

(26) May V.; Kuhn O. Intramolecular Electronic Transitions. *Charge and Energy Transfer Dynamics in Molecular Systems*; WILEY-VCH: Verlag Berlin GmbH, Berlin, **2000**; PP 191-247.

Chapter 3 - Site-Energies of Active and Inactive Pheophytins in the Reaction Center of Photosystem II from *Chlamydomonas reinhardtii*

K. Acharya[1], B. Neupane[1], V. Zazubovich[3], R. T. Sayre[4], R. Picorel[5,6], M. Seibert[5], and R. Jankowiak[1,2,*]

[1]Department of Chemistry and [2]Department of Physics, Kansas State University, Manhattan, KS 66505; [3]Department of Physics, Concordia University, Montreal, Quebec, Canada; [4]New Mexico Consortium, Los Alamos, NM, 87544, and [5]National Renewable Energy Laboratory, Golden, CO 80401

Abstract

It is widely accepted that the primary electron acceptor in various Photosystem II (PSII) reaction centers (RCs) is pheophytin *a* (Pheo *a*) within the D1 protein ($Pheo_{D1}$), while $Pheo_{D2}$ (within the D2 protein) is photochemically inactive. The Pheo site energies, however, have remained elusive, due to inherent spectral congestion. While most researchers over the last two decades assigned the Q_y-states of $Pheo_{D1}$ and $Pheo_{D2}$ bands near 678–684 nm and 668–672 nm, respectively, recent modeling [Raszewski et al. *Biophys. J.* **2005**, *88*, 986–998; Cox et al. *J. Phys. Chem*. B **2009**, *113*, 12364–12374] of the electronic structure of the PSII RC reversed the location of the active and inactive Pheos, suggesting that the mean site energy of $Pheo_{D1}$ is near 672 nm, whereas $Pheo_{D2}$ (~677.5 nm) and Chl_{D1} (~680 nm) have the lowest energies (i.e., the $Pheo_{D2}$-dominated exciton is the *lowest* excited state). In contrast, chemical pigment exchange experiments on isolated RCs suggested that both pheophytins have their Q_y absorption maxima at 676–680 nm [Germano et al. *Biochem.* **2001**, *40*, 11472–11482; Germano et al. *Biophys. J.* **2004**, *86*, 1664–1672]. To provide more insight into the site energies of both $Pheo_{D1}$ and $Pheo_{D2}$ (including the corresponding Q_x transitions, which are often claimed to be degenerate at 543 nm) and to attest that the above two assignments are most likely incorrect, we studied a large number

of isolated RC preparations from spinach and wild-type *Chlamydomonas reinhardtii* (at different levels of intactness) as well as the *Chlamydomonas reinhardtii* mutant (D2-L209H), in which the active branch $Pheo_{D1}$ is genetically replaced with chlorophyll *a* (Chl *a*). We show that the Q_x-/Q_y-region site-energies of $Pheo_{D1}$ and $Pheo_{D2}$ are ~545/680 nm and ~541.5/670 nm, respectively, in good agreement with our previous assignment [Jankowiak et al. *J. Phys. Chem. B* **2002**, *106*, 8803–8814]. The latter values should be used to model excitonic structure and excitation energy transfer dynamics of the PSII RCs.

3.1. Introduction

The recent X-ray structure of the Photosystem II (PSII) reaction center (RC) at 1.9 Å resolution[1] has confirmed that some of the general features of the PSII RC are homologous to those of the bacterial RC (BRC).[2-4] The $S_1(Q_y)$-electronic structure, excitation energy transfer (EET), and primary charge separation (CS) processes in the D_1-D_2-cyt *b*-559 RC complex of PSII (PSII RC) of plants,[5-11] cyanobacteria,[12-16] and algae[17-20] have been the subjects of many time-domain[20-24] and frequency-domain studies[25-30]. Although in recent years consistent progress has been made in our understanding of the electronic structure and CS dynamics of the isolated PSII RC,[12,31-33] an adequate global understanding has yet to be achieved. The key uncertainty in modeling of its optical spectra (independent of the level of the excitonic theory involved) is that different sets of data are interpreted in the context of different pigment site-energies[12,24,31,33-35] that cannot be reliably calculated due to the complex protein environment. Instead, the search for realistic site energies is always guided by experimental constraints and aided by fitting algorithms.[33,34,36-39] In particular, the focus of the current study is on the site energies of the active and inactive pheophytins ($Pheo_{D1}$ and $Pheo_{D2}$, respectively) in the isolated PSII RC from wild-type (WT) *Chlamydomonas (C.) reinhardtii* and its D2-L209H mutant. While most researchers over the last two decades surmised that the Q_y-states of $Pheo_{D1}$ and $Pheo_{D2}$ bands were at ~678–684 nm and ~668–672 nm, respectively, recent modeling[13,16,40] of the electronic structure of the PSII RC reversed the location of the active and inactive Pheos, suggesting that the mean site energy of $Pheo_{D1}$ is near 672 nm, whereas $Pheo_{D2}$ (~677.5 nm) and Chl_{D1} (~680 nm)[13,16,40] have the lowest energies (i.e., the $Pheo_{D2}$ dominated exciton is the *lowest* excited state). The latter would allow one to explain the presence of narrow (persistent) homogeneous hole widths burned at the lowest energy state, as excitation of $Pheo_{D2}$ would not lead to charge

separation.[40] This assumption, however, is not necessary, as a broad distribution of charge separation rates[6,8,23] can explain the possibility of burning very narrow holes. For example, it has been shown that there are fractions of both P680- and P684-type RCs, where charge separation is too slow to compete with fluorescence at 5K.[6,41,42] Besides, a typical fractional

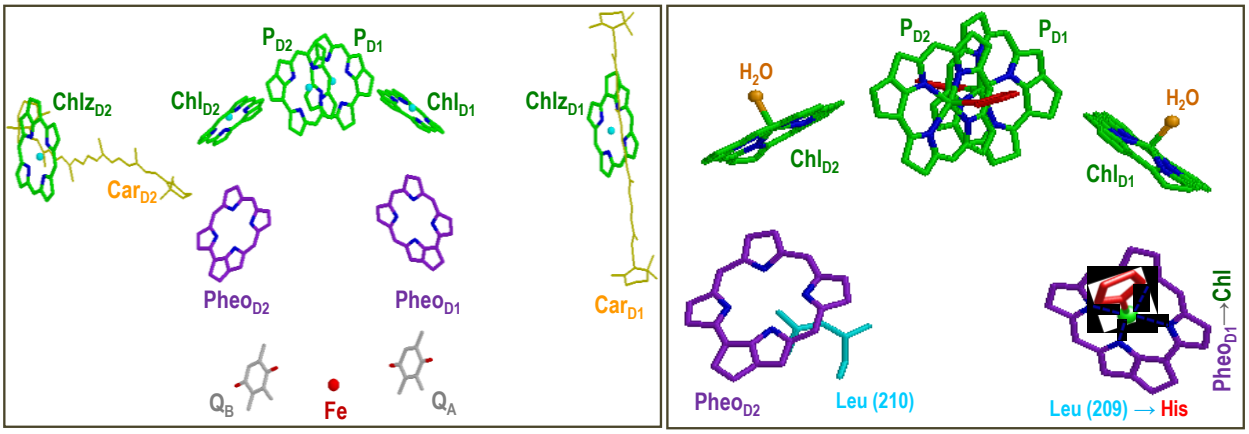

Figure 3-1 Cofactor arrangement in the active (D1) and inactive (D2) branches of the PSII RC based on the crystal structure of *T. vulcanus* at 1.9 Å resolution, PDB ID 3ARC[1]. The left frame shows the arrangement in WT RCs (chls, green; carotenes, yellow; pheophytins, purple; plastoquinones, gray; non-heme iron, red; and nitrogen, blue). The right frame shows the arrangement of selected pigments and their ligands (water, orange; histidine, red; leucine, cyan) in the D2-L209H RC mutant. The substituents of the cofactors are truncated for clarity.

depth of saturated ZPHs at 680 nm are 25% and not 15%, as reported by others[40] based on our previous work.[6] Such holes are not achievable within the Cox *et al.* model[40], as only a 17% fraction of $Pheo_{D2}$ contributes to the lowest state in their model. Thus we favor an interpretation that is also consistent with recent transient absorption experiments at 77K on the isolated PSII RCs from spinach, where the existence of a very slow channel for charge separation was observed.[7] The combination of femtosecond pump-probe transient absorption experiments with selected Pheos exchanged (*i.e.*, chemical exchange of $Pheo_{D1}$ and $Pheo_{D2}$ with 13′-deoxy-13′-hydroxy-pheophytin *a*) suggested that both pheophytins in the PSII RC have their Q_y-transitions

at 676–681 nm.[9,43,44] To provide more insight into the site energies of both $Pheo_{D1}$ and $Pheo_{D2}$, and to prove that the above[9,43,44] assignment is unlikely correct, we compare data obtained for the RC from spinach with those generated for WT *C. reinhardtii* and its D2-L209H mutant. In this mutant the active branch $Pheo_{D1}$ was replaced with chlorophyll *a* (Chl *a*) by site-directed mutagenesis[45] on the *psbD* gene.

Figure 3-1 (left frame) shows a schematic arrangement of the six Chl and two Pheo molecules for the PSII RC from *Thermosynechococus (T.) vulcanus* based on Ref.[1]; the P_{D1} and P_{D2} Chls are analogous to the P_L and P_M BChls of the bacterial special pair, respectively, while the $Chl_{D1,D2}$ an $Pheo_{D1,D2}$ molecules correspond to the monomeric $BChl_{L,M}$ and the $BPheo_{L,M}$ molecules of the BRC.[2-4] The D1 and D2 polypeptides are homologous with the L and M polypeptides of the BRC, respectively.[19,46] By analogy with the BRC, it is also believed that the P_{D1}/P_{D2}, Chl_{D1}, and $Pheo_{D1}$ molecules participate in primary charge separation in the PSII RC.[31-34] An obvious difference between the PSII RCs and BRCs is that the former contains two additional (peripheral) Chls, which are also shown in the left frame of Figure 3-1. In addition, a much larger heterogeneity and spectral congestion of pigments (with comparable couplings) in the PSII RC and the lack of crystals of isolated D1-D2-Cyt b_{559} complexes, make it difficult to describe the excitonic structure of the isolated PSII RC. The right frame of Figure 3-1 shows the pigments along with their ligands of the D2-L209H mutant mentioned above, in which the active $Pheo_{D1}$ has been replaced with chlorophyll a (Chl *a*). The cofactor arrangement in the active (D1) and inactive (D2) branches of the PSII RC was taken from the very recent crystal structure of *T. vulcanus* at 1.9 Å resolution, PDB ID 3ARC.[1]

To our knowledge, there are only a few studies of the isolated algal PSII RC from *C. reinhardtii* because such complexes are difficult to prepare.[12,17-20] We anticipate that the structural asymmetry introduced into the RC complex (*i.e.*, in the case of the *C. reinhardtii* D2-

L209H mutant) will shed more light on the site-energy of the active pheophytin. This strategy of replacing selected bacteriopheophytins (BPheos) with bacteriochlorophylls (BChls) was developed historically in BRCs.[47-49] Similar pigment replacements have been accomplished in PSII RCs using *chemically modified* Pheos along with detergent extraction and pigment reconstitution approaches.[9,43,50] However, it is not clear to what extent the latter approach modifies and/or destabilizes the excitonic structure of the RCs.

Site-directed mutagenesis approaches should, in principle, give more precise replacement and a less distorted system than chemical modification, and have the additional advantage that intact PSII complexes (thylakoids) as well as smaller PSII sub-fractions (including RCs) can be characterized biophysically. It has recently been demonstrated that the introduction of a potential Mg ligand (D1-L210H) over the center of the $Pheo_{D2}$ macrocycle ring resulted in the replacement of $Pheo_{D2}$ with a Chl *a*.[12] In this case, the kinetics of primary charge separation were not substantially altered in the D1-L210H mutant, indicating that the Chl substitution for the $Pheo_{D2}$ in the inactive branch did not significantly perturb the energetics of the primary electron donor/acceptor pair.[12] It was also shown that $Pheo_{D2}$ Q_x band is blue shifted in comparison with the Q_x band of $Pheo_{D1}$ (active).[12]

We present below absorption and hole burned (HB) spectra of WT *C. reinhardtii* and its D2- mutant (D2-L209H), obtained under various conditions as well as some new results from our modeling studies. A discussion on the primary electron donor and the possibility of P_{D1} and Chl_{D1} electron transfer pathways being present in isolated PSII RC will be published elsewhere. In the current study we focus on the assignment of the Q_y- and Q_x-states of $Pheo_{D1}$ and $Pheo_{D2}$. The results reported below indicate that the $Pheo_{D1}$-Q_x and $Pheo_{D2}$-Q_x transitions lie on the low and high energy sides, respectively, of the single Pheo-Q_x absorption band, in perfect agreement

with data obtained previously with the PSII RCs from spinach.[12,28,36,51] We also demonstrate that the replacement of the $Pheo_{D1}$ with a Chl *a* is in agreement with simple modeling studies of the absorption difference spectrum. We show that in contrast to the D1-L210H mutant (with $Pheo_{D2}$ replaced by Chl *a*[12]), where the kinetics of primary charge separation were not substantially altered,[12] the D2-L209H mutant exhibits significant changes in the energetics of the primary electron donor/acceptor pair. Finally, we argue that it is unlikely that $Pheo_{D2}$ dominates the lowest-energy excited state (and contributes to the zero-phonon action (ZPA) spectra) as suggested recently.[40] A new interpretation of the origin of the nonresonant (persistent) hole bleached in the isolated PSII RC is also provided. We anticipate that the data presented in this paper will allow us to refine the models of the electronic structure of the PSII RC by providing additional constraints (*i.e.,* proper site energies of both the active and inactive pheophytins) for future excitonic calculations of optical spectra (research in progress).

3.2. Materials and methods

3.2.1. Preparation of PSII RC from WT C. reinhardtii and its D2-L209H mutant.

Photosystem II RC preparations from *C. reinhardtii* containing ~6 Chls per 2 Pheos in the WT, and ~7 Chls and 1 Pheo in the D2-L209H mutant (note this mutant is incapable of photosynthetic growth because of the absence of an active-Pheo and thus was grown on the dark in TAP medium) were prepared from both thylakoids and PSII-enriched membranes following the method of Nanba and Satoh[5] with important modifications.[20] To obtain the D2-L209H mutant studied in the present work, we used a transgenic (site-directed mutagenesis) approach to modify the pigment composition of the *C. reinhardtii* PSII RC. A histidine, a common Chl ligand, was introduced to the D2 protein over the macrocycle ring of the active branch $Pheo_{D1}$. Thylakoids or PSII-enriched membranes (around 100 mg Chl) were resuspended in buffer A (20

mM Bis-Tris, pH = 6.5, 1.5 mM (w/v) taurine, and 35 mM NaCl), and treated with 6% (w/v) Triton X-100 (final concentration) at a final chlorophyll (Chl) concentration of 0.5 mg Chl/mL. The detergent was added drop-wise from a 30% (w/v) solution, and the suspension was incubated for 2 h at 4^{o}C with gentle stirring in the dark. The solution was centrifuged at 40,000 x g for 30 min, and the resultant supernatant was loaded onto a Toyopearl TSK DEAE 650s column (30 x 1 cm), pre-equilibrated with buffer B (20 mM Bis-Tris, pH = 6.5, 1.5 mM taurine, 35 mM NaCl, and 0.35% [w/v] Triton X-100) at a flow rate of 3–4 mL/min. The large pellet from the centrifugation was still quite green, and it was re-suspended in the same buffer without Triton, incubated for 10 min, and centrifuged again under the same conditions. The new green supernatant was added to the previous one on the column. Note that the final bound green material remained at about the middle of the column in contrast to the observation with similar material isolated from spinach, which remained at the very top of the column. Spinach material seems to bind more strongly to this column than that from Chlamydomonas. A similar observation was reported by Alizadeh *et al.*[18] using the *Chlamydomonas* F54-14 mutant (a PSI- and chloroplastic ATPase-defective double mutant). The column was then washed overnight with the same buffer B at a flow-rate of 3 mL/min until the peak at 435 nm was a little lower that that at 417 nm. At this point, the remaining green material was eluted with a 35–300 mM NaCl linear gradient in the same buffer, 3-mL fractions were collected, and the RCs eluted at around 90 mM NaCl. In the case of the D2-L209H mutant, most of the recovered material showed a room temperature absorption peak at around 675 nm, and the material was stored without further treatment under liquid N_2 until use. WT RCs exhibited an absorption peak at around 675.5 nm (the first 3–4 colored fractions that eluted at around 90 mM NaCl), but the other fractions showed maxima at ≥676 nm, probably due to some contamination with LHCII or PSI

components. The fractions with maxima at around 675.5 nm were pooled for Cu^{2+}-IMAC chromatography as in Ref.[52], using a Chelating Sepharose Fast-Flow (GE Healthcare) column to eliminate some minor Chl *b*-containing pigment–protein complex contaminant. The green material was eluted with a 0–50 mM Imidazol gradient. Pigment quantification of the preparations was done after extraction with 80% (v/v) acetone using the method in Ref.[53] Our typical RC preparation from spinach contained 5.85 Chl/2 Pheo and that from WT Chlamydomonas contained 5.55 Chl/2 Pheo. If we assume 6.0 Chl/2Pheo in spinach we obtained about 5.7 Chl/2 Pheo in our WT Chlamydomonas PSII RC preparation. This somewhat lower Chl content of our preparations compared with other PSII RC material is most probably due to a reproducibly lower carotenoid content in our preparations as compared to those from other laboratories; carotenoid bands were taken into account in our pigment calculations). Using the same quantification methodology, our non-active D2-L209H mutant RCs contained ~7 Chl per 1 Pheo, demonstrating that in this mutant one Pheo is been replaced for one Chl.

3.2.2. Spectroscopic measurements.

The hole burning apparatus used for this study was described in detail elsewhere.[54,55] Briefly, absorption and hole spectra were recorded with a Bruker HR120 Fourier transform spectrometer. Absorption and hole-burned spectra were obtained at a resolution of 4 cm^{-1} and 0.5 cm^{-1}, respectively. A Coherent CR699-21 ring dye laser (linewidth of 0.07 cm^{-1}), pumped with a 6 W Coherent Innova argon-ion laser, was used to burn the holes. The persistent NPHB spectra reported in the figures correspond to the post-burn absorption spectrum minus the pre-burn absorption spectrum. The triplet bottleneck hole spectra correspond to absorption spectrum with laser on minus the spectrum with laser off. Burn intensities and times are given in the figure captions. The sample temperature was maintained at 5 K using a Janis 8-DT Super Vari-Temp

liquid helium cryostat. The excitation source for the fluorescence experiments was a Coherent UV argon-ion laser operating at 496.5 nm. Fluorescence was dispersed at a resolution of 0.1 nm by a Princeton Instrument Acton SP-2300 monochromator, equipped with a back-illuminated, N_2-cooled CCD camera. Care was taken to ensure that reabsorption effects were negligible.

3.2.3. Monte Carlo simulations of the WT minus the mutant RC absorption difference spectrum.

To model absorption changes introduced by the mutation, we carried out simple excitonic calculations using MathCad 12.0. Transition dipole moments and coupling between chromophores were calculated as in Ref.[13] However, due to the significant shift in the position of the central magnesium out of the chlorin plane, which was revealed in the recent crystal structure, the transition dipole moments were taken to extend from the ring I nitrogen (N-B) to the ring III nitrogen (N-D) rather than from the central Mg to N-D, and the center of the Chl molecule was taken to be at the averaged position of the four ring nitrogen atoms, rather than at the central magnesium. A Frenkel Hamiltonian matrix (static lattice approximation) for the PSII RC chromophores was constructed (see section 3.5); for each interaction of the Monte Carlo simulations, site energies were added randomly according to a Gaussian distribution, mimicking the site distribution function (SDF) of the chromophore. A simple fitting algorithm was used to

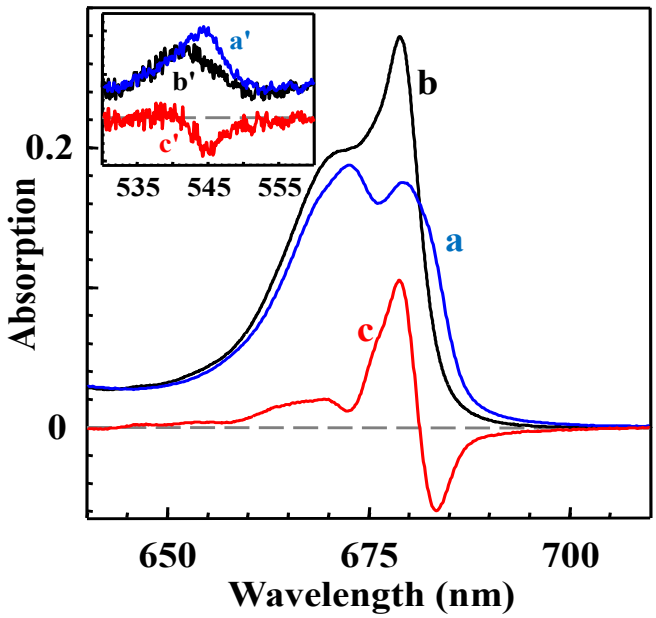

Figure 3-2 Spectra a and b correspond to the absorption spectra of intact WT and D2-L209H mutant RCs, respectively, measured at T = 5K. The areas of curve a and b are scaled to 7.0 and 7.5, respectively, based on the normalized oscillator strength of the cofactors. Curve c is the difference between spectra b and a. The inset shows the corresponding Q_x-region (see text for detail).

find optimized parameters (*i.e.,* site energies and the width of the SDF) to achieve simultaneously good fits to the absorption for the RCs from WT *C. reinhardtii* and the D2-L209H mutant, as well as the difference between the latter two spectra.

3. 3. Results

3.3.1. Low temperature absorption spectra of the RC from WT C. reinhardtii and its D2-L209H mutant—site energies of PheoD1 and PheoD2.

Absorption spectra of the WT RC from *C. reinhardtii* and its D2-mutant are shown in Figure 3-2, as blue (a) and black (b) curves, respectively. According to pigment extraction with 80% (v/v) acetone and comparison with spinach RC data obtained as in Ref.,[53] we established that our WT RC and D2 mutant contained about 6 Chl *a*/2 Pheo *a* and 7 Chl *a*/1 Pheo *a*,

respectively (the measured values were 5.7 and 6.5-7, respectively; however, see the comments in Material and Methods, Section 2.1). Note that our WT RC preparation (see curve a in Figure 3-2) has a 5K absorption maximum near 679.5 nm with a noticeable shoulder near 685 nm. Spectra a and b were normalized over a broad spectral range of 500–700 nm, assuming that the integrated absorbance of the WT PSII and D2-L209H mutant RCs should be about 7.0 (in Chl *a* units) and 7.5, respectively. The difference originates from the fact that the mutant has Chl *a* (instead of $Pheo_{D1}$) in the active D1-protein branch and the Pheo oscillator strength in the protein environment is 50% that of Chl *a*[9,56], for convenience normalized to unity. The difference spectrum is given by the red curve (c) in Figure 3-2. The overall absorption decrease near 684 nm in curve (c) corresponds to about 0.3 in Chl *a* units. The intensity gain at ~679 nm is bigger than the loss at ~684 nm because the oscillator strength of the Chl *a* is higher than that of Pheo *a*. A theoretical description of this spectrum is shown in Figure 3-6. Here we note only that the shape of curve (c) suggests that the site energy of Chl *a* in the $Pheo_{D1}$ binding pocket shifts to the blue; note, this does not mean that the site energy of $Pheo_{D1}$ is located at about 684 nm (see below for details) in agreement with previous data for RCs from spinach.[11,57] The fluorescence from WT *C. reinhardtii* RCs peaks near 685 nm (data not shown).

Curves a′ and b′ in the inset of Figure 3-2 correspond to the normalized Q_x band of the WT *C. reinhardtii* RC and its D2-L209H mutant. The difference between curves a′ and b′ (curve c′) corresponds to the removal of $Pheo_{D1}$ (red curve in the inset), proving that the absorbance difference in Q_y near 684 nm (see curve c) indeed originates from the genetically replaced mutation of Pheo *a* ($Pheo_{D1}$) to Chl *a*. We would like to make it clear that the 684 nm bleach does not reflect the site energy of $Pheo_{D1}$; rather, it reflects changes to the lowest exciton band in the RC mutant (*vide infra*). We hasten to add that the coupling constants between chlorins in the Q_x

region are about one order of magnitude weaker than those in the Q_y-region.[58] This is why the *entire* Q_x absorption band near 544 nm in WT RC corresponds both to the active and inactive pheophytins, since the Q_x band of Chl *a* lies near 580 nm.[59-61] Thus the bleach at ~545 and ~684 nm corresponds definitively to the replacement of active $Pheo_{D1}$ with Chl *a*. This in turn indicates that the Q_x-transition of $Pheo_{D2}$ must be near 541.5 nm; the site energy of Q_y $Pheo_{D2}$ will be discussed below. Here, it is suffice to say that the relative positions of the Q_x-transitions of active and inactive Pheos in *C. reinhardtii* are in good agreement with the same Q_x-transitions observed in isolated RC from spinach, where the localized Q_x-transitions of $Pheo_{D1}$ and $Pheo_{D2}$ were demonstrated to lie at 544.4 and 541.2, respectively.[28,36] In addition, we found that in our most intact WT RC from *C. reinhardtii* the entire Q_x-band lies near 544 nm (not at 543 nm, as typically observed in isolated spinach RCs[9,26,43]). The Q_x bleach of active $Pheo_{D1}$ near 545 nm is in perfect agreement with data obtained for intact spinach PSII core,[62,63] suggesting that our isolated RCs are intact. The theoretical fit of the red spectrum in the main frame of Figure 3-2 (curve c) will be discussed in section 3.5. In view of the above data, we conclude that it is doubtful that the site energy of $Pheo_{D1}$ lies near 672 nm, as assumed recently in Refs.[13,40] (*vide infra*). Thus, it is not likely that the exciton realizations may lead to a predominantly $Pheo_{D2}$ character of the lowest energy exciton, as suggested by Cox *et al.*[40].

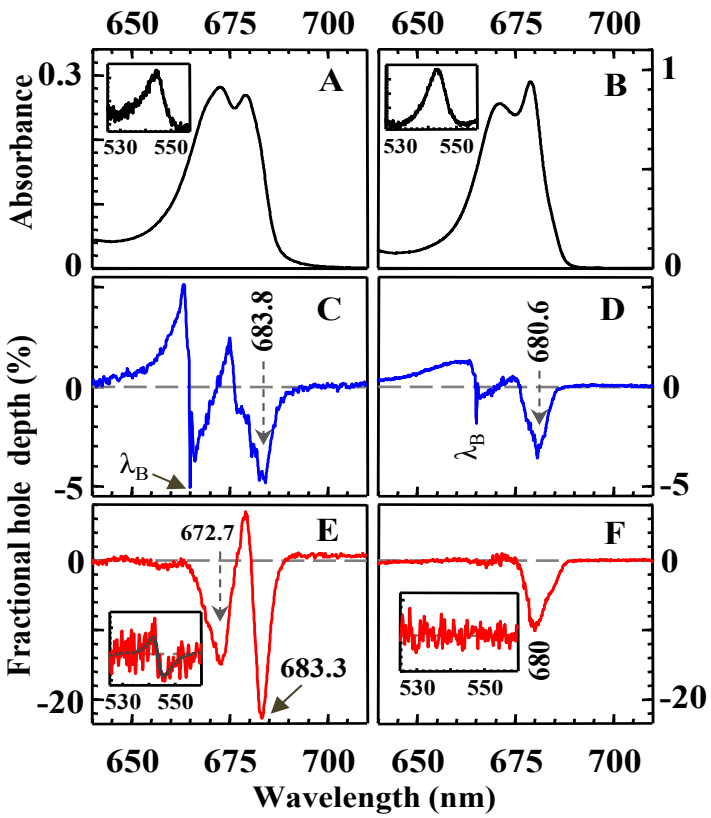

Figure 3-3 Absorption, nonresonant persistent hole, and transient HB spectra obtained for RCs from *C. reinhardtii* and spinach RC are shown in frames A/C/E and B/D/F, respectively. The insets in frames A and B show the Q_x absorption band of both pheophytins near 544 and 543 nm, while those in frames E and F illustrate the Q_x response (in the pheophytin region) in the transient spectra. All HB spectra were obtained with a λ_B of 665 nm and were measured at 5K.

3.3.2. Comparison of absorption, persistent, and transient hole spectra obtained for the RCs from C. reinhardtii and spinach.

Frames A and B in Figure 3-3 show Q_y absorption spectra obtained for RCs from *C. reinhardtii* and spinach, respectively. There is no indication that any of these two samples are contaminated with other antenna complexes, *i.e.,* both have 6 Chl *a* /2 Pheo *a*, and no bleaching and/or emission bands typically observed in PSII antenna complexes.[42,64] The corresponding insets in frames A and B show Q_x absorption band of

pheophytins located near 544 nm (frame A) and 543 nm (frame B). As expected, the more intact sample (frames A, C, and E) has red-shifted peaks of Q_y- and Q_x-absorption bands, as well as the position of the lowest-energy bands, in agreement with spectra obtained for RC from intact PSII core samples.[16,62,63] Frames C and D show (nonresonant) persistent saturated holes obtained with a λ_B of 665.0 nm. Non-resonant holes appear as the result of downhill energy transfer. The hole depths of the broad (saturated) holes, obtained under identical conditions and shown in frames C (*C. reinhardtii*) and D (spinach), are 4.6% and 3.5%, respectively. Although hole shapes are similar, the broad hole in *C. reinhardtii,* located at 683.8 nm, is about 3.2 nm red-shifted in comparison with the hole typically obtained for RCs isolated from spinach.[27,28,65] The origin of the broad 683.8 and 680.6 nm holes will be discussed in section 4.1. Here we only note that both persistent holes shown in frames C and D have weak (and noisy) responses in the Q_x region of $Pheo_{D1}$ near 545 ± 1 nm (data not shown).

In contrast to persistent holes, the transient, non-line narrowed spectra shown in frames E and F (λ_B = 665.0 nm) are very different; the hole in *C. reinhardtii* (frame E) has two components at 672.7 and 683.3 nm with a positive feature near 679 nm. The fractional hole depth at 683.3 nm (measured with a laser intensity (I) of 100 mW) is 22.5%. The large nonresonant transient hole, obtained under identical conditions for spinach RCs, is blue shifted to 680.0 nm (although slightly red-shifted holes near 681–682 nm have been previously observed in isolated RCs from spinach[27,28,65]) and has a smaller fractional depth of 9.8%. Note the shape of this transient hole is exactly the same as previously observed in spinach PSII RCs[27,28,65] with a bleach near 680/681 nm and a weak shoulder near 683/684 nm[28], which we assigned previously to P680 and P684 RCs, respectively[6]. That is, we proposed that in isolated spinach RCs, transient holes at ~680–681 nm and ~684 nm correspond to the triplet bottleneck holes, originating from

P680- and P684-type RCs and reflecting the gross heterogeneity of PSII RCs (the P684–band is the primary electron donor band (P684) of a subset of RCs that are more intact than P680-type RCs).[6] This suggestion is consistent with data presented in Figure 3-3. Another striking difference between the transient holes obtained for *C. reinhardtii* and spinach RCs is in the Q_x region. As previously observed there is no bleaching in this region for transient spectra obtained for spinach RCs (see the inset in frame F), whereas the Q_x Pheo band clearly shifts in *C. reinhardtii* RCs as shown in the inset of frame E. Note that the transient spectrum obtained for isolated RC from *C. reinhardtti* is very similar to the flash-induced ($P684^+Q_A^-$ - $P684Q_A$) absorbance difference spectra of PSII core complexes from WT *Synechocystis sp.* PCC 6803.[15] The latter suggests the presence of Q_A; therefore, an electrochromic shift in the Q_x-region of the pheophytins is possibly due to the formation of the $P684^+Q_A^-$ state, as previously observed in bacterial RCs[64,66,67] and PSII cores[16,62,63] As expected, there was no bleach or shift in the 530–560 nm region in the D2-L209H mutant, since there is no formation of a $P684^+Q_A^-$ state, even if Q_A is present, due to the lack of active $Pheo_{D1}$. This proves that our isolated RCs from *C. reinhardtti* are to a large extent intact with a bleach at 672.7 nm being due to the oxidation of $P_{D1/D2}$ Chls *a*, or, expressed more properly and as discussed by Schlodder *et al*. in the case of *Synechocystis*[15], due to the bleaching of an exciton state dominated by contributions from both P_{D1} and P_{D2} Chls. It has been shown recently that the redox potential (E_m) of P_{D1} for a one-electron oxidation ($E_m(P_{D1})$) is lower than that of P_{D2}, favoring localization of the cationic charge state more on P_{D1}.[68] The positive peak in the transient spectrum (see frame E in Figure 3-3) is related to an electrochromic shift of the pigment(s) contributing to the lowest-energy state (most likely Chl_{D1} and $Pheo_{D1}$), induced by the positive charge on P (most likely P_{D1}[14,15,68]) and a negative charge on plastoquinone Q_A, (Q_A^-). This implies that at least a subpopulation of our *C.*

reinhardtii RCs still possess Q_A, which is typically lost in isolated PSII RCs from spinach. (Theoretical description of these spectra is beyond the scope of this work and will be presented elsewhere). Here we only note that the similarity between our transient spectra in isolated RCs from *C. reinhardtii* (frame E) and WT *Synechocystis* sp. PCC 6803[15], namely $P684^+Q_A^-$-$P684Q_A$ spectra, suggests that the RCs studied in this work contain the largest subpopulation of intact (*isolated*) RCs ever studied before. A very different shape of the transient hole observed in spinach RC (frame F) is most likely the result of disruptive protein-pigment structural perturbations introduced by the isolation procedure. We suggest that in spinach RCs (see frame F) Chl_{D1} is the preferred electron donor with the triplet also localized on Chl_{D1}.[15,69,70] The lack of response near 672.7 nm in spinach RCs supports the notion that RC680 has destabilized D1 and D2 proteins with a significantly weakened excitonic coupling between the P_{D1} and P_{D2} Chls, and as a result, a much weaker absorption band near 673 nm.

3.3.3. Absorption and nonresonant HB spectra obtained for damaged C. reinhardtii RCs.

Spectrum a in frame A of Figure 3-4 shows the absorption spectrum of a RC sample intentionally degraded by leaving it on the bench for several hours at room temperature. Spectrum a in frame B corresponds to WT RC sample diluted with TX-100 detergent. The latter is known to destabilize the D1/D2/Cyt b_{559} RC complex of spinach.[65,71] Curve b in both frames, obtained for control untreated WT RCs, is shown for easy comparison. All spectra were normalized for the same integrated absorbance intensity. Spectra c in both frames (with similar

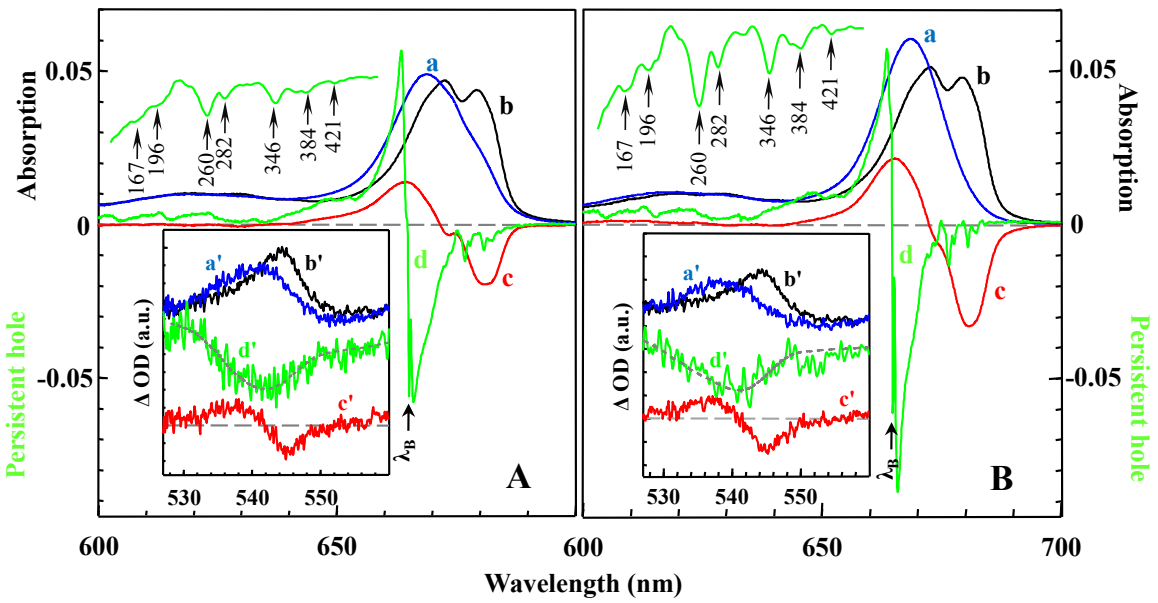

Figure 3-4 ***Frame A*: Absorption spectrum (curve a) of partly damaged PSII RC from *C. reinhardtii* (see text). Curve b is the absorption spectrum obtained for intact WT RCs. Absorption spectra in the corresponding Q_x-region of pheophytins are shown in the inset, as curves a′ and b′, respectively. Curves c and c′ are the difference spectra (i.e., c = a – b and c′ = a′ – b′). The green curve d is the persistent (nonresonant) HB spectrum obtained with λ_B = 664.9 nm; the arrow points to the ZPH. Curve d′ shows the response in persistent HB spectrum in the Q_x-region of pheophytins. The sharp spikes observed in the 675–687 nm spectral range in curves d (re-plotted on a cm^{-1} scale in the upper left insets of frames A and B) are Chl *a* vibronic satellite holes. *Frame B* shows the same spectra, as in frame A, but obtained for WT RCs of *C. reinhardtii* exposed to the excess of TX-100 detergent (see text for details). All spectra were obtained at T = 5 K.**

shapes) shows the difference between spectra a and b, indicating that both procedures destabilize the D1 and D2 proteins and/or the pigments contributing to the lowest energy state(s) in a similar way. (Spectrum a of frame B, as expected, is somewhat more disturbed than spectrum a of frame A). Curves a′ and b′ (and their difference, *i.e.*, curve c′) in the corresponding insets clearly demonstrate that both the Q_y- and Q_x-regions of $Pheo_{D1}$ blue shift

to ~670 nm and ~540 nm, respectively. The sharp spikes observed in the 675–687 nm spectral range in curves d (re-plotted in the upper left insets of frames A and B without a wavelength scale) are pure Chl *a* vibronic satellite holes associated with the ZPH at λ_B; see section 4.2 for discussion.

3.3.4. Optical spectra obtained for the C. reinhardtii D2-L209H mutant.

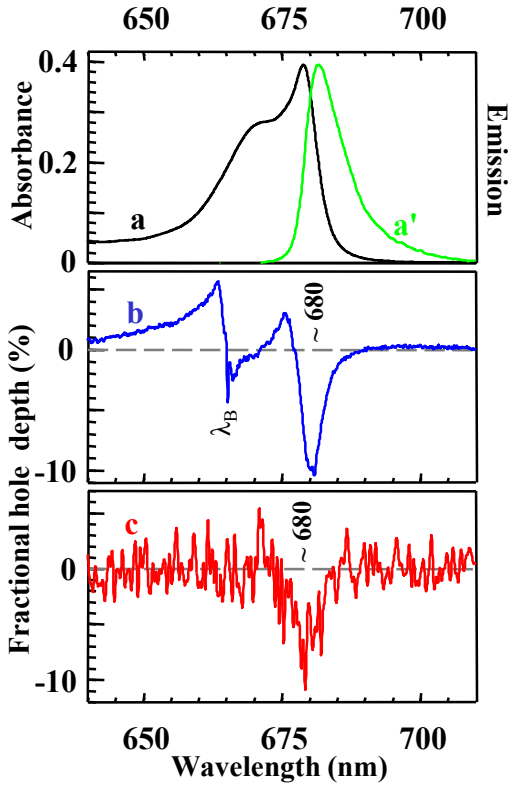

Figure 3-5 Figure 3-5. Curves a, a', b, and c correspond to the absorption, fluorescence, persistent, and transient HB spectra obtained for the D2-L209H mutant of *C. reinhardtii*. Both HB spectra were obtained with a λ_B of 665.0 nm, and recorded at 5 K.

Spectra a and a′ in Figure 3-5 show absorption and emission (with a (0,0)-band maximum near 681 nm) spectra of the D2-L209H mutant. The lowest-energy state (see curve b corresponding to a nonresonant persistent hole obtained with 665 nm excitation) is near 680 nm, revealing a very small Stokes shift of ~20 cm^{-1}. This means that electron-phonon coupling is

very weak (with an estimated Huang-Rhys factor, S of ~0.6, assuming[6] ω_m of 17 cm^{-1}). The fluorescence maximum of the D2- L209H mutant, in comparison to WT RCs, is blue shifted due to a different pigments contributing to the lowest-energy excitonic state. Recall that the absorption spectrum of the D2-L209H mutant, in which the active branch $Pheo_{D1}$ is replaced with Chl *a*, did not reveal (as expected) the Q_x-absorption band near 545 nm assigned to $Pheo_{D1}$(*vide supra*). In light of the above observations, it is interesting to note that the persistent (nonresonant) hole spectrum obtained for the mutant with λ_B = 665.0 nm (curve b in Figure 3-5) has a ~93 cm^{-1} wide hole centered at ~680 nm and no response in the Q_x pheophytin region (data not shown), proving again that $Pheo_{D2}$ does not contribute to the lowest-energy state near 680 nm. The hole near 680 nm can be attributed to downward energy transfer from pigments excited at 665.0 nm to the (blue shifted) lowest-energy excitonic band in the mutant, which is strongly contributed to by Chls (in particular the Chl *a* residing in the $Pheo_{D1}$ binding pocket). This is consistent with data shown in Figure 3-2, as the substituted Chl *a* strongly contributes to the absorption spectrum near 680 nm. In turn, the lack of bleaching at 541. 5 nm (Q_x of $Pheo_{D2}$) in the RC mutant for 665.0 nm excitation, proves that, in contrast to the RCs treated with triton TX-100, the pigments absorbing near 665 nm in the RC mutant transfer energy to the lowest exciton state at 680 nm. As expected, WT RC samples intentionally degraded by leaving them on the bench at room temperature for many hours do not reveal any broad-band bleach near 680 nm in agreement with data shown in Figure 3-4 (see curves d). The identity of the pigment(s) contributing to the low-energy states of WT and mutant RCs will be discussed in section 4.4. Here, we emphasize again that the broad hole near 680 nm is not contributed to by the inactive $Pheo_{D2}$, since the Q_x $Pheo_{D2}$ hole at 541.5 nm is absent. The weak (~6% hole depth) symmetric transient hole (Figure 3-5, curve c) is most likely formed via intersystem crossing and

corresponds to the lowest-energy band (~680 nm) of the mutant, although it cannot be excluded that the shallow transient hole reflects a triplet-bottleneck hole after recombination of the $Chl_{D1}^{+}Chl a^{-}$ state in the D2-L209H mutant (recall that Chl *a* mentioned above resides in the $Pheo_{D1}$ binding pocket). This suggestion needs to be tested via resonant HB and time resolved spectroscopies. Curve b, however, is asymmetric in the higher frequency range due to the presence of an anti-hole typically observed in persistent HB spectra.[42,72] Nevertheless, these data clearly support our above assignment that the mean site energy of $Pheo_{D2}$ is unlikely to lie anywhere close to 677.5 nm and dominate the lowest-energy excited state, as suggested in Refs[31,40]. We hasten to add that our findings also question the assignment of site energies of pheophytins obtained with the *in vitro* exchange experiments, where $Pheo_{D1}$ and/or $Pheo_{D2}$ were replaced by 13^1-deoxo-13^1-hydroxy pheophytin (13^1-OH Pheo).[9,43] The observation reported in Refs[9,43] that both $Pheo_{D1}$ and $Pheo_{D2}$ contribute at the same wavelength to the absorption spectrum, both in the Q_y- and Q_x-regions, could indicate that exchange experiments destabilize RCs or perturb excitonic interactions. The observed bleach near 680 nm and the absorption increase at ~654 nm (the Q_y-transition of replaced 13^1-OH Pheo[9,43]) are not necessarily correlated, *i.e.*, some changes observed near 680 nm could be due to partial damage of RCs and the accompanying changes in the excitonic interactions. Therefore, in light of the data presented in this work, we cannot exclude the possibility that some delta absorbance changes (near 680 nm region) observed in samples going through the chemical exchange process and purification are induced by RC destabilization. In fact, difference spectra reported in Refs[9,43] if not normalized at 624 nm, would be similar to spectra c shown in Figure 3-4 for destabilized RCs.

3.3.5. Monte Carlo simulations of the absorption difference spectra of C. reinhardtii and its D2-L209H mutant.

The red curve in Figure 3-6 (curve c from Figure 3-2) corresponds to delta absorbance spectra obtained for WT RC and its mutant, assuming a dipole strength ratio of Pheo a/Chl a of 0.5.[56] The blue curve (spectrum b) was obtained using excitonic calculations for the Q_y-states using the Frenkel Hamiltonian mentioned above. We used coupling constants calculated by the *ab initio* TrEsp method[13] and the recent X-ray structural data (PDB, file)[1]. The coupling constants (with the exception of the coupling constant (V) for the special pair $V_{PD1\text{-}PD2}$) were very similar to those reported in[13]. Taking into account a considerable wavefunction overlap between P_{D1} and P_{D2} Chls, resulting in Dexter-type exchange coupling, the coupling constant $V_{PD1\text{-}PD2}$ of 150 cm^{-1} was taken from Ref.[13] The site energies were adjusted using our experimental constraints obtained for both the site energies of $Pheo_{D1}$ and of $Pheo_{D2}$, as discussed above. Absorption spectra of *C. reinhardtii* and its D2-L209H mutant were calculated with the same set of parameters with the only adjustment that $Pheo_{D1}$ in WT RC was replaced with Chl *a* in the mutant, and the site energy of Chl a (residing in the $Pheo_{D1}$ binding pocket) was shifted to the blue by 125 cm^{-1} from the site energy of $Pheo_{D1}$ at 14710 cm^{-1}. This shift is consistent with the loss of H-bonding (with Glutamine 130) in Chl *a* residing in the $Pheo_{D1}$ binding pocket. The nice agreement between experimental and calculated difference spectra in the low energy spectral range provides further evidence that $Pheo_{D1}$ in WT RC significantly contributes to the lowest energy exciton state near 684 nm and has a site energy near 680 nm (see section 4.4 for more details).

3.4. Discussion

3.4.1. Nonresonant persistent holes.

Historically, the original assignment of the broad (~120 cm^{-1}) nonresonant persistent hole, typically observed near 680–682 nm[27,28,65] for 665 nm excitation in isolated RCs from spinach, was to a Q_y-state localized on $Pheo_{D1}$.[27] This idea was introduced prior to the introduction of the multimer model.[36,73,74] Subsequent research revealed that *only nonresonant* excitation near 660–670 nm reveals persistent bleaching at the Q_x band assigned to $Pheo_{D1}$,[27] meaning that the Q_x bleach is never observed for saturated holes burned *resonantly* in the 680–686 nm region. In Ref.[6] we provided evidence for highly dispersive primary charge separation kinetics; that is, we have shown that population of either P680* (in RC680, where * ≡ the Q_y-state) or P684* (in RC684, the subset of RCs more intact than RC680) results in both resonant *transient* (due to charge recombination of the primary radical pair) and resonant *persistent* (nonphotochemical) holes. Indeed, one set of parameters (*e.g.* electron-phonon coupling and site distribution function) could be used to simulate all transient and persistent holes burned in the 680–686 nm region. Thus the question arises what is the origin of the broad nonresonant ~680 and ~684 nm persistent holes (as shown in Figure 3-3, frames C and D) accompanied by a clear bleach in the Q_x-region of $Pheo_{D1}$?

We suggest that our original interpretation,[27] namely that this broad hole belongs to the quasi-localized Q_y-band of $Pheo_{D1}$ may actually be correct. We tentatively propose (calculations in progress) that these non-resonant persistent HB spectra could be formed (via CW excitation) during the relatively long lifetime (~2 ms[11,75]) of the triplet-bottleneck of the $^3P680$ or $^3P684$ states that are formed after recombination of the $P680^+Pheo_{D1}^-$ and $P684^+Pheo_{D1}^-$ states, respectively. In these cases, the formation of $^3P680$ or $^3P684$ (if the triplet is localized on Chl_{D1}

[15,69,70]) could partially decouple $Pheo_{D1}$ from the rest of the RC pigments. If $Pheo_{D1}$ has a site energy of ~680 nm, as suggested in this work, it would contribute to the energy trap for EET from states at ~665 nm which are excited by the laser. This indeed could lead to weak broad (~120 cm^{-1}) satellite holes with hole minima near 680 nm and/or 684nm, depending on the quality (*i.e.*, intactness) of the RC sample.[27,28,65] Note that the same process is highly improbable in the case of resonant burning. The RCs, which are resonantly excited at 680-684 nm, may exhibit either slow or fast primary charge separation[7], with persistent HB favoring slow charge separation RCs very strongly (i.e., RCs with fast charge separation and likely triplet formation are not probed). On the other hand, in RCs exhibiting fast charge separation the NPHB into the original lowest-energy state should be very inefficient based on the equation for the spectral hole burning yield[41]:

$$\phi_{SHB} = \frac{\Omega_0 e^{-2\lambda}}{\Omega_0 e^{-2\lambda} + \tau_{CS}^{-1} + \tau_{fl}^{-1}} \quad ,$$

where $\Omega_0 e^{-2\lambda}$ is the NPHB rate, and τ_{cs} and τ_{fl} are the charge separation time and fluorescence lifetime, respectively. Then during the lifetime of the ^{3}P680- or ^{3}P684-triplet states, the narrow zero-phonon lines (ZPL) of the lowest state (now localized on $Pheo_{D1}$) would not be in resonance with the laser, and, as a result, these RCs will become unavailable for further absorption of resonant photons and NPHB. This escape of the lowest-energy state from the resonance with the laser due to triplet formation is obviously irrelevant for nonresonant excitation.

The only difference between (nonresonant) saturated persistent holes (quasi-localized on $Pheo_{D1}$) burned near 665 nm (during the ^{3}P680 and ^{3}P684 triplets, in RC680 and RC684, respectively) is that the corresponding Q_x-/Q_y-transitions depending on sample intactness are at ~544±1/~680.6 nm and ~545±1/683.8 nm, respectively, as discussed above. This is why Q_y-

nonresonant persistent holes have a profile similar to that obtained due to formation (in the presence of dithionite) of stable $Pheo_{D1}^{-}$.[28,36] However, the situation is more complicated in intact RC684 from *C. reinhardtti*, which could contain plastoquinone Q_A, and possibly possess two electron donors, P_{D1} and/or Chl_{D1} (*i.e.*, two charge separation pathways, as recently proposed in Ref[7]). That is, the transient hole in Figure 3-3E may have a contribution from the ^{3}P684 triplet and the long-lived $P^+Q_A^-$ state[76] for a subpopulation of RCs that contain Q_A. The nature of the electron donor(s) and the feasibility of multiple electron transfer pathways in *C. reinhardtii* (including measurements of electron transfer times via resonant HB) is beyond the scope of this manuscript and will be published elsewhere. Here we only note that the ratio of the nonresonant TBHB spectrum (I = 100 mW) to NPHB (saturated persistent hole) in spinach (see Figure 3-3) is about 3.5, while the same ratio in *C. reinhardtii* (obtained under identical conditions; see Figure 3-3) is about 5.5. Interestingly, the ratio of ~3.6 was also observed in destabilized P680-type RCs obtained for *C. reinhardtii*. Since the depth of the saturated persistent hole (nonresonant, λ_B = 665.0 nm, obtained under similar conditions) in: (1) spinach RC near ~680 nm; (2) destabilized RC from *C. reinhardtii* (also at ~680 nm; data not shown); and (3) intact RC from *C. reinhardtii* (~683.8 nm), is only ~3–4%, it is not surprising that the *persistent hole* from a small subset of intact P684-type RCs near 684 nm in *spinach* RCs (revealed as a weak shoulder near 684 nm in a transient hole[65]) has been never observed.

3.4.2. Destabilized (damaged) RC samples.

Recall that curves a and b in Figures 3-4A and 4B correspond to the absorption spectra of damaged and the intact WT RC from *C. reinhardtii*, respectively. In agreement with previous observations[27] the absorption maxima in partly damaged RC samples blue shift to about 670 nm. As a result, the low-energy band near 680 nm disappears, as reflected by curves c. Due to this

damage and as expected, there is no more charge separation as proven by the absence of transient holes. Uncorrelated EET to the lowest-energy exciton state is absent in damaged RC samples, as reflected by the absence of a low-energy, broad satellite holes; instead, only weak sharp vibronic holes are present in the 675–690 nm region. These holes (see Figure 3-4A/B) correspond to the zero-phonon transitions obtained via vibronic excitation. In other words, the differences between the vibronic hole frequencies and the burn frequency (see curves in the upper left corners of Figures 3-4A and 3-4B) correspond to the excited state vibrational frequencies of the pigments contributing to the low-energy wing (*i.e.,* a new Chl *a* dominated low-energy state) of the damaged absorption spectra (curves a). It is not surprising that all/most pigments in the damaged RC contribute to the 665-675 nm spectral region, as it is well known that excess TX-100 detergent modifies excitonic interactions[27,64]; the interesting point, however, is what happens in the Q_x-region, especially since spectra a, a′, and d, d′ in Frames A and B of Figure 3-4 are nearly identical. Recall that the sample described in frame A of Figure 3-4 was not even exposed to excess Triton TX-100. This clearly indicates that the RC of *C. reinhardtii* is extremely sensitive to the conditions of isolation and purification. [17-20] Comparison of spectra c/c′ (obtained as a difference between spectra a/a′ and b/b′ in the Q_y- and Q_x-regions, respectively, in Figure 3-4) with spectra a (damaged RCs) and b (intact RCs) shows that $Pheo_{D1}$ in intact RC sample must contribute to the long wavelength absorption region near 680–684 nm. This questions the validity of the assumption (or data from modeling studies) that the site energy of $Pheo_{D1}$ lies near 672 nm, as suggested in Refs[13,16,31,40]. Interestingly, curves d′, which correspond to the Q_x-region bleach of the HB spectrum (at λ_B = 665.0 nm) suggest that the Q_x band of $Pheo_{D1}$ (in damaged RCs) shifts from about 545 nm to about 540 nm, with the Q_x transition of $Pheo_{D2}$ most likely lying near 541.5 nm, in good agreement with previous findings obtained for PSII RCs isolated

from spinach and those for D1-L210H mutant RCs from *C. reinhardtti*[12]. The latter work identified the Q_x-transition of $Pheo_{D2}$ in *C. reinhardtii* near 542 nm[12] in agreement with our data.

The blue shift of the $Pheo_{D1}$ band in damaged RCs is consistent with Ref.[70], where it was suggested that $Pheo_{D1}$ is likely H-bonded in intact PSII RCs [77], in analogy to $BPheo_L$ in bacterial RCs.[78,79] Thus it appears, based on our data, that this H-bond can be easily broken in destabilized RCs, leading to a blue shift of its site energy. This is consistent with Refs.[78,79] where $Pheo_{D1}$ in PSII from *Synechocystis* and $BPheo_L$ in the active L-branch site of BRCs are red shifted due to the H-bonding to the 13^1-keto substituent. Remarkably, the Q_x-absorption maximum of destabilized $Pheo_{D1}$ is similar to that of $Pheo_{D2}$; that is, now both pheophytins have the Q_x-bands near 540–542 nm (see Figure 3-4A/B, curves a′). This could explain why the reported Q_x absorption band position in RCs varied from sample to sample[9,26,28,36,43]and suggests that both pheophytins likely reside in a protein environment with similar pK_a values. The above assignment of site energies is confirmed by the hole shape in the Q_y-region (see curves d in frames A and B of Figure 3-4) and by the corresponding Q_x-response (curves d′ in both insets) observed in the nonresonant (persistent) HB spectra obtained for 665.0 nm excitation. It appears that 665.0 nm burning (in damaged RCs) bleaches broad holes near 665–673 nm and 540–542 nm (see insets), respectively, which most likely correspond to the Q_y and Q_x bands of *both* pheophytins in destabilized RCs. Note that the broad hole near 665–673 cannot be only due to Chls, as in this case one should not observe any Q_x bleaching of pheophytins. This is, in turn, consistent with our previous work with spinach RC[28,36], where it was shown that the inactive $Pheo_{D2}$ could contribute in the region near 668.3 nm with its Q_x-transition being near 541 nm. In addition, the positions of the persistent (nonresonant) holes in both Q_y- and Q_x-regions excludes the possibility that both $Pheo_{D1}$ and $Pheo_{D2}$ have similar Q_y-transitions near 680 nm, as suggested

in Refs[9,43,44] or near 690 nm, as proposed by recent modeling studies in Ref.[34] As mentioned above, the sharp spikes observed in the 675–687 nm spectral range in curves d of Figure 3-4 (re-plotted in the upper left insets of frames A and B) are Chl *a* vibronic satellite holes associated with the ZPH at λ_B. Their frequencies of 167, 196, 260, 282, 346, 384, and 420 cm^{-1} are very similar to the excited state Chl *a* mode frequencies[80,81,82,83] and to our unpublished data obtained for Chls *a* in CP43 and CP47 antenna complexes. The presence of these weak resonant holes is consistent with our previous findings that TX-100 disrupts an energy transfer pathway from pigments contributing to the high-energy side of the absorption spectrum. Finally, the fact that Q_x-bleaching of $Pheo_{D1}$ occurs near 545 nm, is also in perfect agreement with data obtained for intact isolated RC (*vide supra*) and PSII core samples,[62,63] supporting our conclusion that our *isolated* RC from *C. reinhardtii* contains the largest subpopulation of *intact* RC of PSII studied so far.

3.4.3. More on site energies of $Pheo_{D1}$ and $Pheo_{D2}$.

We emphasize that knowledge of the site energies of the Chls and Pheos is important to understand the excitonic structure and excitation energy transfer in PSII RCs, as they determine the direction of the energy flow. Recall that conclusions made from the experiments with borohydride reduction of the inactive branch $Pheo_{D2}$[84]and exchange of $Pheo_{D2}$[9,43,85], as well as with partial exchange of $Pheo_{D1}$[9,43] with 13^1-hydroxy Pheo (*vide supra*)[9,43], which suggested that both pheophytins have their Q_y absorption maxima at 676–680 nm (at 6 K), are inconsistent with data shown above. In addition, the blue shift of both the Q_x and Q_y transitions of $Pheo_{D1}$ in destabilized RCs (see Figure 3-4) is consistent with resonance Raman spectroscopy data[77], where it was suggested that $Pheo_{D1}$ in the PSII RC is likely H-bonded (as $BPheo_L$ in the BRC[78,79]), with the glutamin residue D1-Gln130 being the likely homologue of the glutamic acid residue L-104

in BRC. That is, in the *Synechocystis* site-directed mutation, D1-Gln130Leu results in the shifting of the Q_x band to shorter wavelength consistent with a disappearance of the $C13^1$=O hydrogen bond. Different Q_x and Q_y positions of $Pheo_{D1}$ and $Pheo_{D2}$ also suggest that only $Pheo_{D1}$ is H-bonded.[70] Thus we suggest that the H-bond of $Pheo_{D1}$ can be easily broken in destabilized RCs, as shown by the blue shift of the Q_y-absorption band in Figure 3-4. Finally, the different Q_y positions of $Pheo_{D1}$ and $Pheo_{D2}$ are consistent with an earlier suggestion in Ref.[77] that one possible distinction between the active and inactive branches of the PSII RC might be the presence of a H-bonded pheophytin on the active branch and the absence of a hydrogen bond on the inactive branch. The latter is consistent with data presented above, but contradictory to conclusions reached in[70] that the Q_x transitions of both pheophytins located at 543 nm imply that both pheophytins have a H-bond to the C_{13}^1=O of equal strength. Other groups also concluded that the $Pheo_{D1}$ contributes to the low-energy state near 681 nm.[5,39,44,86-88] Several earlier studies also indicated that the site-energy of $Pheo_{D2}$ Q_y-state must be located near 668–672 nm[28,36,39,86-88], in agreement with the results presented in this paper.

3.4.4. Excitonic calculations.

In calculations of absorption spectra (and of the difference spectrum shown in Figure 3-6), inhomogeneous broadening was treated via Monte Carlo methods, while homogenous broadening was included by convoluting the calculated spectra with an assumed single site (SSA) spectrum for absorption. The parameters used for the SSA curve (i.e.,zero phonon line width = 0.5 cm^{-1}, S = 0.6, ω_m = 17 cm^{-1}) were taken from[6]. Vibrational modes of Chl *a* were adopted from[83]. For simplicity we neglected lifetime broadening effects on homogenous linewidths. All pigment site energies tested so far, which can describe the absorption spectra of WT RC and its D2-L209H mutant, as well as their difference shown in Figure 3-6, have in

common that the site energy of $Pheo_{D1}$ must be near 679–681 nm, in agreement with our experimental data reported above, and previously published results.[5,28,36,39,44,86-88]

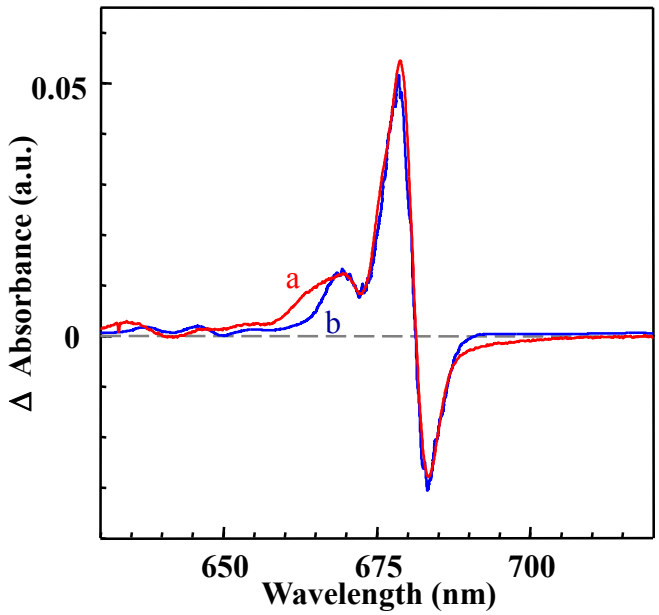

Figure 3-6 The red curve a (curve c from Figure 3-2) corresponds to absorbance difference spectrum obtained for WT RC and its D2-L209H mutant, assuming a dipole strength ratio of Pheo a/Chl a of 0.5[56]. The blue curve (spectrum b) was obtained using excitonic calculations (see text).

The other common property of the parameter sets resulting in good fits to the difference spectrum shown in Figure 3-6 is that the site energy of $Pheo_{D2}$ used in the modeling was near 670 nm. In addition, our modeling data confirm that the site energies of P_{D1} and P_{D2} found by Renger's group[13,31] are correct and must lie in the 665–667 nm region. We also confirm that the Chl_{D1} site energy must be red shifted to about 678 nm in agreement with Ref.[31] and various calculations of triplet-bottleneck spectra.[13] Discussion of site energies for PSII RCs, along with simultaneous fits of WT and mutant RC absorption, emission, triplet-bottleneck holes, and transient $P_{D1}^{+}Q_A^{-}$ - $P_{D1}Q_A$ spectra is beyond the scope of this work, and will be reported

elsewhere. Here we only say that site energies of $Pheo_{D1}$ and $Pheo_{D2}$ near 679–681 nm and ~670 nm, respectively, provide a unified description of all our optical spectra.

4. Conclusions.

A large number of isolated RC preparations from spinach and wild-type *Chlamydomonas reinhardtii* (at different levels of intactness), as well as the D2-L209H mutant, in which the active branch $Pheo_{D1}$ has been genetically replaced with Chl *a*, have been studied by HB spectroscopy. This work provides direct evidence that the biochemical treatment used to isolate D1-D2-Cytb559 RC complex may change optical properties of the RC pigments. It appears, however, that RCs with similar properties to those observed in intact PSII cores can be obtained; the latter is of critical importance, as optical spectra of PSII cores are more difficult to interpret due to possible contributions from CP43 and CP47 antenna pigment complexes.[16,34,69,89] The results presented here offer no support for the recent assignments[13,16,31,40] that site energies of $Pheo_{D1}$ and $Pheo_{D2}$ are at 672 nm and 677.5 nm, respectively. It is also unlikely that both pheophytins contribute to the absorption near 676–681 nm region as proposed in Refs.[9,43,44,90] In contrast, we have demonstrated that the Q_x-/Q_y-region site-energies of $Pheo_{D1}$ and $Pheo_{D2}$ are most likely at ~545/~680 nm and ~541.5/~670 nm, respectively, in good agreement with our previous assignment.[28,36] These values should be used to model excitonic structure and excitation energy transfer dynamics of the PSII RC. We also propose that the nonphotochemical (nonresonant) persistent holes at ~680 and ~684 nm (depending on the sample intactness), obtained via higher-energy excitation (e.g., λ_B = 665.0 nm) are, at least in part, the result of burning in the decoupled $Pheo_{D1}$ Q_y-state during the lifetime of the long lived $^3Chl_{D1}$ triplet bottleneck-state in RCs without Q_A. On the other hand, the narrow (lifetime limited) resonant holes[25,91] as well as the saturated resonant holes burned in the 678–686 nm spectral region of the

PSII RC (with no bleaching in the Q_x band of the pheophytins) are not bleached in the $Pheo_{D2}$ dominated low-energy exciton band, as suggested in[13,31,40]. On the contrary, the experimentally observed distribution of hole widths in both persistent and transient HB spectra[6,41,92] must be associated with highly dispersive primary charge separation kinetics in destabilized RC680 and intact RC684.

Abbreviations: Bacterial reaction center (BRC); Charge separation (CS); Charge separation time (τ_{cs}); Chlorophyll (Chl); Continuous wave (CW); Cytochrome b_{559} (Cyt b_{559}); D1/D2-side pheophytins ($Pheo_{D1}$/$Pheo_{D1}$); D1/D2-side special pair chlorophyll monomers (P_{D1}/P_{D2}); D1-side accessory chlorophyll (Chl_{D1}); Excitation energy transfer (EET); Fluorescence lifetime (τ_{fl}); Glutamin (Gln); Huang-Rhys factor (*S*); L/M-side bacteriochlorophylls ($BChl_{L,M}$); L/M-side bacteriopheophytins ($BPheo_{L,M}$); Laser intensity (I); Non-photochemical hole burning (NPHB); Photochemically active/inactive polypeptide chains in PSII RC (D1/D2) and in BRC (L/M); Photosystem II (PS II); Reaction center (RC); Single site absorption (SSA); Site distribution function (SDF); Triplet-bottleneck hole burning (TBHB); Wild-type (WT); Zero-phonon action (ZPA); Zero-phonon hole (ZPH)

Acknowledgements

This work was supported by the NSF ARRA Grant (CHE-090795) to R.J. Partial support to KA was provided by the NSF EPSCoR Grant. We thank M. Reppert (MIT) for insightful discussion and comments. V.Z. acknowledges support by NSERC; R.T.S. acknowledges support from USDOE, Photosynthetic Antennae Research Center; R.P. acknowledges support by MICINN (Grant AGL2008-00377) in Spain, and M.S. by the US Department of Energy's

Photosynthetic Systems Program within the Chemical Sciences, Geosciences, and Biosciences Division of the Office of Basic Energy Sciences under NREL Contract #DE-AC36-08-GO28308. M.S. also acknowledges the NREL Pension Program.

References

(1) Umena, Y.; Kawakami, K.; Shen, J.-R.; Kamiya, N. *Nature* **2011**, *473*, 55-60.

(2) Deisenhofer, J.; Epp, O.; Miki, K.; Huber, R.; Michel, H. *Nature* **1985**, *318*, 618-624.

(3) Michel, H.; Deisenhofer, J. *Biochem.* **1988**, *27*, 1–7.

(4) Deisenhofer, J. ; Michel. H. *Annu. Rev. Biophys. Biophys. Chem.* **1991**, *20*, 247–266.

(5) Nanba, O.; Satoh, N.; *Proc. Natl. Acad. Sci. U. S. A.* **1987**, *84*, 109–122.

(6) Riley, K. J.; Jankowiak, R.; Rätsep, M.; Small, G. J., Zazubovich, V. *J. Phys. Chem. B* **2004**, *108*, 10346–10356.

(7) Romero, E.; van Stokkum , I. H.; Novoderezhkin, V. I.; Dekker, J. P.; van Grondelle, R. *Biochem.* **2010**, *49*, 4300–4307.

(8) Prokhorenko, V. I.; Holzwarth, A. R. *J. Phys. Chem. B* **2000**, *104*, 11563–11578.

(9) Germano, M.; Shkuropatov, A. Ya.; Permentier, H.; de Wijn, R.; Hoff, A. J.; Shuvalov, V. A.; van Gorkom, H. J. *Biochem.* **2001**, *40*, 11472–11482.

(10) Germano, M.; Gradinaru, C. C.; Shkuropatov, A. Ya.; van Stokkum, I. H. M.; Shuvalov, V. A.; Dekker, J. P.; van Grondelle, R.; van Gorkom, H. J. *Biophys. J.* **2004**, *86*, 1164–1672.

(11) Groot, M.-L.; Peterman, E. J. G.; van Kam, P. J. M.; van Stokkum, I. H. M.; Dekker, J. P.; van Grondelle, R. *Biophys. J.* **1994**, *67*, 318–330.

(12) Xiong, L.; Seibert, M.; Gusev, A. V.; Wasielewski, M. R.; Hemann, C.; Hille, C. R; Sayre, R. T. *J. Phys. Chem. B* **2004**, *108*, 16904–16911.

(13) Raszewski, G.; Diner. B. A.; Schlodder, E.; Renger, T. *Biophys. J.* **2008**, *95*, 105–119.

(14) Diner, B. A.; Schlodder, E.; Nixon, P. J.; Coleman, W. J.; Rappaport, F.; Levergne, J.; Vermaas, W.F. J.; Chisholm, D. A. *Biochem.* **2001**, *40*, 9265–9281.

(15) Schlodder, E.; Coleman, W. J.; Nixon, P. J.; Cohen, R. O.; Renger, T.; Diner, B. A. *Phil. Trans. R. Soc. B* **2008**, *363*, 1197–1202.

(16) Cox, N.; Hughes, J. L.; Steffen, R.; Smith, P. J.; Rutherford, W.; Pace, R. J.; Krausz, E. *J. Phys. Chem. B* **2009**, *113*, 12364–12374.

(17) Andronis, C.; Merry, S.A.P.; Durrant, J.; R.; Klug, D. R.; Barber, J.; Nixon, P. J. *Photosynth. Res.* **1999**, *62*, 205–217.

(18) Alizadeh, S.; Nixon, P. J.; Telfer, A.; Barber, J.; *Photosynth. Res.* **1995**, *43*, 165–171.
(19) Xiong, J.; Subramanian, S.; Govindjee *Photosynth. Res.* **1998**, *56*, 229–254.
(20) Wang, J.; Gosztola, D.; Ruffle, S. V.; Hemann, C.; Seibert, M.; Wasielewski, M. R.; Hille, R.; Gustafson, T. L.; Sayre, R. T. *Proc. Natl. Acad. Sci. U. S. A.* **2002**, *99*, 4091–4096.
(21) Shelaev, I. V.; Gostev, F. E.; Nadtochenko, V. A.; Shkuropatov, A. Ya.; Zabelin, A. A.; Mamedov, M. D.; Semenov, A. Yu.; Sarkisov, O. M.; Shuvalov, V. A. *Photosynth. Res*. **2008**, *98*, 95–103.
(22) Holzwarth, A. R.; Müller, M.; Reus, M.; Nowaczyk, M.; Sander, J.; Rögner, M. *Proc. Natl. Acad. Sci. U. S. A*. **2006**, *103*, 6895–6900.
(23) Myers, J. A.; Lewis, K. L. M.; Fuller, F. D.; Tekavec, P. F.; Yocum, C. F.; Ogilvie, J. P. *J. Phys. Chem. Lett.* **2010**, *1*, 2774–2780.
(24) Abramavicius, D.; Mukamel, S. *J. Chem. Phys*. **2010**, *113*, 184501–1:184501–13.
(25) den Hartog, F. T. H.; Vascha, F.; Lock, A. J.; Barber, J.; Dekker, J. P.; Völker, S. *J. Phys. Chem. B.* **1998**, *102*, 9174–9180.
(26) Dědic, R.; Lovčinskỳ, M.; Vácha, F.; Hala, J. *J. Lumin*. **2000**, *87-89*, 809–811.
(27) Tang, D.; Jankowiak, R.; Seibert, M.; Yocum, C. F.; Small, G. J. *J. Phys. Chem.* **1990** *24*, 6519–6522.
(28) Jankowiak, R.; Rätsep, M.; Picorel, R.; Seibert, M.; Small, G. J. *J. Phys. Chem. B* **1999**, *103*, 9759–9769.
(29) Zazubovich, V.; Jankowiak, R.; Riley, K.; Picorel, R.; Seibert, M.; Small, G. J. *J. Phys. Chem. B* **2003**, *107*, 2862–2866.
(30) Jankowiak, R.; Rätsep, M.; Hayes, J.; Zazubovich, V.; Picorel, R.; Seibert, M.; Small, G. J. *J. Phys. Chem. B* **2003**, *107*, 2068–2074.
(31) Raszewski, G.; Saenger, W.; Renger, T. *Biophys. J.* **2005**, *88*, 986–998.
(32) Madjet, M. E.; Abdurahman, A.; Renger, T. *J. Phys. Chem. B* **2006**, *110*,17268–17281.
(33) Novoderezhkin, V. I.; Dekker, J. P; van Grondelle, R. *Biophys. J.* **2007**, *93*, 1293–1311.
(34) Novoderezhkin, V. I.; Romero, E.; Dekker, J. P.; van Grondelle, R. *ChemPhysChem* **2011**, *12*, 681–688.
(35) Saito K, Mukai, K.; Sumi, H. *Chem. Phys. Lett*. **2005**, *401*, 122–129.

(36) Jankowiak, R.; Hayes, J. M.; Small, G. J. *J. Phys. Chem. B* **2002**, *106*, 8803–8814.

(37) Reppert, M.; Zazubovich, V.; Dang, N. C.; Seibert, M.; Jankowiak, R. *J. Phys. Chem. B* **2008**, *112*, 9934–9947.

(38) Reppert, M.; Acharya, K.; Neupane, B.; Jankowiak, R. *J. Phys. Chem. B* **2010**, *114*, 11884–11898.

(39) Vasil′ev, S.; Orth, P.; Zouni, A.; Owens, T. G.; Bruce, D. *Proc. Natl. Acad. U. S. A*. **2001**, *98*, 8602–8807**.**

(40) Cox, N.; Hughes, J.; Rutherford, A.W.; Krausz, E. *Physics Procedia* **2010,** *3***,** 1601–1605.

(41) Herascu, N.; Ahmouda, S.; Picorel, R.; Seibert, M.; Jankowiak, R.; Zazubovich, V. J. *Phys. Chem. B*. **2011** (in press).

(42) Jankowiak, R.; Reppert, M.; Zazubovich, V.; Pieper, J.; Reinot, T. *Chem. Rev*. **2011,** *111*, 4546–4598.

(43) Germano, M.; Shkuropatov, A. Ya.; Permentier, H.; Khatypov, R. A.; Shuvalov, V. A.; Hoff, A. J.; van Gorkom, H. J. *Photosynth. Res*. **2000**, *64*, 189–198.

(44) Yruela, I.; Torrado, E.; Roncel, M.; Picorel, R. *Photochem. Photobiol*. **2001**, 67, 199–206.

(45) Xiong, L. Modification of the Protein Matrix around Active- and Inactive Pheophytins by Site-Directed Mutagenesis, Affects on Energy And Electron Transfer Processes in Photosystem II. Ph. D. Dissertation, The Ohio State University, Columbus, Ohio, **2002**.

(46) Kálmán, L.; Williams, J. C.; Allen, J. P. *Photosynth. Res*. **2008**, *98*, 643–655.

(47) Kirmaier, C.; Gaul, D.; DeBey, R.; Holten, D.; Schenck, C. C. *Science* **1991**, *251*, 922–927.

(48) Heller, B. A.; Holten, D., Kirmaier, C. *Science* **1995**, *269*, 940–945.

(49) Chirino A. J.; Lous, E. J.; Huber, M.; Allen, J. P.; Schenck, C. C.; Paddock, M. L.; Feher, G.; Ress, D. C. *Biochem.* **1994**, *33*, 4584–4593.

(50) Gall, B.; Zehetner, A.; Scheer, H. *FEBS Lett*. **1998**, 434, 88–92.

(51) Mimuro, M.; Tomo, T.; Nishimura, Y.; Yamazaki, I.; Satoh, K. *Biochim. Biophys. Acta* **1995**, *1232*,81–88.

(52) Vacha, F., Joseph, D. M., Durrant, J. R., Telfer, A., Klug, D. R., Porter, G., Barber, J. *Proc. Natl. Acad. Sci. U. S.A.* **1995**, *92*, 2929–2933

(53) Eijckelhoff, C.; Dekker , J. P. *Photosynth. Res*. **1997**, *52*, 69–73

(54) Dang, N. C.; Zazubovich, V.; Reppert, M.; Neupane, B.; Picorel, R.; Seibert, M.; Jankowiak, R. *J. Phys. Chem. B* **2008**, *112*, 9921–9933.
(55) Neupane, B; Dang, N. C.; Acharya, K.; Reppert, M.; Zazubovich, V.; Picorel, R.; Seibert, M.; Jankowiak, R. *J. Am. Chem. Soc.* **2010**, *132*, 4214–4229.
(56) Årsköld, S. P.; Masters, V. M.; Prince, B. J.; Smith, P. J.; Pace, R. J.; Krausz, E. *J. Am. Chem. Soc*. **2003**, *125*, 13063–13074.
(57) Peterman, E. J. G.; van Amerongen, H.; van Grondelle, R.; Dekker, J. P. *Proc. Natl. Acad, Sci. U. S. A*. **1998**, *95*, 6128–6133.
(58) Pearlstein, R. M. In *Photosynthesis: Energy Conversion by Plants and Bacteria*; Ed., Govindjee ; Academic press: New York, 1982; Vol. 1, pp. 293–330.
(59) Hughes, J. L.; Razeghifard, R.; Logue, M., Oakley, A.; Wydrzynski, T.; Krausz, E. *J. Am. Chem. Soc*. **2006**, *128*, 3649–3658.
(60) Housssier, C.; Sauer, K.; *J. Am. Chem. Soc*. **1970**, *92*, 779–791
(61) Shipman, L. L.; Cotton, T. M.; Norris, J. R.; Katz, J. J. *J. Am. Chem. Soc*. **1976**, *98*, 8222–8230.
(62) Krausz, E.; Hughes, J. L.; Smith, P.; Pace, R.; Årsköld, S. P. *Photochem. Photobiol. Sci*. **2005**, *4*, 744–753.
(63) Hughes, J. L.; Smith, P.; Pace, R.; Krausz, E. *Biochim. Biophys. Acta* **2006**, *1757*, 841–851.
(64) Jankowiak, R.; Small, G. J. In *The Photosynthetic Reaction Centers*; Eds. Norris J. and Deisenhofer J.; Academic Press: New York,1993; p133.
(65) Chang, H.-C.; Jankowiak, R.; Reddy, N. R. S.; Yocum, C. F.; Picorel, R.; Seibert, M., Small, G. J. *J. Phys. Chem.* **1994**, *98*, 7725–7735.
(66) Steffen, M. A.; Lao, K.; Boxer, S. G. *Science* **1994**, *264*, 810–816.
(67) Reddy, N. R. S.; Kolaczkowski, S. V.; Small, G. J. *Science* **1993**, *260*, 68–71.
(68) Saito, K.; Ishida, T.; Sugiura, M.; Kawakami, K.; Umena, Y.;Kamiya, N.; Shen, J.-R.; Ishikita, H. *J. Am. Chem. Soc.* **2011**, DOI: 10.1021/ja203947k.
(69) Renger, T.; Schlodder, E. *ChemPhysChem* **2010**, *11*, 1141–1153.
(70) Diner, B. A.; Rappaport, F. *Annu. Rev. Plant Biol*. **2002**, *53*, 551–580.

(71) Seibert, M. In *The Photosynthetic Reaction Centers*; Eds., Norris J. and Deisenhofer J.; Academic Press: New York,1993; p. 319.
(72) Jankowiak, R.; Hayes, J. M.; Small, G. J. *Chem. Rev* **1993**, *93*, 1471–1502.
(73) Durrant, J. R.; Klug, D. R.; Kwa, S. L. S.; van Grondelle, R.; Porter, G.; Dekker, J. P. *Proc. Natl. Acad. Sci. U. S. A.* **1995**, *92*, 4798–4802.
(74) Tetenkin, V. L.; Gulyaev, B. A.; Seibert, M.; Rubin, A. B. *FEBS Lett.* **1989**, *250*, 459–463.
(75) van Kan, P. J. M.; Otte, S. C. M.; Kleinherenbrink, F. A. M.; Nieveen, M. C.; Aartsma, T. J.; van Gorkom, H. J. *Biochim. Biophys. Acta.* **1990**, *1020*, 146–152.
(76) van Mieghem, F.; Brettel, K.; Hillmann, B.; Kamlowski, A.; Rutherford, A. W.; Schlodder, E. *Biochem*. **1995**, *34*, 4798–4813.
(77) Moënne-Loccoz, P.; Robert, B.; Latz, M. *Biochem*. **1989**, *28*, 3641–3645.
(78) Bylina, E. J.; Kirmaier, C.; McDowell, L.; Holten, D.; Youvan, D. C. *Nature* **1988**, *336*, 182–184.
(79) Clyton, R. K.; Yamamoto, T.; *Photochem. Photobiol*. **1976**, *24*, 67–70.
(80) Pieper, J.; Voigt, J.; Small, G. J. *J. Phys. Chem. B* **1999**, *103*, 2319–2322.
(81) Gillie, J. K.; Small, G. J. Golbeck, J. H. *J. Phys. Chem*. **1989**, *93*, 1620–1627.
(82) Avarmaa, R. A.; Rebane, K. K. *Spectrochimica Acta* **1985**, *41A*, 1365–1380.
(83) Rätsep, M.; Pieper, J.; Irrgang, K-D.; . Freiberg, A. J. Phys. Chem. B 2008, 112, 110–118.
(84) Shkuropatov, A. Y.; Khatypov, R. A.; Volsh-chukova, T. S.; Shkuropatova, V. A.; Owens, T. G.; Shuvalov, V. A. *FEBS Lett.* **1997**, *420*, 171–174.
(85) Shkuropatov, A. Y.; Khatypov, R. A.; Zverreva, M. G.; Shkuropatova, V. A.; Owens, T. G.; Shuvalov, V. A. *FEBS Lett*. **1999**, *450*, 163–167.
(86) Konermann, L.; Holzwarth, A. R. *Biochem*. **1996**, *35*, 829–842.
(87) Mimuro, M.; Tomo, T.; Nishimura, Y.; Yamazaki, I.; Satoh, K. *Biochim. Biophys. Acta* **1995**, *1232*, 81–88
(88) Stewart, D. H.; Nixon, P. J.; Diner, B. A.; Brudvig, G. W. *Biochem.* **2000**, *39*, 14583–14594.
(89) Vassiliev, S.; Bruce, D. *Photosynth. Res*. **2008**, *97*, 75–89.
(90) Saito, K.; Mukai, K.; Sumi, H. *Chem. Phys. Lett.* **2005**, *401*, 122–129.

(91) den Hartog, F. T. H.; Dekker, J. P.; van Grondelle, R.; Völker, S. *J. Phys. Chem. B* **1998**, *102*, 11007–11016.
(92) Groot, M.-L.; Dekker, J. P; van Grondelle, R.; den Hartog, F. T. H.; Völker, S. *J. Phys. Chem*. **1996**, *100*, 11488–11495.

Chapter 4 - Primary Electron Donor(s) in Isolated Reaction Center of Photosystem II from *Chlamydomonas reinhardtii*

Khem Acharya[1], Valter Zazubovich[2], Mike Reppert[3], and Ryszard Jankowiak[1,4,*]

[1]Department of Chemistry and [4]Department of Physics, Kansas State University, Manhattan, KS 66506; [2]Department of Physics, Concordia University, Montreal, Quebec, Canada; [3]Department of Chemistry, MIT, Cambridge, MA 02139

Abstract

Isolated reaction centers (RCs) from wild-type *Chlamydomonas (C.) reinhardtii* of Photosystem II (PSII), at different levels of intactness, were studied to provide more insight into the nature of the charge-separation (CS) pathway(s). We argue that previously studied D1/D2/Cyt_{b559} complexes (referred to as RC680), with Chl_{D1} serving as the primary electron donor, contain destabilized D1 and D2 polypeptides and, as a result, do not provide a representative model system for the intact RC within the PSII core. The shapes of non-resonant transient hole-burned (HB) spectra obtained for more intact RCs (referred to as RC684) are very similar to $P^+Q_A^-$ - PQ_A absorbance difference and triplet minus singlet spectra measured in PSII core complexes from *Synechocystis* PCC 6803 [Schlodder et al. *Phil. Trans. R. Soc. B* **2008**, *363*, 1197]. We show that in the RC684 complexes both P_{D1} and Chl_{D1} may serve as primary electron donors, leading to two different charge separation pathways. Resonant HB spectra cannot distinguish the CS times corresponding to different paths, but it is likely that the zero-phonon holes (ZPHs) observed in the 680-685 nm region (corresponding to CS times of ~1.4–4.4 ps) reveal the Chl_{D1} pathway; conversely the observation of charge-transfer (CT) state(s) in RC684 (in the 686-695 nm range) and the absence of ZPHs at $\lambda_B > 685$ nm, likely stems from the P_{D1} pathway, for which CS could be faster than 1 ps. This is consistent with the finding of Krausz et al. [*Photochem. Photobiol. Sci.* **2005**, 4, 744] that CS in intact PSII core complexes can be initiated at low temperatures with fairly long-wavelength excitation. The lack of a clear shift of HB spectra as a function of excitation wavelength within the red-tail of the absorption (i.e. 686–695 nm) and the absence of ZPHs suggests that the lowest-energy CT state is largely homogeneously broadened. On the other hand, in usually studied destabilized

RCs, i.e. RC680, for which CT states have never been experimentally observed, Chl_{D1} is the most likely electron donor.

4.1. Introduction

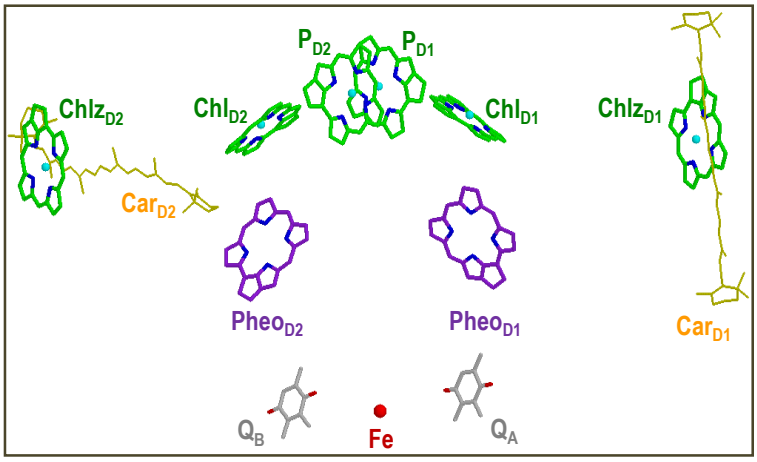

Figure 4-1 Cofactor arrangement in the active (D1) and inactive (D2) branches of photosystem II reaction center from crystal structure of *T. vulcanus* at 1.9 Å resolution, PDB ID 3ARC.[2] The cofactors are color coded as, chls: green, carotenes: yellow, pheophytins: purple, plastoquinones: gray, non-heme iron: red, and Nitrogen: blue. The substituents of the cofactors are truncated for clarity.

Photosystem II (PSII), the only protein complex capable of evolving oxygen, performs the primary charge separation (CS) in the D1/D2/Cyt_{b559} reaction center (RC)[1] in oxygenic photosynthesis (plants, cyanobacteria, and algae). According to the recent X-ray crystal structure[2] (from *T. vulcanus*) the PSII RC complex contains six chlorophyll (Chl) and two pheophytin (Pheo) molecules, two plastoquinones (Q_A and Q_B), two β-carotene molecules (Car_{D1} and Car_{D2}), a cytochrome b-559 (Cyt b-559), and a non-heme iron. Figure 4-1, based on the recent crystal structure of PSII (PDB ID 3ARC)[2], shows a schematic arrangement of the six Chls, two Pheos, Q_A, Q_B, Car_{D1} and Car_{D2} molecules and a non-heme iron (Fe). This structure further confirmed that the amino acid sequences of the membrane bound polypeptides D1 and D2 subunits of PSII RC are homologous to their counterparts L and M subunits, respectively, of purple bacterial RC (BRC), whose crystal structure[3] has been solved at atomic resolution earlier. The P_{D1} and P_{D2} Chls are structurally analogous to the P_L and P_M BChls of the bacterial special pair, respectively, while the $Chl_{D1,D2}$ and $Pheo_{D1,D2}$ molecules correspond to the monomeric $BChl_{L,M}$ and $BPheo_{L,M}$ molecules (where the subscripts represent the respective polypeptide

chains to which the chlorines are bound).[4] Unlike in BRC, PSII RC contains two additional peripheral Chls, bound by the histidines of D1 and D2 polypeptides, and sometimes referred to as $Chlz_{D1}$ and $Chlz_{D2}$.[5] In both BRC and PSII RCs, the pigments are organized and function in a similar way, with a structural pseudo-C_2 structural symmetry but functional asymmetry of their two branches D1/L and D2/M.[6] By analogy with the BRC, it is believed that the D1 protein chain of PSII RC is photochemically active, and thus the P_{D1}/P_{D2}, Chl_{D1}, and $Pheo_{D1}$ molecules participate in primary charge separation.[1] The two Chl monomers, P_{D1} and P_{D2}, form a dimer with a partial structural overlap, stabilized by van der Waals interaction of about −17 kcal mol^{-1}.[7] Differences in the immediate environment of the two pigments of the dimer cause localization of the major portion of dimer's HOMO at the monomer P_{D1}.[7] It has also been recently shown that redox potential (E_m) of P_{D1} for one electron oxidation ($E_m(P_{D1})$) is lower than that of P_{D2}, favoring the localization of the cationic charge of the primary charge transfer (CT) state on P_{D1}.[8]

Since the first isolation of the PSII RC in 1987 by Nanba and Satoh[9], its biophysical processes, including excitation energy transfer (EET) and primary charge separation (CS), have been the subject of many studies: spectral hole-burning (SHB),[10-14] stark spectroscopy[15], photon echo,[16] time-resolved fluorescence,[17] visible pump-probe[18], 2D spectroscopy,[19] mutagenesis studies[20-23], and theoretical calculations.[24-26] Although in recent years consistent progress has been made in comprehending the electronic structure and charge transfer dynamics of PSII RC, [25,27,28] an adequate global understanding of this complex system has yet to be achieved.

One significant obstacle to our understanding of the PSII RC is that, in contrast to the BRC (which can be isolated and crystallized while maintaining full functional), the PSII RC is considerably more fragile during isolation and interrogation procedures[29] and retains only limited PSII functionality in its isolated form.[28] Although isolation and purification protocols have been

consistently improved over the years, these complexes are highly fragile and the right choice of buffer and detergent is critical; for example, use of Triton X-100 has been found to significantly affect the low temperature absorption and persistent hole spectra and to disrupt the charge transfer from accessory Chl *a* to the active pheophytin ($Pheo_{D1}$).[11] Moreover, it has been reported that some integral parts of the native PSII RC, i.e. Q_A and Q_B secondary electron acceptors, as well as 4-Mn clusters, are lost during the isolation.[9,21] It has also been suggested that the isolated RC samples possess two subsets of RCs, destabilized RC680 and more intact RC684, the latter being vulnerable and changing to RC680 upon biochemical manipulation.[13,30] In this regard, it is likely that after isolation, the coupling between P_{D1} and P_{D2} is weakened, resulting in the blue-shifted absorption spectrum. Our current data also suggest (see section 3.1) that all previously studied RCs from spinach were destabilized with the electronic structure significantly different with respect to that observed in intact PSII core[27,31] complexes, calling into question the validity the use of the isolated RCs as model systems of intact RC in PSII core.

In addition to these sample preparation considerations, the PSII RC is considerably more difficult to study than its purple bacterial counterpart due to the inherent spectral congestion of the Q_y absorption region of the PSII RC.[32] In contrast to the three well-resolved absorption bands per 6 pigments of the BRC from *Rps. Viridis*[33], the low temperature Q_y-region absorption spectrum of the PSII RC displays only two obvious Q_y bands corresponding to 8 pigments (6 Chl and 2 Pheo). This severe spectral congestion both makes it very difficult experimentally to selectively excite any particular state (or pigment) and introduces significant uncertainty in theoretical interpretation of the transient absorption data in both time- and frequency-domain experiments since ultrafast energy-equilibration, radical pair formation and excitation energy transfer all happen in the same narrow spectral region.[34]

Thanks in part to these technical difficulties, there are still numerous issues to be addressed regarding primary CS processes in the PSII RC. For example, the question of whether the primary electron donor is P_{D1} or Chl_{D1}[27,28,34,35] is still controversial. Also, the site energies of RC pigments reported in various papers are not consistent.[17,24,26,35,36] A recent modeling study[24,36] of the electronic structure of PSII RC has suggested that the mean site energy of $Pheo_{D1}$ is near 672 nm, whereas that of $Pheo_{D2}$ is at ~ 677.5 nm. We show that the Q_x-/Q_y-region site-energies of $Pheo_{D1}$ and $Pheo_{D2}$ in PSII RC are ~545/680 nm and ~541.5/670 nm, respectively.[37] Furthermore, although spectral features interpreted as belonging to the primary CT state were experimentally observed in the intact PSII core[31], such features have never been identified in the isolated PSII RC; moreover, the nature of the suggested CT state still remains to be unequivocally resolved.

In order to provide more insight into the nature of the PSII RC, and resolve the aforementioned issues, we focus our SHB studies on the isolated RCs obtained from *Chlamydomonas (C.) reinhardtii*. To our knowledge, there are only a few studies of the isolated algal PSII RC from *C. reinhardtii* because of the difficulties of their preparation.[5,20,21,38] *C. reinhardtii,* a unicellular green alga flagellate possessing a single chloroplast, is an important model for the fundamental studies of photosynthesis as well as for molecular biology studies.[39] In this manuscript, we present optical spectra such as low-T absorption, and transient hole-burned (HB) spectra obtained for isolated PSII RC from *C. reinhardtii*, at different levels of intactness, studied during the last five years. A new assignment of the Q_x- and Q_y-region site energies of $Pheo_{D1}$ and $Pheo_{D2}$ (based on mutational and modeling study, and incompatible with[24,36]) is published elsewhere.[37] Here we report the comparison of our RC data with those previously obtained for the isolated spinach RC[10-14] and the PSII core[27,31,36], and demonstrate that

previously studied isolated D1/D2/Cytb559 complexes had destabilized D1 and D2 polypeptides and therefore do not provide a proper model system for the intact RC within the PSII core. Our results reported below indicate that the nature of the primary electron donor in isolated PSII RC depends on its intactness. Our findings should be useful for future modeling of the excitonic structure, which should provide a more complete picture of the EET pathways and charge separation (CS) in PSII core complexes.

4.2. Experimental section

Photosystem II RC complexes from *C. reinhardtii* containing 6 Chls per 2 Pheos from both thylakoids and PSII-enriched membranes following the method of Nanba and Satoh[9], with important modifications[21], were prepared by Dr. R. Picorel in Dr. M. Seibert's laboratory at NREL (Golden, CO). Preparation of isolated RCs from both thylakoids or PSII-enriched membranes and their basic spectroscopic characterization and pigment analysis is described in [37].

The hole burning apparatus and measurements were described in detail elsewhere.[40] Briefly, a Bruker HR125 Fourier transform spectrometer and a Janis 8-DT Super Vari-Temp liquid helium cryostat were used to measure the absorption and HB spectra at 5 K. Non-resonant and resonant HB spectra were recorded at a resolution of 4 and 0.5 cm^{-1}, respectively. For some non-resonant HB a 496.5 nm Coherent Innova 200 argon ion laser was employed. For resonant HB experiments, a tunable Coherent CR699-21 ring dye laser (Exciton LD688; range 650-710 nm; linewidth of 0.07 cm^{-1}) was used, pumped by a 532 nm Spectra-Physics Millennia diode laser. The latter laser system was also used to obtain nonresonant HB spectra with 665.0 nm excitation. The laser output was stabilized using LPC from Brockton Electro-Optics Corp. Sample temperature was read and stabilized with a Lakeshore Cryotronic model 330 temperature

controller. The transient spectra reported in this work correspond to the difference of absorption spectrum with laser on and absorption spectrum with laser off. This difference is due to dynamic depopulation of the singlet ground state for the duration of the (long) lifetime of either triplet state (triplet-bottleneck hole) or charge-separated state. Burn intensities and times are given in the figure captions.

4.3. Results

4.3.1 Low temperature absorption spectra for isolated RC of C. reinhardtii.

Frames A – C of Figure 4-2 show the Q_y- (main frames) and Q_x-region (respective insets) absorption spectra obtained for three RC samples from *C. reinhardtii* (out of ten samples studied). The grey dashed curves in frames A and B of Figure 4-2 correspond to the absorption spectrum from frame C (shown for comparison). These data are representative of variability observed in both absorption and transient HB spectra (frames E–F) of isolated RCs studied in our laboratory. Samples whose absorption spectra are shown in frames A–C of Figure 4-2 will be referred to as RC_{S1}, RC_{S2} and RC_{S3} respectively. Absorption spectra are normalized at the Q_x transition of the pheophytins (Pheos) and are similar (but not identical) to those typically observed in the PSII RC of spinach.[10-14,32] The integrated absorption in all three samples is

similar, in agreement with pigment extraction analysis, which showed that all preparations had a

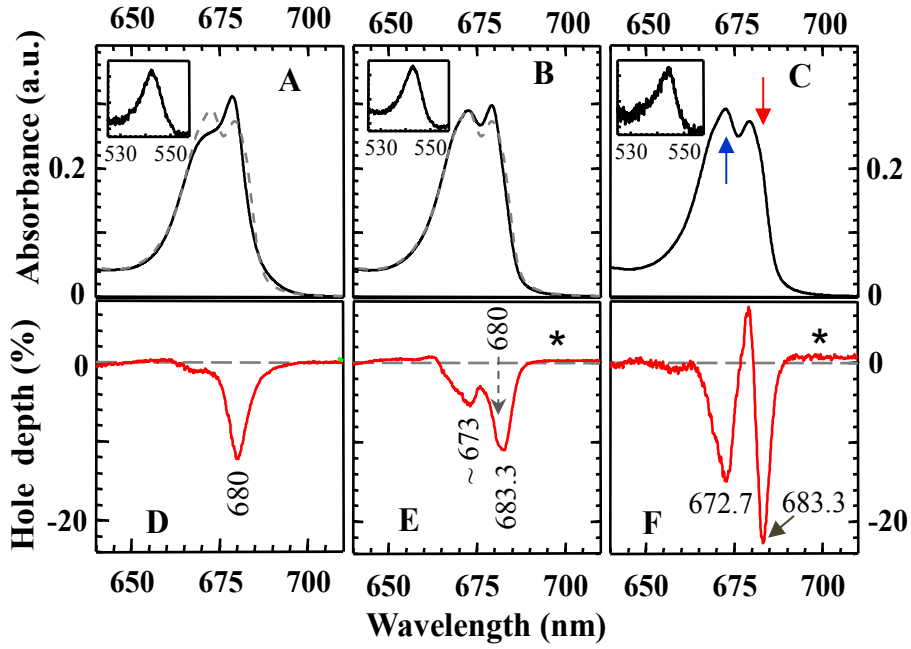

Figure 4-2 Normalized absorption spectra (at Q_x transition of Pheos) of three representative RC samples RC_{S1}, RC_{S2}, and RC_{S3} (obtained from *C. reinhardtii*) are shown in the frames A, B, and C, respectively. Corresponding transient HB spectra are shown in frames D, E, and F. The insets in frames A, B and C show the Q_x absorption band of pheophytins. All HB spectra were obtained with λ_B = 665.0 nm and laser intensity of ~100 mW/cm^2. The dotted gray curve in frames A and B is the absorption spectrum from frame C and is shown for easy comparison. All spectra were measured at T = 5 K.

similar number of Chls per two Pheos (i.e. 6.0±0.5 Chl *a* per 2 Pheo *a*), as discussed in[37]. Furthermore, there was no indication that any of these samples were contaminated with antenna complexes, *i.e.* no bleaching and/or emission characteristic for PSII antenna complexes[41,42] was observed. Comparison of the three frames reveals that the major differences between absorption spectra of RC_{S1}, RC_{S2}, and RC_{S3} samples occur near 673 nm and 684 nm. The comparison of the Q_x-regions, on the other hand, shows similar spectral shapes with the same integrated area, but with a slightly red-shifted Q_x-band of pheophytins in RC_{S3}. The maxima of the Pheo Q_x-band in

RC_{S1}, RC_{S2}, and RC_{S3} are at 542.5, 543.0 (most frequently observed Q_x-transition wavelength of both pheophytins[43-45]), and 544.2 nm, respectively. The position of the most red-shifted RC_{S3} Q_x-band is similar to that observed in intact PSII core complexes[31,46], suggesting that the RC_{S3} sample is the most intact one. Based on the above-mentioned discrepancies in the Q_x- and Q_y-regions (along with varied intensities near ~673 nm and at ~684 nm) we suggest that RC_{S1}, RC_{S2}, and RC_{S3} consist of varying proportions of different subpopulation of RCs, in agreement with our earlier RC680/RC684 model for isolated RCs from spinach[13,32]; see section 4.1 for discussion.

4.3.2. Nonresonant transient HB spectra.

Frames D, E, and F in Figure 4-2 show transient holes obtained for RC_{S1}, RC_{S2}, and RC_{S3} samples, respectively, with excitation wavelength (λ_B) of 665.0 nm at T = 5 K. As described in the experimental section, transient holes in our measurements are due to dynamic depopulation of the singlet ground state for the duration of the (long) lifetime of either triplet state (triplet-bottleneck hole) or charge-separated state. The transient HB signal thus serves as a specific indicator on the presence of these types of excited states. Note that the positions/shapes and depths of the transient holes in frames D, E and F are significantly different. For example, the transient hole spectrum of RC_{S1} (frame D) has a bleach at ~680 nm, typically observed in isolated RC from spinach,[11,12,14] while those of RC_{S2} (frame E) and RC_{S3} (frame F) have pronounced bleaches at ~673 nm and at ~683–684 nm. Also note that the delta absorption in the longer wavelength (> 690 nm) region in frame D (and in Refs[11,12,14]) is zero, while a weak positive delta absorption (see asterisks) is observed in frame E and, especially, in frame F (see also Figure 4-5 below). Note that while the transient hole of RC_{S1} is similar to those of previously studied RCs,[10,32,47] and to flash-induced ($^3P - {}^1P$) absorption spectra of PSII cores,[23,48] the transient hole obtained for RC_{S3} is similar (though not perfectly identical) to flash-induced

($P680^+Q_A^-$ - $P680Q_A$) absorption difference spectra of the intact PSII core[22,27,30,48]. These differences in optical spectra of different RC preparations, in particular in transient holes, suggest a large heterogeneity of all isolated RCs studied so far, most likely due to the presence of different RC subpopulations, with the RC_{S1} transient HB features arising largely from a long-lived triplet state and the RC_{S3} spectra from transient chemical oxidation and accompanying electrochromic shifts (i.e. $P^+Q_A^-$ - PQ_A). In this light, we will argue below that some of our more intact RCs contain plastoquinone, Q_A, which is lost in isolated RCs from spinach.[9,21] We will also argue that the spectra shown for RC_{S1} in frames A and D of Figure 4-2 correspond to the destabilized RCs (referred to as RC680), which are similar to the often studied isolated RCs from spinach [11,12,14], whereas the data shown for RC_{S3} in frames C and F represent the most intact isolated RCs studied so far. The latter closely resembles the RCs within PSII cores.[27,31,36] Intact RCs will be referred to as RC684. The data in frames B and E can be understood assuming that RC_{S2} sample represents a mixture of RC_{S1} and RC_{S3} samples (see Figure 4-4A for details).

Figure 4-3 shows the comparison of two transient holes (λ_B = 665.0 nm) obtained for our most intact sample (RC_{S3}; curve a) and partly damaged RC_{S3d} (obtained by allowing the RC_{S3} sample to interact with a buffer/glycerol mixture at room temperature in the presence of light for about five minutes; curve b). Curves a and b are normalized at ~673 nm. Interestingly, the difference between the spectra of damaged and intact samples (red curve c = b – a) reveals contribution resembling a transient hole typically observed in RC680 (i.e. to transient spectra of many previously studied RCs isolated from spinach.[10,32,47]), clearly indicating that RC684 are not stable after isolation and are very sensitive to sample handling procedures. Note that the hole in curve c (peaking at ~680 nm) is also very similar to the transient hole reported in frame D of Figure 4-2 (RC_{S1} sample).

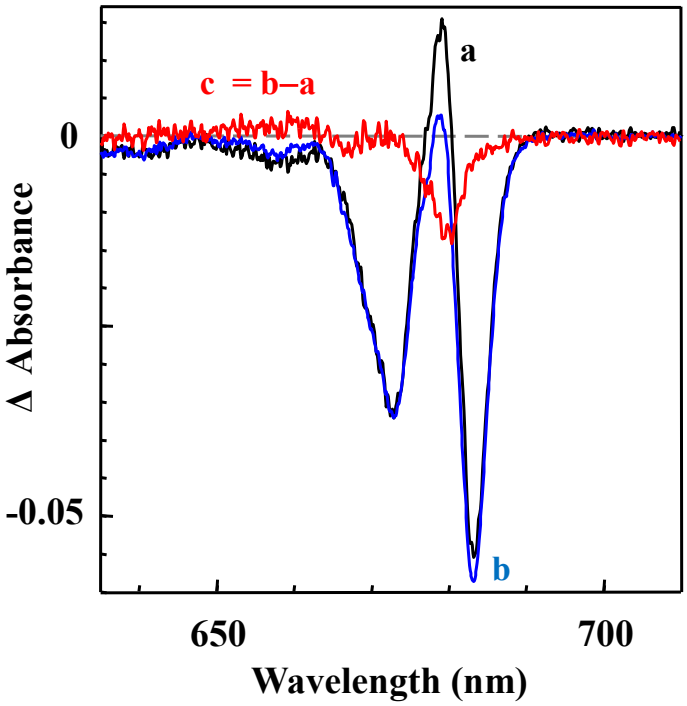

Figure 4-3. Transient HB spectra. Curves a and b represent the transient HB spectra of intact and partly damaged RC_{S3d} obtained with λ_B = 665.0 nm and laser intensities I = 100 mW/cm^2, respectively. The difference between curves b and a is shown as curve c.

Frames A and B of Figure 4-4 show that the shapes of transient HB spectra in RC_{S2} and RC_{S3} depend on excitation wavelength (although for RC_{S3} the effect is significantly smaller than for RC_{S2}). The curves a (a') and b (b') were obtained with λ_B of 665.0 nm and 496.5 nm, respectively. Note that curves a and b in frame A for RC_{S2}, when normalized at ~673 nm bleach, have significantly different behavior near 680 nm, in contrast to curves a' and b' in frame B (RC_{S3}). Although we will not make any assumptions as to why exactly excitation at different wavelengths results in preferential transient bleaching of different pigments in the RC or of different RC sub-populations in the heterogeneous samples, the very existence of qualitative

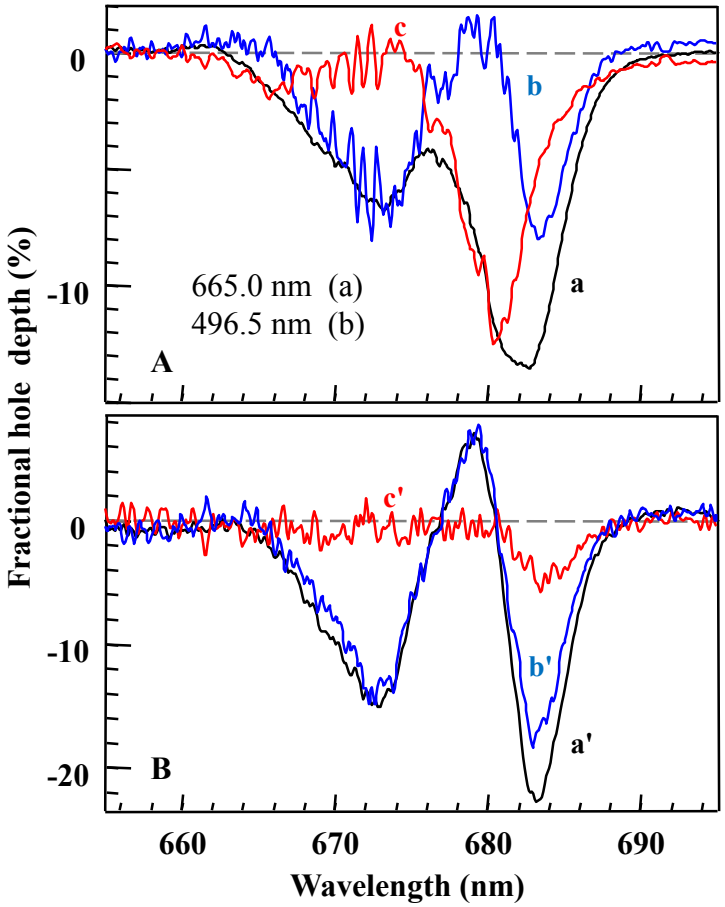

Figure 4-4 Transient HB spectra. Frames A and B represent the transient HB spectra of RC_{S2} and RC_{S3}, respectively, obtained with λ_B of 665.0 nm (curves, a/a') and 496.5 nm (curves, b/b'). The red curves c/c' are obtained as the difference of a/b and a'/b', which correspond to triplet bleach in RC680 and RC684, respectively.

differences between transient holes obtained with λ_B of 665.0 nm and 496.5 nm indicates the presence of such different subpopulations. Thus, the differences between transient holes reflect selected/amplified contributions from one or another subpopulation. The difference between spectra a and b in Frame A (RC_{S2}; curve c) exhibits a major bleach at 680 nm. This bleach is very similar to that observed in RC_{S1} (Figure 4-2D) and isolated spinach RCs[10,32,47]. Note that this hole is also nearly indistinguishable from curve c in Figure 4-3 corresponding to deliberately destabilized sample RC_{S3d}. On the other hand, the difference between spectra a′ and b′, in Frame

B, exhibits major contribution at ~684 nm. The fact that near 684 nm one transient hole (curve a') is deeper than another (curve b') may have interesting implications that are discussed in Section 4.3. Here we only mention that these differences are likely connected to the presence of two different sub-populationsof intact isolated RCs, namely with Q_A present and absent. Note that a similar band near 684 nm (manifested as a weak shoulder) was often observed in isolated spinach RC in transient HB experiments,[13,32,49] and by a selective 685 nm excitation in evolution-associated difference spectra (EADS) in time-resolved experiments[34], although the origin of such contribution was interpreted differently (see section 4.3). Spectrum b' (frame B) has more positive absorbance near 680 nm than spectrum b (in frame A). This is consistent with RC_{S2} having more contribution from the destabilized RC680 complexes. This also agrees with the major bleach in curve a' (RC_{S3} sample; Figure 4-4B) being red-shifted (to ~683.3 nm) in comparison with curve a obtained for RC_{S2} and shown in Figure 4-4A (~682 nm).

A weak but distinct positive absorption feature is observed in the transient HB spectra of the RC_{S3} and RC_{S2} samples in the long wavelength region (690–860 nm). The main frame of Figure 4-5 shows a close-up view of this feature observed in the nonresonant transient HB spectrum (λ_B = 665 nm, I = 100 mW/cm^2). The positive transient response is the strongest in RC_{S3} sample, although similar behavior was also observed in RC_{S2}, in particular for the resonant excitation at λ_B = 682.0 nm as shown in the left inset of Figure 4-5 for four different laser burn intensities (1, 5, 50, and 150 mW/cm^2). Although a full discussion of these features will be provided in Section 4.2 below, we should note here that similar absorbance increase have been observed in chemically oxidized RCs[50] and flash-induced ($P684^+Q_A^-$ - $P684Q_A$) absorbance difference spectra of PSII core complexes from WT *Synechocystis sp.* PCC6803[22,27,48], which should possess intact RCs. We stress that such behavior has never been observed in (isolated)

destabilized RC680 complexes previously studied under identical conditions. In agreement with our earlier observations on transient response in the 670 – 690 nm region, the similarity of these spectra to flash-induced ($P684^{+}Q_A^{-}$ - $P684Q_A$) difference spectra suggest that at least some fraction of the RC684 samples studied here retain the attached plastoquinone Q_A and are capable

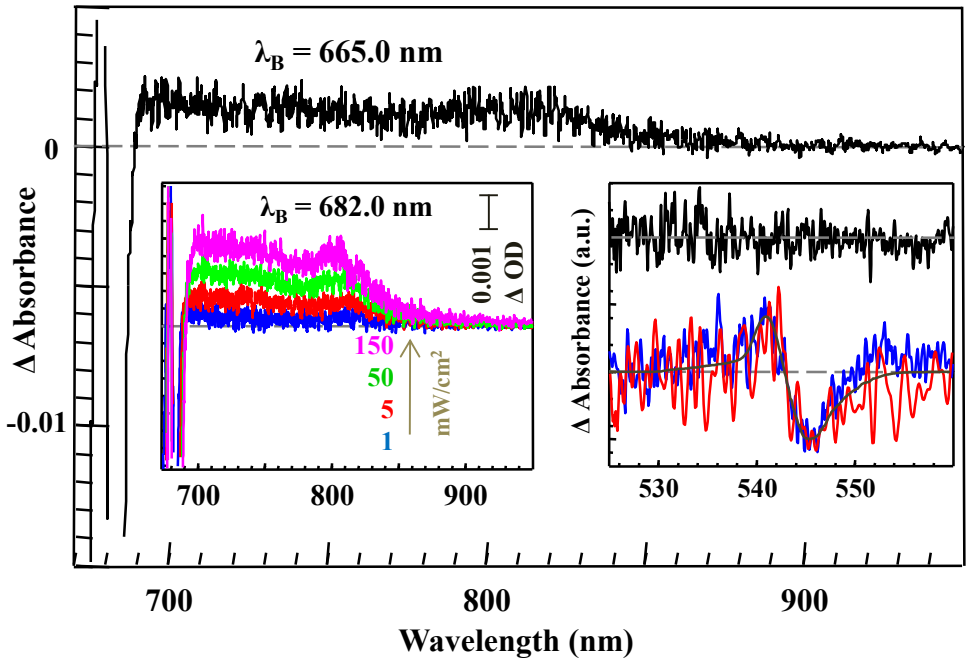

Figure 4-5 Transient hole-burned spectra of various RC samples. In the main frame, black curve represents the absorbance due to the oxidation of P_{D1} of RC_{S3}, obtained with λ_B of 665 nm and intensity of 100 mW/cm^2. Left inset corresponds to the absorption of P_{D1}^{+} in RC_{S2} obtained with λ_B of 682 nm and laser burn intensities (I) of 1, 5, 50, and 150 mW/cm^2. Right inset represents the electrochromic shift in Pheo Q_x-band of spinach RC sample (black), RC_{S2} (blue), and RC_{S3} (red) obtained with λ_B of 665.0 nm.

of forming the transient $P684^{+}Q_A^{-}$ state. By the same token, the absence of this response in RC680 preparations suggest that isolated RC680 and RC684 samples may possess different charge separation pathways as will be discussed in more detail in sections 4.1–4.3. Note, however, that our attempts to directly identify the presence of Q_A in RC_{S3} via extraction of

cofactors and subsequent mass spectrometry and NMR experiments were inconclusive, most likely due to very small amounts of these highest-intactness RCs available for these measurements.

4.3.3. Resonant hole-burned (HB) spectra.

Figure 4-6 shows nonresonant transient HB spectrum (4 cm^{-1} resolution) obtained with λ_B = 496.5 nm (dashed black line), and resonant transient HB spectra (0.5 cm^{-1} resolution) for RC_{S3} sample obtained with λ_B = 682.0 (green curve a), 684.0 (red curve b), 686.0 (brown curve c), and 688.0 nm (blue spectrum d). The transient hole depicted as curve c′ was obtained with λ_B = 686.0 nm, after the persistent nonresonant hole was saturated with 496.5 nm laser excitation. Curve c reveals an extremely weak ZPH, as indicated by the brown arrow at 686.0 nm. Similar spectra were obtained for RC_{S2} at $\lambda_B \geq 682$ nm. Note that all spectra exhibit bleaching near 673 nm (revealed for the first time in the resonant transient HB spectra of isolated PSII RCs) and in the 684–686 nm region. However, a ZPH coincident with the burn wavelength is clearly observed only for λ_B in the 680–685 nm range. Both depth and width of the ZPH increase with illumination intensity. We note that ZPH widths (2.4–7.6 cm^{-1} at 682 nm, depending on depth/intensity, data not shown for brevity) are related to the primary CS time (τ_{CS}). These ZPH widths (with an example shown in the insert of Figure 4-6) correspond to τ_{CS} in *C. reinhardtii* (at 682–684 nm) in the range of 1.4–4.4 ps, in agreement with previous data obtained for primary CS in spinach RCs.[13,14,18,19,35] The values of τ_{CS} were obtained by using[41,51]

$$\Gamma_{hom}\,(cm^{-1}) = (1/2\pi c\tau_{fl} + 1/2\pi c\tau_{CS}) + 1/\pi c T_2^{*} \approx 1/2\pi c\tau_{CS}\,,$$

where τ_{fl} is the fluorescence lifetime and T_2^{*} is the "pure" dephasing time. At T = 5 K, $\tau_{fl} >> T_2^{*} >> \tau_{CS}$, and charge separation time has the major effect on the ZPH width.

ZPHs were nearly absent at 686.0 nm and entirely absent at 688.0 nm and longer wavelengths; the spectra obtained at λ_B of 690–695 nm region (not shown here) were very noisy due to extremely low absorption in that spectral region, but their shape was similar to that represented by curve d. Given the optical density changes in the hole profiles shown in Figure 4-6, it is apparent that the spectra obtained at longer λ_B are a manifestation of stronger electron-

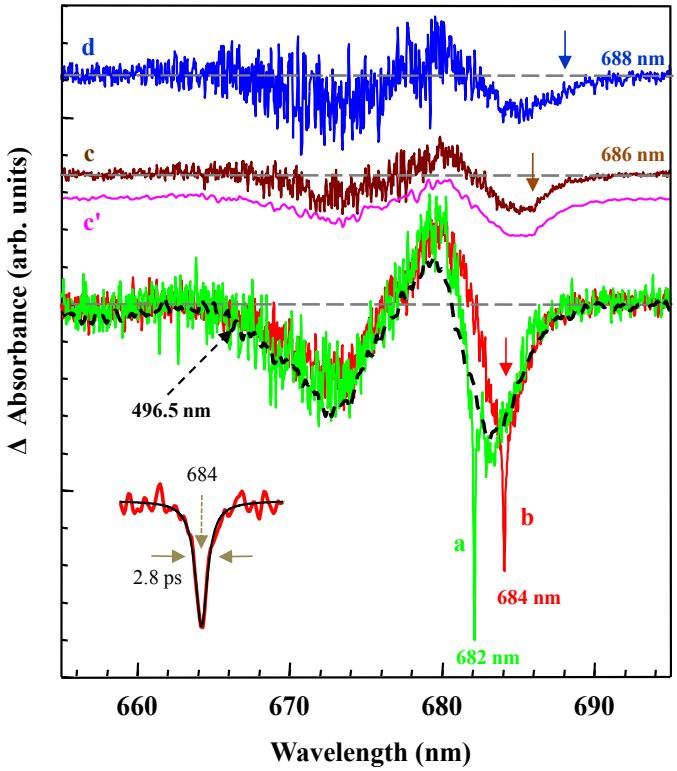

Figure 4-6 Resonant transient HB spectra obtained for RC_{S3} sample. Spectra a, b, c, and d (resolution 1 cm^{-1}) were obtained with λ_B of 682.0, 684.0, 686.0, and 688.0 nm, respectively. Black dashed curve was obtained at λ_B = 496.5 nm. The inset corresponds to the Lorentzian fit (black curve) of ZPH of curve b.

(protein) phonon coupling. This is a signature of the state with significant charge transfer (CT) character (possibly either between two of the P chlorophylls or involving P_{D1} and Chl_{D1}). We also stress that illumination at 690–695 nm results in formation of a bleach near 673 nm and

positive absorption (in the 690–860 nm region), which is a signature of a cation residing on P_{D1} (i.e. P_{D1}^{+}).[23,48]

4.4. Discussion

Taken as a whole, the HB results presented above establish that isolated RCs from *C. reinhardtii* contain a mixture of destabilized (RC680) and intact RCs (RC684), with RC_{S3} samples containing the largest fraction of RC684. Moreover, based on long-wavelength transient absorption features typically ascribed to the $P684^{+}Q_A^{-}$ state, it would seem that the more intact RC684 fraction most likely contains RCs both with and without Q_A; the presence of Q_A allows electron transfer beyond $Pheo_{D1}$ leading to a long-lived $P^{+}Q_A^{-}$ state. This state is responsible for significant bleaching near 673 nm and electrochromic shifts (both observed in the isolated PSII RC for the first time). The absence of a quinone leads to charge recombination resulting in triplet formation, with the associated triplet bleach located near 680 nm (in RC680) or near 684 nm (in RC684). In this context, it is useful to note that recent mutational studies by Schlodder et al.[23] have suggested that the ~673 nm bleach in flash-induced ($P680^{+}Q_A^{-}$ - $P680Q_A$) difference spectra is due to an excitonic state with the strongest contribution from the P_{D1} pigment of the special pair. On the other hand, the triplet-minus-singlet ($^3P - {}^1P$) response near 684 nm is likely due to a triplet state localized on Chl_{D1}. Because of the observed P^{+} transient absorption, stronger P_{D1}-P_{D2} interaction expected in RC684, a bleach near 673 nm, and the electrochromic shift of $Pheo_{D1}$ due to Q_A^{-} formation, we suggest that the primary electron donor in RC684, by analogy to BRC[52,53], might be one of the Chls in the so called P_{D1}/P_{D2} special pair. Since the major portion of the HOMO is localized on P_{D1} chlorophyll,[7] the electron release most likely occurs along the P_{D1} path. In what follows we further discuss the possibility that isolated RCs from *C. reinhardtii* possess two alternative CS pathways within the RC684 (P_{D1} and Chl_{D1} primary

donors). We also consider the localization of the cation radical and provide more insight into the triplet state formed in RC680 (near 680 nm) and intact RC684 (near 684 nm) by charge recombination of the primary radical pair(s), in a fraction of RC684 without Q_A. A possibility of triplet – triplet transfer in RC684 (i.e. $^3P_{D1} \rightarrow {}^3Chl_{D1}$) is also briefly discussed.

4.4.1. Absorption spectra of RC684 and RC680 RCs isolated from C. reinhardtii.

The results presented above indicate that RC_{S3} sample contains largest subpopulation of intact RC684 (with or without Q_A). However, comparison of many different optical spectra obtained for ten RC preparations revealed that RC_{S3} also likely contains a subpopulation (~ 40%; see discussion below related to Figure 4-7) of RC680 complexes. Its presence (manifested via the 680 nm transient hole) is not directly revealed in the transient spectra of RC_{S3} (see Figure 4-4B), due to the significantly deeper transient holes formed in the intact RC684 fraction of the sample; for example, the maximum fractional transient hole depth at 683.3 nm (I = 100 mW/cm^2) is ~22 % in RC_{S3} (see frame F) compared to ~10 % in RC_{S2} (frame E). The latter, with the relatively higher content of RC684 in RC_{S3} sample, minimizes the relative contribution from the transient holes near 680 nm originating from destabilized RC680. The contribution from RC680 near 680 nm in RC_{S3} must be small, as 496.5 and 665.0 nm excitation (Figure 4-4B), in contrast to RC_{S2} preparation (see data in Figure 4-4A) did not result in any difference in transient holes near 680 nm.

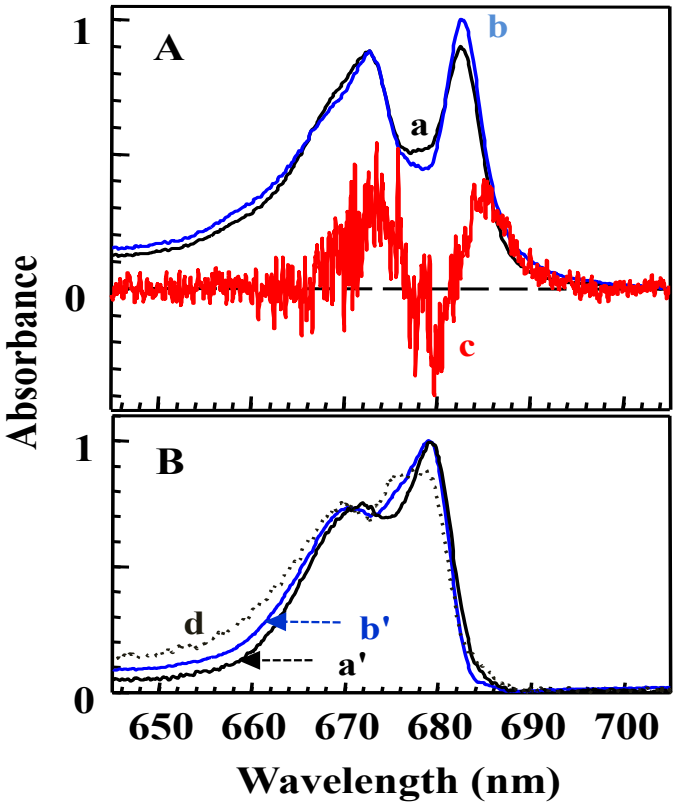

Figure 4-7 Extracted absorption spectra for RC684 (frame A) and RC680 (frame B) complexes. The curves a/b and a′/b′ correspond to the extracted absorption spectra of two subsets of RCs, RC684 (intact) and RC680 (destablished) complexes, respectively (see text for details). Transient spectrum c (inverted curve d from Figure 7) shows a good agreement with the low-energy absorption tail of extracted absorption spectrum of RC684. Curve d (in frame B) was obtained as the difference of absorption spectra of intact and partly damaged RC_{S3} preparation, which corresponds to the destabilized RC680.

Guided by the data shown in Figures 4-2–4, and unpublished results, as well as earlier studies[13,31,32], we attempted to extract individual absorption spectra of the RC684 and RC680 subpopulations. The resulting putative absorption spectra are shown in Figure 4-7 (frames A and B, respectively). Curve a in Figure 4-7A (assigned to the absorption of intact RC684 complexes) was obtained by subtracting scaled contributions of the absorption spectra of RC_{S2} (a mixture of RC680 and RC684) and RC_{S1} (mostly RC680) from the absorption spectrum of RC_{S3}. Curve b

was obtained likewise by subtracting a typical absorption spectrum of spinach RC[13,14] (instead of the RC_{S1}) from RC_{S3}. Note that low-energy part of spectrum c in Figure 4-7A, corresponding to the inverted HB spectrum (curve d in Figure 4-6) obtained at λ_B = 688.0 nm, fits very well the low-energy absorption tail of the intact RC684 complexes.

Based on this putative absorption spectrum for the intact RC684 complex, one can extract the representative absorption spectra of RC680 (curve a' and b' in Figure 4-7B) by subtracting the RC684 absorption spectrum from the absorption spectra measured for various less-intact RC preparations. Such difference spectra (curves a' and b') are indeed very similar to the absorption spectra of typically studied RC680 complexes, which exhibited similar absorption maximum and triplet-bottleneck hole (bleach) near 680 nm, as well as no response near 673 nm. To demonstrate that this assignment is realistic, one should compare curves a′ and b′ with spectrum d (in frame B of Figure 4-7), which was obtained as the difference between the absorption spectra of intact RC_{S3} sample (Figure 4-2C) and partly damaged RC_{S3} (i.e. RC_{S3d}; not shown for brevity), respectively. Recall that the difference between transient holes shown in Figure 4-3 (obtained for the above two samples) revealed more transient hole with bleaching near 680 nm in the damaged sample (see curve c in Figure 4-3) proving that RC684 indeed converts to RC680. This is why spectrum d in Figure 4-7B is similar to a typical absorption of destabilized RC680. Thus we conclude that our analysis is consistent with our RC680/RC684 model for isolated spinach RCs[13,32,49], proving that RC680 are destabilized products of more intact RC684 complexes. None of spinach RCs discussed in[13,32,49], however, contained Q_A as it was lost during the preparation procedure. This is most likely why in spinach RCs (mostly RC680 with a small contribution from RC684, both fractions without Q_A) only the triplet-bottleneck holes near 680 nm (major) and 684 nm (minor) have been observed, but not the 673 nm hole.

These findings pose many relevant questions; for example: 1) Which optical spectra should be fitted using theoretical structure-based models to describe electronic structure and/or electron transfer dynamics in intact RCs? 2) Are both channels of charge separation (i.e. P_{D1} and Chl_{D1} paths) operational in *intact* RCs (i.e. RC684) and destabilized RC680? 3) Why does the triplet-bottleneck bleach in RC680 (no Q_A) shifts to the blue by ~4 nm in comparison with that in RC684 (also with no Q_A)?; and 4) does the Chl_{D1} act as the primary electron donor at physiological temperatures? Some of these questions will be briefly addressed in Section 4.3. First, we focus on the origin of electrochromic shift and the possibility that a fraction of intact RC684 from *C. reinhardtii* may possess the secondary plastoquinone, Q_A.

4.4.2. On triplet formation and the nature of the electrochromic shift in RC684.

For a moment we focus only on the electrochromic shift and the general shapes of transient HB spectra discussed above. The blue and red curves in the right insert of Figure 4-5 show the effect of $P^+Q_A^-$ formation on the Q_x-region of pheophytins in the RC_{S2} and RC_{S3} samples, respectively. These curves correspond to transient spectra after the persistent hole was saturated. A clear blue shift of the Q_x-transition of pheophytins is observed, in agreement with data obtained for intact PSII core samples,[31] and suggesting that a significant subpopulation of RCs in RC_{S3} (and RC_{S2}) contains plastoquinone Q_A, whose reduction to Q_A^- leads to the electrochromic shift of the active $Pheo_{D1}$ residing in the vicinity of Q_A. The gray (smooth) curve is shown to help the reader to perceive the electrochromic shift. (Modeling study of the optical spectra reported here is beyond the scope of this paper and will be published elsewhere). Note that no electrochromic shifts have ever been observed in the spinach RC samples, as shown by the black top curve in the right inset

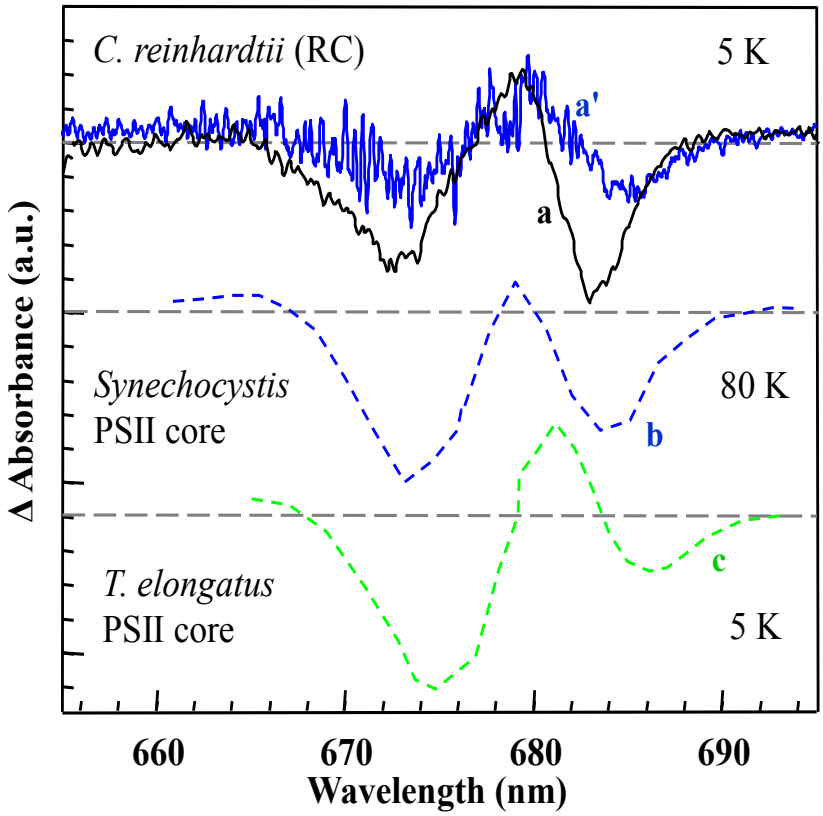

Figure 4-8 Comparison of various ($P^+Q_A^-$– PQ_A) spectra: curve a (black) represents the ($P^+Q_A^-$– PQ_A) obtained for the isolated RC_{S3} from *C. reinhardtii,* adopted from curve b' of Figure 4B. Curve (a') is resonant transient HB spectrum of RC_{S3} sample obtained at the 688.0 nm. Spectra b and c are the flash induced absorption difference ($P^+Q_A^-$– PQ_A) spectra of PSII core complexes from *Synechocystis* sp. PCC 6803 at 80 K[23] and *T. elongatus* at 5 K[30], respectively.

of Figure 4-5. The same is true for positive absorption increase due to P^+ formation. This is consistent with the absence of Q_A in the isolated RC680 complexes from spinach and RC_{S1} sample from *C. reinhardtti.* As shown in Section 3.2, non-resonant transient holes of RC_{S2} and RC_{S3} samples (Figures 4-2 and 4-4) are very different from the non-resonant transient holes typically observed in spinach, as well as from those observed for RC_{S1} (Figure 4-2D), for which the major bleach is near 680 nm, with no accompanying bleach near 673 nm or positive

absorption increase in the long-wavelength region (> 690 nm). The most interesting finding, however, is that RC_{S3} sample (extracted directly from thylakoids)[37] has Q_y transient hole spectrum similar to that of flash-induced ($P^+Q_A^-$ - PQ_A) absorbance difference spectrum obtained for PSII core.[22,27,30,48]

Curve a in Figure 4-8 corresponds to spectrum b' of Figure 4-4B. We believe that this spectrum may still contain a small contribution from the triplet-bottleneck hole due to $^3Chl_{D1}$ with a main bleach near 684 nm, observed in intact RC684 without Q_A (see curve c′ in Figure 4B). That is, spectrum a might be a mixture of triplet and ($P^+Q_A^-$ - PQ_A) contributions. Spectrum a′ was obtained with λ_B of 688.0 nm and is shown for comparison. Spectra b and c in Figure 4-8 correspond to transient ($P^+Q_A^-$ - PQ_A) spectra obtained for *Synechocystis* sp. PCC6803[22,27,48] and *T. elongatus*[27,30] PSII core complexes, at 80 K and 5 K, respectively. Comparison of spectra a/a′, b, and c clearly suggests that transient spectra measured for our sample RC_{S3} are similar to transient ($P^+Q_A^-$ - PQ_A) spectra observed in more intact PSII core complexes,[22,27,30,48] where RCs are not affected by the removal of the CP43 and CP47 antenna complexes. We note that the entire shapes of both resonant and non-resonant transient holes in our isolated RCs and in the PSII cores[22,27,30,50] are not only contributed to by the CS per se, but also by the electrochromic shifts of Chl_{D1} and $Pheo_{D1}$ due to charges residing on P_{D1} and Q_A respectively during the transient hole measurement.

Recombination from the $P^+Q_A^-$ state occurs with a characteristic time of about 2–5 ms.[54] In our experimental approach the 684 nm part of the contribution of this state to transient holes cannot be directly distinguished from the holes of triplet-bottleneck nature (see next paragraph). Thus, it is possible that bleaching near 684 nm in RC_{S3}, (curve a of Figure 4-8), still carries a small contribution from the Chl_{D1} triplet. In fact, the differences between the depths of 684 nm

transient holes a′ and b′ (Figure 4-4) and differences in 673/684 nm hole depth ratios for RC_{S3} and PSII cores (Figure 4-8) speak in favor of such a possibility. Taking into account that in PSII core the RC triplet is only observed if Q_A is removed or reduced,[48,55] it is natural to suggest that in our transient HB experiments in either RC680 or RC684 the triplet is also observed only in the absence of Q_A. The triplet in RC684 (with Q_A lost) is most likely localized on Chl_{D1} ($^3Chl_{D1}$), as $^3P_{D1}$ triplet would yield a hole which is significantly blue-shifted (to about 675 nm)[24], in agreement with our calculations (data not shown). The lifetime of such triplet state should be similar to that of the Chl *a* at 5 K (τ = 1.4 ms)[56] and thus should be shorter than the lifetime expected for $P684^+Q_A^-$, i.e. shorter than 2–5 ms.[54,57-59] Due to the longer lifetime of $P_{D1}^+Q_A^-$ (in RC684 with Q_A present) in comparison with the lifetime of the triplet state in RC684 or RC680 (no Q_A), the contribution to a triplet-bottleneck hole near 680 nm (from a fraction of RC680 still present in RC_{S3}) can be expected to be minor and buried under other features in spectra shown in Figure 4-4B. The triplet-bottleneck hole in RC684 (no Q_A) is observed at 684 nm (see curve c′ in Figure 4-4B). However, it is not clear if $^3Chl_{D1}$ in intact RC684 without Q_A is formed directly by charge recombination ($Chl_{D1}^+Pheo_{D1}^- \rightarrow {}^3Chl_{D1}$) or if $^3P_{D1}$ triplet is formed originally, followed by a fast triplet energy transfer to Chl_{D1} (i.e. $P_{D1}^+Chl_{D1}^-Pheo_{D1} \rightarrow P_{D1}^+Chl_{D1}Pheo_{D1}^- \rightarrow {}^3P_{D1} \rightarrow {}^3Chl_{D1}$)[56] Assuming that the presence or absence of Q_A does not affect the very first step of the charge separation, and that P_{D1} is the primary electron donor in RC684, one should favor the latter mechanism of triplet formation on Chl_{D1}. No response near 673 nm is expected if $^3P_{D1} \rightarrow {}^3Chl_{D1}$ transfer is fast enough (~50 ns)[56] compared to $^3Chl_{D1}$ lifetime. The shape and the minimum of the nonresonant hole c′ in Figure 4-4B is consistent with measured T – S spectra for PSII core from *Synechocystis* with Q_A reduced (blocking electron transfer beyond $Pheo_{D1}$) where

it was shown that (at low temperatures) the main bleach is located near 683 nm, in agreement with the RC triplet being localized on accessory Chl_{D1}[48].

The presence of well-defined ZPH for λ_B of 682–684 nm, combined with the absence of ZPH for $\lambda_B \geq 686$ nm (see Figure 4-6) suggests that mixing between the CT state(s) and lowest-energy excited state increases at longer wavelengths. Holes burned at $\lambda_B \geq 688.0$ nm (the noisy spectra for λ_B of 690- 695 nm are not shown) were very similar to those obtained at $\lambda_B = 686.0$ and 688.0 nm, suggesting that there is(are) a low-lying CT state(s) that might be largely homogeneously broadened (although see discussion below of homogeneous vs. inhomogeneous broadening). It is also tempting to suggest, although results presented in this paper do not provide enough evidence, that narrow ZPHs, which are not due to the CT state, belong to the Chl_{D1} primary CS path. Thus, the CS may occur from both the special pair (most likely P_{D1}) and Chl_{D1}, depending on a particular realization of the static energetic disorder.[26] We anticipate that theoretical modeling of our transient HB spectra (research in progress) will shed more light on excitonic structure of intact RC684 and on the mixing of the special pair Chls with a low-energy CT state(s) whose maximum(a) is(are) likely near 688–695 nm.

4.4.3. Charge separation pathway(s) in RC680 and RC684.

Our transient HB spectra provide a new insights into the Chls that contribute to the long lived (>1 ms) excited and radical pair state(s) in *C. reinhardtii*. In RC684 with Q_A present the shape of the transient HB spectrum is due to formation of a long-lived (2–5 ms) $P_{D1}^{+}Q_A^{-}$ state, accompanied by electrochromic shifts. That is, the negative and positive changes in the transient spectra near 682–690 and 677–681 nm regions, respectively, are contributed to by the electrochromic shifts of pigments residing close to P_{D1} and Q_A, i.e., Chl_{D1} and $Pheo_{D1}$ respectively. The bleach near 673 nm and the increase of absorption at >690 nm are signatures of

the $P_{D1}^{+}Q_A^{-}$ formation (specifically P_{D1}^{+}); see data in Figure 4-8. However, transient HB spectra in RC684 complexes (with Q_A present) cannot distinguish between the following sequences of events: $P_{D1}\mathbf{Chl_{D1}^{+}Pheo_{D1}^{-}}Q_A \rightarrow \mathbf{P_{D1}^{+}}Chl_{D1}\mathbf{Pheo_{D1}^{-}}Q_A \rightarrow \mathbf{P_{D1}^{+}Q_A^{-}}$ and/or $\mathbf{P_{D1}^{+}Chl_{D1}^{-}}Pheo_{D1}Q_A \rightarrow \mathbf{P_{D1}^{+}}Chl_{D1}\mathbf{Pheo_{D1}^{-}}Q_A \rightarrow \mathbf{P_{D1}^{+}Q_A^{-}}$ as the lifetime of the final state is much longer than the characteristic times of the intermediate steps. That is, observation of $P_{D1}^{+}Q_A^{-}$ does not exclude the possibility that Chl_{D1} can serve as a primary electron donor. In addition, the shape of nonresonant transient HB spectra characterized by a single bleach near 680 nm (in RC680) or 684 nm (in RC684) in a subpopulation of RCs without Q_A (and no evidence of oxidation of P_{D1}) does not prove that electron transfer starts at Chl_{D1} ($P_{D1}\mathbf{Chl_{D1}^{+}Pheo_{D1}^{-}} \rightarrow {}^3Chl_{D1}$), as ${}^3Chl_{D1}$ in RC684 can be also obtained via the sequence: $\mathbf{P_{D1}^{+}Chl_{D1}^{-}}Pheo_{D1} \rightarrow \mathbf{P_{D1}^{+}}Chl_{D1}\mathbf{Pheo_{D1}^{-}} \rightarrow {}^3P_{D1} \rightarrow {}^3Chl_{D1}$, especially if the triplet-triplet transfer is fast.[56] Thus, it is likely that Chl_{D1} can also serve as primary electron donor in PSII RC if it is strongly enough contributing to the lowest exciton state. Therefore, our data are consistent with the recent conclusion reached by Romero et al.,[34] based on time-resolved spectroscopic experiments, that both P_{D1} and Chl_{D1} paths are possible, In particular, it has been suggested in[34] that the very weak shoulder near 672–673 nm observed in recent 77 K transient absorption experiments on spinach RCs (i.e. in the species-associated difference spectra (SADS) obtained with laser pump pulse duration of ~100 fs and 10 nm fwhm) reflects a contribution from the P_{D1} path for CS, though no clear evidence was presented. Therefore, this pathway, if present in the spinach RC[34,35], most likely operates only in a very small subpopulation of intact spinach RCs (i.e. RC684), but not in destabilized RC680, which (with weakened P_{D1}-P_{D2} coupling) are responsible for the major bleach near 680 nm in all spinach RC transient absorption spectra published so far.

The fact that RC680-dominated samples reveal a major response (bleaching) near 680 nm[11,12,14] (and not at 684 nm as in RC684 complexes) shows that these RCs have lost Q_A and the interaction between D1 and D2 proteins in RC680 is altered. Weaker coupling (i.e. smaller wave function overlap) between the Chls constituting the special pair (P_{D1}/P_{D2}) in RC680 could lead to the well-documented (preferential) charge separation pathway in RC680 starting from the accessory Chl_{D1} (Chl_{D1} path), with the major bleach near 680 nm[1,24] as a signature. In these destabilized RC680 (D1/D2/Cyt_{b559} proteins) one would not expect the negative signal (bleach) near 673 nm due to oxidation of P_{D1}. This is consistent with the major ~680 nm bleach observed in isolated RCs from spinach; namely, SADS indicated that the $(Chl_{D1}Pheo_{D1})^*$ state decays in 3 ps forming $Chl_{D1}^{+}Pheo_{D1}^{-}$ radical pair[34] while the $P_{D1}^{+}Pheo_{D1}^{-}$ formation was assigned to be faster. Regarding the latter pathway, the authors claimed that contributions from high exciton states, P_{D1} and/or P_{D2}, and Chl_{D1}, were observed at 660, 667, and 680 nm, respectively[34], in agreement with the $(P_{D1}P_{D2}Chl_{D1})^* \rightarrow P_{D2}^{+}P_{D1}^{-} \rightarrow P_{D1}^{+}Chl_{D1}^{-}$ process. However, clear bleaches near 672/673 nm and 684 nm (as in our RC684) have not been observed, suggesting that this P_{D1} pathway in spinach RCs was present only in a minor subpopulation of more intact RC684. On the other hand, very recent modeling of the same transient absorption kinetics data (by the same group) suggested[35] that it is the $Chl_{D1}^{+}Pheo_{D1}^{-}$ formation that corresponds to the fastest component (0.7 ps).

The fact that there is a distribution of CS times and variable λ_B-dependent (due to disorder) mixing with CT states complicates the so-called model-dependent "target analysis" of composite transient absorption spectra. The absence of ZPHs at $\lambda_B \geq 686$ nm (see Figure 4-6) suggests the presence in RC684 of low-lying CT state(s) characterized by very strong electron-phonon coupling, in agreement with Krausz et al. who showed that excitation wavelengths as

long as 695.0 nm (T = 1.7 K), can induce CS in PSII core and thus Q_A^- formation.[31,60] On the other hand, a very small shift of the $P^+Q_A^-$ holes near 673 and 684 nm for λ_B of 686, 688, 690, and 695 nm is consistent with the presence of a weakly absorbing (and predominantly homogeneously broadened) CT state(s) lying near 688–695 nm. This assignment is in agreement with[31] where a weak (homogeneously broadened) CT state was hypothesized to be present in the PSII core (hidden beneath the CP47 lowest-energy state centered at 690 nm). The homogeneously broadened character of the CT state is analogous to that observed in bacterial RCs, with well-established strong electron phonon coupling.[61,62] However, Novoderezhkin et al.[26] suggested that the absence of ZPHs does not automatically imply very large S-values (leading to large homogeneous broadening) since the relative intensities of zero-phonon and vibrationally excited transitions will depend on the degree of mixing of each CT mode with higher-energy exciton states, which in turn depends on the relative displacement of the CT and exciton state potential energy surfaces along each vibrational mode. In short, they argued that preferential mixing of vibrationally excited modes of the (dark) CT state with the (bright) exciton states, may lead to an effective suppression of the CT state ZPL even in the absence of strong local electron-phonon coupling. Furthermore, it should be noted that Krausz et al.[31] argued that the CT state in PSII core extends far beyond 700 nm (700–730 nm), a notion that requires further confirmation, as the long absorption tail in PSII core is strongly contributed to by antenna complexes, and no such absorption was revealed in our intact isolated RC684 complexes. Note that RC684 has a major bleach ~4 nm to the red (at ~684 nm; see curve c′ in Figure 4-4B) in comparison with the ~680 nm bleach observed in destabilized RC680. It remains to be determined whether the 4 nm blue-shift of the triplet-bottleneck hole in RC680 is due to a shift in the site energy of $Pheo_{D1}$, or, as arbitrarily assumed in[24], due to a blue-shift of the site energy of

Chl_{D1}. Both states of affairs are possible since, based on our preliminary modeling studies, both $Pheo_{D1}$ and Chl_{D1} contribute to the lowest-energy excitonic state[37]. It cannot be excluded that the blue shift of the site energy of $Pheo_{D1}$ in RC680 is due to the the H-bond to $Pheo_{D1}$[1,54] being broken[37,63]. This would be consistent with the observed blue shift of the Q_x- transition of $Pheo_{D1}$ and a blue shift of the broad nonresonant triplet-bottleneck hole (λ_B = 665.0 nm) in RC680 when compared to RC684.

In summary, our data suggest the following:

(1) Spectra shown in Figures 4-6 and 4-8 can be explained only assuming that major cation in intact RCs is localized on P_{D1}.[27]

(2) A fraction of intact RC684 must contain Q_A (with a positive charge on P_{D1} and negative charge on Q_A during our transient HB measurements, $P_{D1}^{+}Q_A^{-}$ - $P_{D1}Q_A$). An electrochromic shift with a zero crossing near 681 nm in the Q_y and near 543 nm in the Q_x regions is consistent with a blue shift of the site energies of active $Pheo_{D1}$ and in part Chl_{D1} (see curve a in Figure 4-8 and the right inset (lower curves) in Figure 4-5). This data is in agreement with transient profiles reported for the PSII core in Ref.[22,27,30,48]

(3) Charge separation in intact RCs in *C. reinhardtii* (RC684) most likely starts from P_{D1} pigment, although Chl_{D1} being a primary donor for a fraction of RC684 cannot be excluded.

Although our findings are consistent with the original suggestion that isolated RCs (in spinach) may posses$_s$ two parallel electron-transfer pathways, one starting at Chl_{D1} and one at P_{D1}[34], with the relative contribution of each pathway determined by the particular realization of disorder[34,35], we suggest that the major transient contribution peaked at 680 nm observed in these

papers originated from the Chl_{D1} path in destabilized RC680, while the minor P_{D1} path contribution was due to a small subpopulation of more intact RC684 complexes. (Recall that triplet localization on Chl_{D1} in RC680 and RC684 leads to transient holes near 680 nm (see curves c in Figures 4-3 and 4-4) and 684 nm (curve c′ in Figure 4-4), respectively). Bear in mind that these contributions can be only observed in RCs without Q_A. Our assignment is also supported by the fact that transient absorption spectra reported in[34] exhibited a small red shift to ~682 nm of the major bleach for 685 nm excitation with fs laser with a bandwidth of ~10 nm. The explanation provided in[34,35] was that the red-shift is caused by photoselection of a subpopulation from the inhomogeneous distribution. Although under such experimental conditions a weak photoselection from the inhomogeneous distribution can be present, it is much more likely that, in agreement with transient HB spectra, that these spectra were contributed to by two distinct subpopulations, as discussed above. In other words, transient spectra with bleaching near ~673/685 nm and ~680 nm correspond to different subsets of the ensemble of RCs, i.e. intact RC684 (with P_{D1} and Chl_{D1} as the primary electron donor) and destabilized RC680 (with only Chl_{D1} as the primary electron donor) complexes, respectively. We think both P_{D1} and Chl_{D1} pathways may be highly operational for particular realizations of disorder being responsible for the very efficient CS in PSII RC at physiological temperatures, as room temperature protein motions can lead to large conformational protein disorder.[17] Thus, it appears the conformational protein dynamics modulating pigment-pigment and pigment-protein interactions leads not only to efficient excitation energy transfer but also to efficient and fast electron transfer times, utilizing two different CS pathways.

4.5. Concluding remarks.

Comprehensive HB studies of a large number of *isolated* PSII RC samples with different levels of intactness indicate that isolated RCs from *C. reinhardtii* are highly fragile and sensitive to the isolation/purification protocols and sample handling/preparation procedures. This is in agreement with previous reports that harsh biochemical treatment (necessary to isolate RCs) can modify both optical spectra and redox properties of protein's cofactors.[13,32,64] As a result, the nature of the primary electron donor in *isolated* PSII RCs from *C. reinhardtii* depends on the intactness of the protein. Our data clearly suggest that isolated RCs from *C. reinhardtii* possess three RC fractions referred to as destabilized RC680 (no Q_A), more native RC684 (no Q_A), and a small fraction of native RC684 with Q_A present, in different proportions. We argue that all isolated RCs studied so far contained mostly RC680 (i.e. destabilized RCs; no Q_A), with a major single-band bleaching near 680 nm in the transient hole spectra as well as Chl_{D1} path for CS. On the other hand, two different CS pathways (P_{D1} and Chl_{D1}) are possible in RC684, with the former likely being dominant. We show, for the first time, that transient HB spectra obtained for our most intact RCs (RC_{S3} sample; with a significant fraction of RC684 possessing Q_A) are similar to transient delta absorption spectra of ($P^+Q_A^-$ - PQ_A) observed in the PSII core[27,30]. In particular, transient HB spectra in RC684 revealed contributions from both a longer lived $P^+Q_A^-$ state (most likely formed by both P_{D1} and Chl_{D1} pathways for CS) and triplet-bottleneck holes near 684 nm (localized on Chl_{D1}) formed either directly via the Chl_{D1} CS path or via the P_{D1} CS path plus triplet-triplet transfer ($^3P_{D1} \rightarrow {}^3Chl_{D1}$). Resonant HB cannot distinguish different paths by the CS times, but it is clear that primary CS (most likely via the Chl_{D1} pathway) occurs on the ps time scale of about 1.4 – 4.4 ps. In contrast, we propose that CS in RC684 via the P_{D1} pathway could be even faster; since HB spectra burned at $\lambda_B > 686$ nm do not show ZPHs, the CS time

via the P_{D1} pathway cannot be obtained from HB spectra. We demonstrate that the destabilization of isolated D1/D2/Cyt_{b559} protein complexes (i.e. RC680) not only eliminates (or significantly decreases) contribution from the RC684 (and, as a result, the P_{D1} CS pathway), as observed in spinach RCs,[34] but also modifies the site energies of the pigments participating in the Chl_{D1} path for CS along the D1 protein (Section 4.3), shifting its triplet-bottleneck hole by ~90 cm^{-1} (~ 4 nm) towards high energy. The lack of P_{D1} path in RC680 is most likely caused by a modified (i.e. decreased) overlap of the π-electron wavefunctions between P_{D1} and P_{D2} and/or P_{D1}/P_{D2} and Chl_{D1} cofactors, as well as possible conformational changes in the D1/D2 protein.

Acknowledgements

This work was supported by the Chemical Sciences, Geosciences and Biosciences Division, Office of Basic Energy Sciences, Office of Science, U.S. Department of Energy; grant EC9987 to RJ. Partial support at the early stage of this project was provided by the DOE EPSCoR Grant (DE-FG02-08ER46504) and DOE BES to RJ. VZ acknowledges support by NSERC. We thank Chen Lin for mass spectrometry and NMR measurements using extracts of RC_{S3} sample and acknowledge our collaborators Dr. Michael Seibert (from NREL, Golden, CO) and Dr. Rafael Picorel (CSIC, Zaragoza, Spain) for kindly providing us with the isolated RC complexes and useful discussions.

References

(1) Diner, B. A.; Rappaport, F. *Annu. Rev. Plant Biol*. **2002**, *53*, 551-580.
(2) Umena, Y.; Kawakami, K.; Shen, J.-R.; Kamiya, N. *Nature* **2011**, *473*, 55-60.
(3) Deisenhofer, J.; Epp, O.; Miki, K.; Huber, R.; Michel, H. *Nature* **1985**, *318*, 618-624.
(4) Deisenhofer, J.; Epp, O.; Miki, K.; Huber, R.; Michel, H. *J. Mol. Biol.* **1984**, *180*, 385-398.
(5) Xiong, J.; Subramanian, S.; Govindjee *Photosynth. Res.* **1998**, *56*, 229-254.
(6) Trebst, A. *Z. Naturforsch. C 41 c* **1986**, 240-245.
(7) Lill, N. S. O. *Phys. Chem. Chem. Phys.* **2011,** *13,* 16022-16027.
(8) Saito, K.; Ishida, T.; Sugiura, M.; Kawakami, K.; Umena, Y.; Kamiya, N.; Shen, J.-R.; Ishikita, H. *J. Am. Chem. Soc.* **2011**, *133*, 14379-14388.
(9) Nanba, O.; Satoh, N. *Proc. Natl. Acad. Sci. U. S. A.* **1987**, *84*, 109-122.
(10) Tang, D.; Jankowiak, R.; Seibert, M.;Yocum, C.F.; Small, G. J. *J. Phys. Chem.* **1990**, *17*, 6519-6522.
(11) Tang, D.; Jankowiak, R.; Seibert, M.; Small, J. G. *Photosynth. Res.* **1991**, *27*, 19-29.
(12) Zazubovich, V.; Jankowiak, R.; Riley, K.; Picorel, R.; Seibert, M.; Small, G. J. *J. Phys. Chem. B* **2003**, *107*, 2862-2866.
(13) Riley, K. J.; Jankowiak, R.; Rätsep, M.; Small, G. J.; Zazubovich, V. J. *Phys. Chem. B* **2004**, *108*, 10346-10356.
(14) Jankowiak, R.; Rätsep, M.; Hayes, J.; Zazubovich, V.; Picorel, R.; Seibert, M.; Small, G. J. *J. Phys. Chem. B* **2003**, *107*, 2068-2074.
(15) Frese, R. N.; Germano, M.; de Weerd, F. L.; Van Stokkum, I. H. M.; Shkuropatov, A. Y.; Shuvalov, V. A.; van Grokon H. J.; Van Grondelle, R.; Dekker, J. P. *Biochemistry* **2003**, *42*, 9205-9213.
(16) Prokhorenko, V. I.; Holzwarth, A. R. *J. Phys. Chem. B* **2000**, *104*, 11563-11578.
(17) Novoderezhkin, V.I.; Andrizhiyevskaya, E. G.; Dekker, J. P.; van Grondelle, R. *Biophysical Journal* **2005**, *89*, 1464-1481.
(18) Groot, M.-L.; van Mourik, F.; Eijckelhoff, C.; van Stokkum, I. H. M.; Dekker, J. P.; van Grondelle, R. *Proc. Natl. Acad. Sci. U.S.A.* **1997**, *94*, 4389-4394.
(19) Myers, J. A.; Lewis, K. L. M.; Fuller, F. D.; Tekavec, P. F.; Yocum, C. F.; Ogilvie, J. P. *J. Phys. Chem. Lett.* **2010**, *1*, 2774-2780.
(20) Alizadeh, S.; Nixon, P. J.; Telfer, A.; Barber, J. *Photosynth. Res.* **1995**, *43*, 165-171.
(21) Wang, J.; Gosztola, D.; Ruffle, S. V.; Hemann, C.; Seibert, M.; Wasielewski, M. R.; Hille, R.; Gustafson, T. L.; Sayre, R. T. *Proc. Natl. Acad. Sci. U.S.A.* **2002**, *99*, 4091-4096.
(22) Diner, B. A.; Schlodder, E.; Nixon, P. J.; Coleman, W. J.; Rappaport, F.; Levergne, J.; Vermaas, W.F. J.; Chisholm, D. A. *Biochemistry* **2001**, *40*, 9265-9281.
(23) Schlodder, E.; Coleman, W. J.; Nixon, P. J.; Cohen, R. O.; Renger, T.; Diner, B. A. *Phil. Trans. R. Soc. B* **2008**, *363*, 1197-1202.

(24) Raszewski, G.; Saenger, W.; Renger, T. *Biophys. J.* **2005**, *88*, 986-998.
(25) Raszewski, G.; Diner. B. A.; Schlodder, E.; Renger, T. *Biophysical J.* **2008**, *95*, 105-119.
(26) Novoderezhkin, V. I.; Dekker, J. P; van Grondelle, R. *Biophys. J.* **2007**, *93*, 1293-1311.
(27) Renger, T.; Schlodder, E. *ChemPhysChem* **2010**, *11*, 1141-1153.
(28) Cox, N.; Hughes, J.; Rutherford, A.W.; Krausz, E. *Physics Procedia* **2010, *3*,** 1601-1605.
(29) Seibert, M.; In *The Photosynthetic Reaction Center* Deisenhofer, J.; Norris, J.; Eds; Academic Press: New York, 1993, Vol. I, pp. 319-356.
(30) Hillmann, B.; Brettel, J. K.; van Mieghem, F.; Kamlowski, A.; Rutherford, A. W.; Schloder, E. *Biochem.* **1995**, *34*, 4814-4827.
(31) Krausz, E.; Hughes, J. L.; Smith, P.; Pace, R.; Årsköld, S. P. *Photochem. Photobiol. Sci*. **2005**, *4*, 744-753.
(32) Chang, H.-C.; Jankowiak, R.; Reddy, N. R. S.; Yocum, C. F.; Picorel, R.; Seibert, M., Small, G. J. *J. Phys. Chem.* **1994**, *98*, 7725-7735.
(33) Reddy, N. R. S.; Kolaczkowski, S. V.; Small, G. J. *Science* **1993**, *260*, 68-71.
(34) Romero, E.; van Stokkum, I. H.; Novoderezhkin, V. I.; Dekker, J. P.; van Grondelle, R. *Biochem.* **2010**, *49*, 4300-4307.
(35) Novoderezhkin, V. I.; Romero, E.; Dekker, J. P.; van Grondelle, R. *ChemPhysChem* **2011**, *12*, 681-688.
(36) Cox, N.; Hughes, J. L.; Steffen, R.; Smith, P.J.; Rutherford, W.; Pace, R.J.; Krausz, E. *J. Phys. Chem. B* **2009**, *113*, 12364-12374.
(37) Acharya, K.; Neupane, B.; Zazubovich, V.; Sayre, R. T.; Picorel, R.; Seibert, M.; Jankowiak, R. *J. Phys. Chem. B* **2012**, DOI: 10.1021/jp3007624.
(38) Xiong, L.; Seibert, M.; Gusev, A. V.; Wasielewski, M. R.; Hemann, C.; Hille, C. R; Sayre, R. T. *J. Phys. Chem. B* **2004**, 108, 16904-16991.
(39) Rochaix, J.-D. *Annu Rev Genet* **1995**, *29*, 209-230.
(40) Riley, K. J.; Zazubovich, V.; Jankowiak, R. *J. Phys. Chem. B **2006***, *110*, 22436-22446.
(41) Jankowiak, R.; Reppert, M.; Zazubovich, V.; Pieper, J.; Reinot, T. *Chem. Rev*. **2011,** *111,* 4546-4598.
(42) Jankowiak, R.; G. J. Small, In *The Photosynthetic Reaction Centers*; Eds. Norris J. and Deisenhofer J.; Academic Press: New York,1993; pp. 133-177.
(43) Germano, M.; Shkuropatov, A. Ya.; Permentier, H.; de Wijn, R.; Hoff, A. J.; Shuvalov, V. A.; van Gorkom, H. J. *Biochem.* **2001**, *40*, 11472-11482.
(44) Dědic, R.; Lovčinskŷ, M.; Vácha, F.; Hala, J. *J. Lumin*. **2000**, *87-89*, 809-811.
(45) Germano, M.; Shkuropatov, A. Ya.; Permentier, H.; Khatypov, R. A.; Shuvalov, V. A.; Hoff, A. J.; van Gorkom, H. J. *Photosynth. Res*. **2000**, *64*, 189-198.

(46) Hughes, J. L.; Smith, P.; Pace, R.; Krausz, E. *Biochim. Biophys. Acta* **2006**, *1757*, 841-851.

(47) Jankowiak, R.; Rätsep, M.; Picorel, R.; Seibert, M.; Small, G. J. *J. Phys. Chem. B* **1999**, *103*, 9759-9769.

(48) Schlodder, E; Renger, T.; Raszewski, G; Coleman, W. J.; Nixon, P. J.; Cohen, R. O.; Diner, B. A *Biochemistry* **2008**, *47*, 3143-3154.

(49) Herascu, N.; Ahmouda, S.; Picorel, R.; Seibert, M.; Jankowiak, R.; Zazubovich, V. *J. Phys. Chem. B.* **2011**, *115*, 15098-15109.

(50) Allakhverdiev, S. I.; Ahmed, A.; Tajmir-Riahi, H.-A.; Klimov, V. V.; Carpentier, R. *FEBS Lett.* **1994**, *339*, 151-154.

(51) Jankowiak, R.; Hayes, J. M.; Small, G. J. *Chem. Rev* **1993**, *93*, 1471-1502.

(52) Madjet, M. E.; Müh, F.; Renger, T. *J.Phys. Chem. B* **2009**, *113*, 12603-12614.

(53) Kálmán, L.; Williams, J. C.; Allen, J. P. *Photosynth. Res* **2008**, *98*, 643-655.

(54) Moënne-Loccoz, P.; Robert, B.; Latz, M. *Biochem*. **1989**, *28*, 3641-3645.

(55) Vass, I.; Styring, S.; Hundal, T.; Koivuniemi, A.; Aro, E.-M.; Anderson, B. *Proc. Natl. Acad. Sci. U. S. A.* **1992**, *89*, 1408-1412.

(56) Rutherford, A.W.; Paterson, D. R.; Mullet, J.E. *Biochim. Biophys. Acta* **1981**, *635*, 205-214.

(57) Noguchi, T.; Tomo, T.; Kato, C. *Biochemistry* **2001**, *40*, 2176-2185.

(58) Mathis, P.; Vermeglio, A. *Biochem. Biophys. Acta* **1975**, *396*, 371-381.

(59) Hillmann, B.; Schlodder, E. *Biochem. Biophys. Acta* **1995**, *1231*, 76-88.

(60)Hughes, J. L.; Prince, B. J.; Krausz, E.; Smith, P. J; Pace, R. J.; Riesen, H. *J. Phys. Chem. B*. **2004**, *108*, 10428-10439.

(61) Renger, T. *Phys. Rev. Lett.* **2004**, *93*, 188101-1: 188101-4.

(62) Neupane, B.; Jaschke, P.; Saer, R.; Zazubovich, V.; Beatty, J. T.; Jankowiak, R. *J. Phys. Chem. B*, **2012**, DOI:10.1021/jp300304r.

(63) Hughes, J. L.; Cox, N.; Rutherford, A. W.; Krausz, E.; Lai, T.-L.; Boussac, A.; Sugiura, M. *Biochem. Biophys. Acta* **2010**, *1797*, 11-19.

(64) Krausz, E.; Cox, N.; Årsköld, S. P. *Photosynth. Res.* **2008**, *98*, 207-217.

Chapter 5 - Conclusion and Future Direction

A number of isolated antenna proteins (CP43 and CP47) and reaction centers (RC)–the constituents of oxygen-evolving photosystem II core complexes–have been studied in our group over the years, using state-of-the art-techniques such as low-*T* absorption, emission and hole-burning (HB) spectroscopies and sophisticated spectral-simulation algorithms. We have reported many low-*T* optical spectra of *intact* photosynthetic protein complexes. Modeling of reliable experimental optical spectra provided more insight into some of the long-standing unresolved issues such as lowest-energy state(s), energy of fluorescence origin band(s), excitonic energy transfer (EET), charge separation (CS) dynamics, and more reliable assignment of site energies of pigments residing in protein environments. The present work establishes that the lowest-energy state of CP47 is near 693 nm, i.e., energetically below the primary electron-donor state of the PSII RC that is expected to lie near 685 nm.[1,2,3] This means that at room temperature the energy of the primary electron-donor state is within reach of thermal energy *kT*. The lowest Q_y-state (~693 nm) is characterized by weak electron-phonon coupling with a Huang-Rhys factor S~1±0.2, an Γ_{inh} of 180 cm^{-1}, and a mean phonon frequency of 20 cm^{-1}. HB and absorption data indicate that the lowest-energy state has a smaller oscillator strength than that corresponding to one Chl, in contrast to earlier assignments.[4,5] Importantly, intact CP47 complexes do not reveal any contribution from triplet-bottleneck (transient) holes, which were previously observed in singlet-minus-triplet spectra, suggesting that the transient hole previously observed near 684 nm originated from partially destabilized complexes. We have shown that the fluorescence origin band of the intact CP47 antenna protein complex of PSII from spinach does not shift in the temperature range of 5–77 K, and has very different temperature dependence than previously reported in.[6] It has been shown that the emission maximum of CP47 and its bandwidth strongly

depend on the degree of bleaching of the low-energy state(s) and/or destabilization of the protein complex. The 695 nm emission shifts continuously to shorter wavelengths reaching, due to photobleaching, a position of ~692 nm at saturated HB conditions. This process is reversible by cycling the temperature. In contrast, the emission peaks previously observed near 685 nm and ~691 nm characteristic of destabilized complexes[7] cannot be eliminated by temperature cycling. We suggest that both the ~685 nm and ~690 emissions in the PSII core could originate from destabilized or photo-damaged complexes. Thus the slow EET dynamics observed in[8] may not be characteristic of the intact CP47 antenna, showing again that the EET dynamics in PSII deserves further study.

From *C. reinhardtii* WT-RC and its mutant D2-L209H (in which the active branch $Pheo_{D1}$ has been genetically replaced with chlorophyll *a* (Chl *a*)) studies and Monte Carlo simulations, we have demonstrated that the Q_x-/Q_y-region site-energies of $Pheo_{D1}$ and $Pheo_{D2}$ are most likely at ~545/~680 nm and ~541.5/~670 nm, respectively, in good agreement with our previous assignment.[9,10] Our results presented here offer support neither for the recent assignments[11,12,13,14] that site energies of $Pheo_{D1}$ and $Pheo_{D2}$ are at 672 nm and 677.5 nm, respectively,[11,12,13,14] nor for the assignment that both pheophytins contribute to the absorption near 676–681 nm region as proposed in.[15,16,17,18] The transient hole-burned spectra of the most intact RCs revealed that transient holes have contribution from both triplet-bottleneck (localized on Chl_{D1}) and long lived (~ ms) $P^+Q_A^-$ state. We have established that isolated RC samples are a mixture of RC680 (destablished) and RC684 (intact) complexes. It has been shown that transient HB spectra in RC684 are very similar to $P^+Q_A^-$ - PQ_A spectra measured in PSII core,[19,20] providing the first evidence that RC684 represent *intact* isolated RC that also possesses the secondary electron acceptor, Q_A. We also revealed two possible charge separation pathways in

isolated RCs. For example, the shape of $P^+Q_A^-$ - PQ_A transient holes clearly suggests that the primary electron donor (major pathway) in intact RC684 (with Q_A) from *C. reinhardtii* is P_{D1} and/or P_{D2} of the special Chl pair (analogous to P_L and P_M, the special BChl pair of the bacterial RC). However, Chl_{D1} can also be the primary electron donor (minor pathway) in RC684 (with no Q_A) and destablished RC680, as reflected by the typically observed bleach at ~684 nm and 680 nm, respectively, (and no response at ~673 nm expected for oxidation of P_{D1}) in triplet-bottleneck holes.

In summary, the results presented in this work highlight that it is important to work with intact samples; otherwise it will be difficult to compare data generated in different laboratories. While working with highly fragile and light sensitive protein complexes, we were able to develop sample preparation protocols required for the measurement of low-*T* optical spectra. We anticipate proper characterization of intact CP43, CP47, and isolated (RCs) complexes provide more insight into the structure function relationship of PSII core. Our assignment of pigment site energies should be useful to model the excitonic structure, which should provide a more complete picture of the EET pathways and charge separation (CS) in PSII core complexes.

There is still more to learn about the remarkable phenomena in photosynthesis in order to be well-equipped for the energy needs of humans by the conversion and utilization of solar energy. In the future, we are planning to measure low temperature CD, LD and time-domain spectra of our intact samples in collaboration with other labs. We believe that simultaneous fit of both linear and non-linear spectra of intact samples by applying a more advanced theory (Redfield approach;[21,22,23] research in progress) using experimental constraints will provide a more coherent picture of excitonic structure and dynamics in these complex biological systems. Our HB data of intact isolated RC samples indicate that, like in PSII core, the excited-state

manifold most likely includes a primary charge separation (CT) state that is strongly mixed with the pure exciton states. Future calculations should account for a coupling to a CT state. However, the nature of this state (homogeneously versus inhomogeneously broadened) needs to be resolved first. High pressure and Stark HB studies (accessible in our lab) applied to PSII RC could provide more information on the nature of CT state(s).

References

(1) Hughes, J. L.; Krausz, E.; Smith, P. J.; Pace, R. J.; Riesen, H. *Photosynthesis Res.* **2005**, *84*, 93.

(2) Jankowiak, R.; Rätsep, M.; Hayes, J.; Zazubovich, V.; Picorel, R.; Seibert, M.; Small, G. J. *J. Phys. Chem. B* **2003**, *107*, 2068.

(3) Jankowiak, R.; Tang, D.; Small, G. J.; Seibert, M. J. Phys. Chem. 1989, 93, 1649.

(4) De Weerd, F. L.; van Stokkum, I. H. M.; van Amerongen, H.; Dekker, J. P.; van Grondelle, R. Biophys. J. **2002**, *82*, 1586.

(5) de Weerd, F. L.; Palacios, M. A.; Andrizhiyevskaya, E. G.; Dekker, J. P.; van Grondelle, R. *Biochemistry* **2002**, *41*, 15224.

(6) Groot, M.; Peterman, E. J. G.; van Stokkum, I. H. M.; Dekker, J. P.; van Grondelle, R. *Biophys. J.* **1995**, *68*, 281.

(7) Neupane, B.; Dang, N. C.; Acharya, K.; Reppert, M.; Zazubovich, V.; Picorel, R.; Seibert, M.; Jankowiak, R. *J. Am. Chem. Soc.* **2010**, *132*, 4214.

(8) Krausz, E.; Hughes, J. L.; Smith, P.; Pace, R.; Peterson Årsköld, S. *Photochem. Photobiol. Sci.* **2005**, *4*, 744.

(9) Jankowiak, R.; Rätsep, M.; Picorel, R.; Seibert, M.; Small, G. J. *J. Phys. Chem. B* **1999**, *103*, 9759.

(10) Jankowiak, R.; Hayes, J. M.; Small, G. J. *J. Phys. Chem. B* **2002**, *106*, 8803.

(11) Raszewski, G.; Diner. B. A.; Schlodder, E.; Renger, T. *Biophys. J.* **2008**, *95*, 105.

(12) Cox, N.; Hughes, J. L.; Steffen, R.; Smith, P. J.; Rutherford, W.; Pace, R. J.; Krausz, E. *J. Phys. Chem. B* **2009**, *113*, 12364.

(13) Raszewski, G.; Saenger, W.; Renger, T. *Biophys. J.* **2005**, *88*, 986.

(14) Cox, N.; Hughes, J.; Rutherford, A.W.; Krausz, E. *Physics Procedia* **2010, *3*,** 1601.

(15) Germano, M.; Shkuropatov, A. Ya.; Permentier, H.; de Wijn, R.; Hoff, A. J.; Shuvalov, V. A.; van Gorkom, H. J. *Biochem.* **2001**, *40*, 11472.

(16) Germano, M.; Shkuropatov, A. Ya.; Permentier, H.; Khatypov, R. A.; Shuvalov, V. A.; Hoff, A. J.; van Gorkom, H. J. *Photosynth. Res*. **2000**, *64*, 189.

(17) Yruela, I.; Torrado, E.; Roncel, M.; Picorel, R. *Photochem. Photobiol*. **2001**, 67, 199.

(18) Saito, K.; Mukai, K.; Sumi, H. *Chem. Phys. Lett.* **2005**, *401*, 122.

(19) Hillmann, B.; Brettel, J. K.; van Mieghem, F.; Kamlowski, A.; Rutherford, A. W.; Schloder, E. *Biochem*. **1995**, *34*, 4814.

(20) Renger, T.; Schlodder, E. *ChemPhysChem* **2010**, *11*, 1141.

(21) Yang, M.; Fleming, G. R. *Chem Phys* **2002**, *275,* 355.

(22) Redfield, A.G. *IBM J. Res. Dev.* **1957,** *1*, 19.

(23) Renger, T.; May, V.; Kühn, O. *Phys Rep* **2001** *343*, 138.

Appendix A - New Insight into the Electronic Structure of the CP47 Antenna Protein Complex of Photosystem II: Hole Burning and Fluorescence Study

Bhanu Neupane, Nhan C. Dang, Khem Acharya, Mike Reppert, Valter Zazubovich, Rafael Picorel, Michael Seibert, and Ryszard Jankowiak

Abstract

We report low temperature (T) optical spectra of the isolated CP47 antenna complex from Photosystem II (PSII) with a low-T fluorescence emission maximum near 695 nm and not, as previously reported, at 690-693 nm. The latter emission is suggested to result from three distinct bands: a lowest-state emission band near 695 nm (labeled F1) originating from the lowest-energy excitonic state A1 of intact complexes (located near 693 nm and characterized by very weak oscillator strength) as well as emission peaks near 691 nm (FT1) and 685 nm (FT2) originating from subpopulations of partly destabilized complexes. The observation of the F1 emission is in excellent agreement with the 695 nm emission observed in intact PSII cores and thylakoid membranes. We argue that the band near 684 nm previously observed in singlet-minus-triplet spectra originates from a subpopulation of partially destabilized complexes with lowest-energy traps located near 684 nm in absorption (referred to as AT2) giving rise to FT2 emission. It is demonstrated that varying contributions from the F1, FT1, and FT2 emission bands led to different maxima of fluorescence spectra reported in the literature. The

fluorescence spectra are consistent with the zero-phonon hole action spectra obtained in absorption mode, the profiles of the non-resonantly burned holes as a function of fluence, as well as the fluorescence line-narrowed spectra obtained for the Q_y-band. The lowest Q_y-state in absorption band (A1) is characterized by an electron-phonon coupling with the Huang-Rhys factor S of ~1 and an inhomogeneous width of ~180 cm^{-1}. The mean phonon frequency of the A1 band is 20 cm^{-1}. In contrast to previous observations, intact isolated CP47 reveals negligible contribution from the triplet-bottleneck hole, i.e. the AT2 trap. It has been shown that Chls in intact CP47 are connected *via* efficient excitation energy transfer to the A1 trap near 693 nm and that the position of the fluorescence maximum depends on the burn fluence. That is, the 695 nm fluorescence maximum shifts blue with increasing fluence, in agreement with non-resonant hole burned spectra. The above findings provide important constraints and parameters for future excitonic calculations, which in turn should offer new insight into the excitonic structure and composition of low-energy absorption traps.

Conclusions

We have shown that absorption, emission, and persistent NPHB spectra of CP47 complexes, diluted from solutions stored at high optical density followed by sonication, dark thermal equilibration, and mixing with cryoprotectants (50/50 v/v) shortly before experimentation, exhibit less contribution from destabilized complexes and provide new insight into the nature of the electronic structure of intact CP47. The present work establishes that the lowest-energy state of CP47 is near 693 nm, i.e., energetically below the primary electron-donor state of the PSII RC that is expected to lie near 685 nm.[1-3] This means that at room temperature the energy of the primary electron-donor state is within reach of thermal energy *kT*. The lowest Q_y-state (~693 nm, A1 band) is characterized by weak electron-phonon coupling with a Huang-

Rhys factor S~1±0.2 and an Γ_{inh} of 180 cm^{-1}. The mean phonon frequency of the lowest energy trap A1 is 20 cm^{-1}. HB and absorption data indicate that the A1 state has a small oscillator strength, i.e., it is much smaller than the oscillator strength corresponding to one Chl, in contrast to earlier assignments.[4,5] This in turn suggests that Chls absorbing at higher energies steal a significant amount of the oscillator strength from Chls contributing to the A1 trap, in agreement with a positive anti-hole feature at high energy in the persistent non-resonant hole spectra (see Fig. 2). This fact should help to identify the A1 state pigments (see excitonic calculations in Ref.[6]). Fluorescence of intact complexes was shown to be strongly dependent on the excitation power density. Different maxima of fluorescence spectra reported in the literature are attributed to varying contributions from several distinct emission bands (F1, FT1, and FT2) originating from intact and destabilized CP47 complexes, as well as potentially from shifts in these fluorescence bands due to HB if high-fluence was used. The above conclusions are consistent with the ZPH-action spectra obtained in absorption mode, the profiles of the non-resonantly and resonantly burned holes, as well as the FLN spectra obtained for the Q_y band. Importantly, intact CP47 complexes do not reveal any contribution from triplet-bottleneck (transient) holes, which were previously observed in singlet-minus-triplet spectra, suggesting that the transient hole near 684 nm originates from partially destabilized complexes. Finally, we suggest that the absorption spectrum of intact CP47 reported in this work along with the absorption spectrum of the CP43 complex published recently[7] should allow extraction the real absorption spectrum of the intact reaction center residing in the intact PSII core complexes and shed more light on possible contaminations, charge-transfer emission in PSII core from spinach, and unusual fluorescence temperature dependence observed previously in CP47 complexes.

References

(1) Hughes, J. L.; Krausz, E.; Smith, P. J.; Pace, R. J.; Riesen, H. *Photosynthesis Res*. **2005**, *84*, 93.

(2) Jankowiak, R.; Rätsep, M.; Hayes, J.; Zazubovich, V.; Picorel, R.; Seibert, M.; Small, G. J. *J. Phys. Chem. B* **2003**, *107*, 2068.

(3) Jankowiak, R.; Tang, D.; Small, G. J.; Seibert, M. *J. Phys. Chem.* **1989**, *93*, 1649.

(4) De Weerd, F. L.; van Stokkum, I. H. M.; van Amerongen, H.; Dekker, J. P.; van Grondelle, R. *Biophys. J.* **2002**, *82*, 1586.

(5) de Weerd, F. L.; Palacios, M. A.; Andrizhiyevskaya, E. G.; Dekker, J. P.; van Grondelle, R. *Biochemistry* **2002**, *41*, 15224.

(6) Reppert, M.; Acharya, K.; Neupane, B.; Jankowiak, R. *J. Phys. Chem. B* **2010**, *114*,11884.

(7) Dang, N. C.; Zazubovich, V.; Reppert, M.; Neupane, B.; Picorel, R.; Seibert, M.; Jankowiak, R. *J. Phys. Chem. B* **2008**, *112*, 9921.

Appendix B - Supporting Information for the Chapter number two: Experimental Strategy and Fitting Algorithm for Temperature Dependent Fluorescence Spectra.

K. Acharya, B. Neupane, M. Reppert, X. Feng, and R. Jankowiak

SI 1. Temperature dependence of emission spectra.

The fluorescence lineshape function at a given temperature T is calculated using the standard expression:[1]

$$D(\omega;T) \propto e^{-S} \int_{-\infty}^{\infty} e^{-i\omega t + S\cdot G(t;T)} dt$$

where $G(t;T) = \int_{-\infty}^{\infty} e^{-i\omega t}\left(1+n(\omega;T)\right)J(\omega) + n(-\omega;T)J(-\omega)d\omega$, S is the Huang-Rhys (HR) factor, $n(\omega;T)$ is the thermal occupation number for a phonon with frequency ω, and $J(\omega)$ is the spectral density function.

Using a series expansion for the exponent, this formula can be re-cast to obtain

$$D(\omega;T) \propto e^{-S(T)} \sum_{R=0}^{\infty} \frac{S(T)^R}{R!} l_R(-\omega;T)$$

where $S(T) = \int_{-\infty}^{\infty} p(\omega;T)d\omega$, $p(\omega;T) = \left(1+n(\omega;T)\right)J(\omega) + n(-\omega;T)J(-\omega)$, $l_0(\omega;T)$ is a delta function representing the zero-phonon line (ZPL), $l_1(\omega;T) = S(T)^{-1} \cdot p(\omega;T)$, and for $R > 1$,

$l_R(\omega;T)$ is the convolution $l_1(\omega;T)$ with itself *R*-1 times. For numerical calculations, the sum was truncated after a number of terms sufficient to account for 99.99% of the total intensity of the phonon-sideband (PSB).

For the m^{th} excitonic state (m = 1, 2,…, 16), the bulk emission spectrum is calculated as

$$F_m(\omega;T) \propto \omega^3 \cdot f(\overline{\omega}_m;T) \cdot \int_{-\infty}^{\infty} D(\omega-\omega_m;T) \cdot Z(\omega_m) d\omega_m$$

where $Z(\omega_m)$ is a zero-phonon emission distribution function including both probability of occurrence and oscillator strength, and $f(\overline{\omega}_m;T)$ is the Boltzmann population of a state with *average* excitation energy $\overline{\omega}_m$ at temperature *T*. The distributions $Z(\omega_m)$ were obtained from Monte Carlo simulations.[2] The total emission spectrum is obtained as the sum of the spectra from each excitonic state. For our present calculations, we assumed a HR factor of *S = 1* for all states. Note that in[2] a lower HR factor of *S = 0.5* was assumed (somewhat arbitrarily) for upper excitonic states (m > 1), while *S = 1* was assigned to the lowest state based on experimental HB data. In the current work, it was found that S = 1 provides a better fit to high-temperature data; since the calculations in[2] are not very sensitive to this parameter for the higher energy states (as noted in that work), it appears that a value of S = 1 is more reasonable for all states. The spectral density function $J(\omega)$ was obtained by extraction from experimental difference spectra for the CP47 complex and is defined by

$$J(\omega) = \frac{1}{11}\sum_{i=1}^{3} \frac{f_i \cdot \theta_i^{-a}}{(a_i-1)!} w^{a_i-1} \exp\left(-\frac{\omega}{\theta_i}\right)$$

with $(f_1,a_1,\theta_1)=(4,2,30)$, $(f_2,a_2,\theta_2)=(4,2,100)$, and $(f_3,a_3,\theta_3)=(3,4,6)$ with θ_i in cm^{-1}.

SI 2. Spectroscopic measurements.

Fluorescence spectra were obtained with an excitation wavelength of 496.5 nm from the Coherent Innova 200 Ar^+ ion laser. Other excitation wavelength s were obtained using a tunable Coherent CR699-21 ring dye laser (linewidth of 0.07 cm^{-1}, laser dye: DCM Special (Exciton)), pumped by a 6-W Coherent Innova 90 Ar^+ ion laser. Fluorescence was dispersed by a 300-mm focal length monochromator and detected by a PI Acton Spec-10 (1340 x 400) CCD camera. The FWHM spectral resolution for the fluorescence spectra was ~0.1 nm. For fluorescence measurements, the OD of the samples (at the maximum of the Q_y band) was reduced to 0.1 per 1 cm sample thickness (at the absorption maximum), and the sample thickness reduced to ~ 1 mm to ensure that re-absorption effects were negligible. All spectra were corrected for the wavelength sensitivity of the detection system. The sample temperature was maintained at 5 K (unless otherwise specified) using a Janis 8-DT Super Vari-Temp liquid helium cryostat. The temperature was stabilized and measured with a Lakeshore Cryotronic model 330 temperature controller.

SI 3. CP47 complexes. We hasten to add that the CP47 complexes studied in this work did not aggregate. Efforts were made to use the correct detergent concentration of β-DM (i.e. 0.03%). It is well known that aggregates are typically formed by significantly lowering the β-DM concentration, i.e. far below the critical micelle concentration[3]. No indication of aggregation was observed in high-resolution spectroscopy experiments[4] or size exclusion chromatography/HPLC experiments**.** For completeness, Figure S1 shows the fluorescence spectrum of an intact CP47 sample with a β-DM concentration of 0.03% (solid line) in ethylene glycol/glycerol glass at 5 K. The dotted curve is shown for comparison and corresponds to the CP47 sample diluted directly 1:1 with ethylene glycol/glycerol matrix

decreasing the concentration of β-DM by a factor of two (i.e. 0.015%). The spectra are nearly indistinguishable with a maximum near 695 nm. Partial aggregation was observed, however, at much lower concentrations of β-DM (<0.01%) as reflected by stronger fluorescence intensity near 700 nm (data not shown).

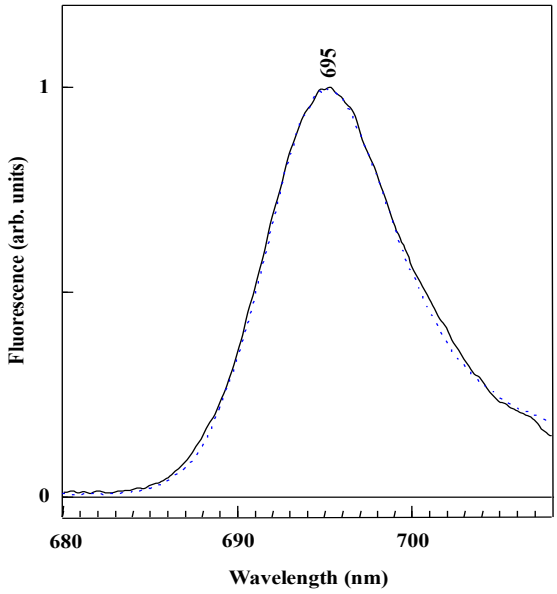

Figure B-1 Emission spectra of CP47 complex at T = 5 K with two different concentrations of β-DM; solid black line (0.03%) and dotted blue line (0.015%).

References

(1) May V.; Kuhn O. Intramolecular Electronic Transitions. *Charge and Energy Transfer Dynamics in Molecular Systems*; WILEY-VCH: Verlag Berlin GmbH, Berlin, **2000**; PP 191-247.

(2) Reppert, M.; Acharya, K.; Neupane, B.; Jankowiak, R. Lowest Electronic States of the CP47 Antenna Protein Complex of Photosystem II: Simulation of Optical Spectra and Revised Structural Assignments *J. Phys. Chem. B* **2010**, *114*,11884.

(3) Van Oort, B.; van Hoek, A.; Ruban, A.V.; and van Amerongen, H. Aggregation of Light-harvesting Complex II leads to formation of efficient excitation energy traps in monomeric and trimeric complexes, *FEBS Letters* **2007**, *581,* 3528–3532.

(4) Neupane, B.; Dang, N. C.; Acharya, K.; Reppert, M.; Zazubovich, V.; Picorel, R.; Seibert, M.; Jankowiak, R. Insight into the Electronic Structure of the CP47 Antenna Protein Complex of Photosystem II: Hole Burning and Fluorescence Study. *J. Am. Chem. Soc.* **2010**, *132*, 4214-4229.